

**TRANSMISSION LINE FEATURES AND THEIR INFLUENCE ON
GHz CONDUCTOR LOSS**

by

Tracey S Vincent

A Dissertation

Submitted to the Graduate Faculty of

Worcester Polytechnic Institute

in partial fulfillment of the requirements for the degree of

Doctor of Philosophy

in

Materials Science and Engineering by

2009

Approved:

Isa Bar-On, Advisor. Professor of Mechanical Engineering

Approved:

**Richard D Sisson, George F. Fuller Professor. Director of Manufacturing Engineering and
Material Science Program.**

ABSTRACT

Transmission loss needs to be considered in the design of telecommunication systems. If telecommunication systems have high transmission loss, the signals lose too much of their strength, which results in poor reception in television networks and lost calls in cellular networks. Total transmission loss, in the MHz-GHz range, has several different loss components, some of which are poorly characterized. Conductor loss is the largest loss component and the most difficult to predict. It is known that the conductor geometry or features influences the conductor loss. However, current numerical, analytical and empirical tools do not accurately predict this loss component, and there is little experimental data available to explain and show the impact of these conductor geometries. The conductor shape is heavily influenced by the ceramic substrate surface roughness, and this is especially true for printed circuit boards fabricated with thick-film technology. The two conductor features of interest are the conductor-edge angle and conductor-ceramic interface. For thick-film circuits, the edge of the conductor does not have a square cross section but has a tapered shape or angle. The conductor-ceramic interface is also rough at the micron scale. Since the current density is concentrated at the extremities of the conductor then these features, conductor-ceramic interface and conductor edges, can potentially have a large impact on conductor loss. For this study, the surfaces of ceramic substrates were subjected to different surface finishes that resulted in distinctly different surface characteristics. This in turn resulted in a range of conductor-ceramic interfaces and conductor-edge angle geometries.

The impact of the conductor-edge angle and conductor-ceramic interface features on conductor loss was measured over a range of frequencies and conductor conductivities to ascertain the level of their contribution. It was shown quantitatively that the conductor-edge angle was significantly altered by the surface roughness and heavily influenced the conductor loss result. The consensus for decades has been that greater surface roughness causes the ceramic-conductor interface geometry to have a greater impact on conductor loss, increasing the conductor loss. However, this study has shown that greater surface roughness also causes the conductor-edge angle feature to have a smaller or reduced impact on conductor loss, improving the conductor loss result - this has not been considered previously. Focusing on only one of these features can give an anomalous loss prediction; both features need to be considered for the calculation of conductor loss for thick-film applications. The low frequency loss results are as expected but the high frequency (greater than 5GHz) results depend on edge angle and therefore thick-film paste viscosity, and substrate surface roughness.

Acknowledgements

I would like to give many thanks to my advisor, Professor Isa Bar-On, for providing me the opportunity to work on this project, for her support, assistance, encouragement, advice, humor, sassiness, and overall guidance throughout this study.

To my advisory committee: Professor Isa Bar-On, Professor of Mechanical Engineering, Director, Alternative Fuel Economics Laboratory (AFEL), Professor Richard D Sisson, Director of Manufacturing and Materials Engineering, Professor Christopher Brown, Professor of Mechanical Engineering, Director of Surface Metrology Lab, Dr John Sharp, Group leader at Napier University, Edinburgh, Scotland and Ron Barnett, of National Instruments and Owner of GeoMat Insights LLC, my sincere gratitude for being members of my advisory committee, for their active participation and their kind support.

Special thanks to Professor Sisson for pointing me in the direction of many rewarding experiences and opportunities, for example, the ceramics congress in Verona Italy, funded by the NSF, and encouraging me to teach, “introduction to material science” in term D 2009. Thank you also for your open door policy and your advice on many issues over these years.

Thank you also to Professor Brown for accepting me into the Surface Metrology group and for many interesting discussions at Surface lab meeting and dinners.

Also, I would like to express my appreciation to Brendan Powers, Torbjorn S Bergstrom and Omair Paracha, for their interesting discussions and ideas, their friendship, and for helping me with the surface measurements and methodology and to Bouquan Li, Lab Manager, and Mohammad Maniruzzaman, Research Assistant Professor of Mechanical Engineering, Materials Science and Engineering for their help and training on various microscopes and machinery. My sincere thanks to Rita Shilansky and Susan Milkman for their assistance, and help throughout.

To Barry Industries, Attleboro, MA, acknowledgement and appreciation for the use of their thick-film fabrication technology, for their processing techniques and knowledge and making all the samples used in this study and for being my employer for over five years. Specifically my gratitude extends to Barry Employees: Michael Ehlert, Dave Murphy, Joe Timoteo, Scott Pouliot and Peter Barnwell. Thanks also to DuPont, Research Triangle Park, NC, specifically Michael Smith and John Crumpton for the Fodel samples and LTCC knowledge.

Additionally, I would like to thank all in the materials and manufacturing departments for providing a friendly and encouraging atmosphere.

Last but never least; I would like to express my sincere gratitude to Brian Pierce for his consistent, altruistic support. Brian, you are the best friend anyone could hope for.

This thesis is dedicated to my grandparents Samuel Scott Hay and Anne Miller Hay. The wittiest people I have ever known. Miss you.

TABLE OF CONTENTS

ABSTRACT	ii
ACKNOWLEDGEMENTS	iv
LIST OF TABLES	ix
LIST OF FIGURES	x
1.0 INTRODUCTION	1
1.1 MICROELECTRONICS AND MICROELECTRONIC PACKAGING	1
1.2 BACKGROUND FOR PROBLEM STATEMENT I – ELECTRICAL LOSS DUE TO MATERIALS PROPERTIES	3
1.3 BACKGROUND FOR PROBLEM STATEMENT II - CONDUCTOR LOSS AND SKIN EFFECT	6
1.4 PROBLEM STATEMENT - CONDUCTOR TOPOGRAPHY INFLUENCE ON CONDUCTOR LOSS FOR A MICROSTRIP STRUCTURE	11
1.5 RESEARCH OBJECTIVE	14
1.6 PUBLICATIONS AND PRESENTATIONS	15
1.7 THESIS ORGANIZATION	16
2.0 CHAPTER II	17
2.1 LITERATURE REVIEW	17
2.1.1 Conductor loss and Skin effect	17
2.2.1 Conductor topography influence on conductor loss for a microstrip structure: Conductor -ceramic Interface topography	18

2.2.2	Conductor Topography: Conductor Edge Angle	20
3.0	CHAPTER III	22
	PAPER #1.....	23
	INTRODUCTION.....	24
	THEORY.....	26
	EXPERIMENTAL PROCEDURES.....	33
	RESULTS	38
	DISCUSSION	50
	CONCLUSIONS:	55
4.0	CHAPTER IV	60
	PAPER #2.....	61
	INTRODUCTION.....	62
	EXPERIMENTAL METHOD	63
	RESULTS	67
	DISCUSSION	72
	CONCLUSION	74
5.0	CHAPTER V: FURTHER WORK	78
6.0	CHAPTER VII: CONCLUSION	82
	REFERENCES FOR THESIS (EXCLUDING CHAPTERS III AND IV).....	84
7.0	APPENDIX A.....	88
8.0	APPENDIX B	105
9.0	APPENDIX C	125
10.0	APPENDIX D.....	127

LIST OF TABLES

Table Number		Page
1.1	Summary of commercially available simulation tools and their prediction of conductor loss	5
3.1	Surface finish processes description with average roughness result	32
3.2	Skin depth for conductor lines with different conductivities	37
3.3	Roughness parameters, Ra and Rt for AlN surfaces with four finishing processes	40
4.1	Aluminum nitride surface finish processes	64
4.2	Student t-test results for each combination of measured conductor edge angles for both AlN 11 and AlN 33	69

LIST OF FIGURES

Figure Number		Page
1.1	<i>Metal wire with AC signal at GHz frequencies showing current I, induced internal magnetic fields, H and current loops, I_w.</i>	8
1.2	<i>An illustration of three transmission structures common for signals in the GHz frequency range, the distribution of the electric and magnetic fields, and the corresponding current density. The circuit structures are shown for comparison and are assumed to have similar conductivities, dielectric constants and operating at similar frequencies at similar scale.</i>	10
1.3	<i>An illustration noting the three conductor geometries, that are thought to influence conductor loss.</i>	13
3.1	<i>Illustration of losses for microstrip topology at GHz frequencies</i>	28
3.2a	<i>Diagram of skin depth phenomena in microstrip topology</i>	30
3.2b	<i>Legend of skin depth phenomena for given frequencies</i>	30
3.3	<i>Comparing measured conductor loss from a lapped surface with the theoretical loss derived from eq.3.3.</i>	32
3.4	<i>Diagram of skin depth phenomena in microstrip topology, front cross-section view: a, is a given skin depth for a GHz frequency signal with square cross section edges, b, is a given skin depth for a GHz frequency signal with cross section edges at an angle, common for circuits made by thick-film processing.</i>	33
3.5	<i>An example length-scale analysis on a cartoon profile, showing the increase in measured length as the scale, or step length decreases. All the nominal lengths are</i>	34

110 μ m

3.6	<i>Photograph of an AlN substrate with conductor with two sets of three conductor lines with nominal lengths: 10, 20, and 40mm. The serpentine line is used to measure bulk conductivity.</i>	38
3.7a	<i>Height map measurement of chemically etched surface.</i>	38
3.7b	<i>Height map measurement of honed surface</i>	39
3.7c	<i>Height map measurement of lapped surface</i>	39
3.8	<i>Length-scale plots [ASME B46 2000] for the four surface treatments on the AlN substrates. The error bars represent +/- one standard deviation on the six profile measurement of each surface.</i>	41
3.9	<i>ALN11 conductor losses versus frequency for all four substrates</i>	42
3.10	<i>ALN33 conductor losses versus frequency on all four substrates</i>	43
3.11	<i>ALN 23 conductor losses versus frequency on all four substrates</i>	44
3.12	<i>Loss vs. Average roughness</i>	45
3.13	<i>Loss vs. relative length at four different frequencies and at three scales of observation for the four different surface finishes using conductor line ALN11.</i>	46
3.14	<i>Loss vs. relative length at four different frequencies and at three scales of observation for the four different surface finishes using conductor line ALN33.</i>	47
3.15	<i>Loss vs. relative length at four different frequencies and at three scales of observation for the four different surface finishes using conductor line ALN23.</i>	48
3.16	<i>Conductor edge angle vs. relative length at three scales of observation for the three differentiable surface finishes using conductor lines ALN11 and ALN33.</i>	49
3.17	<i>Transmission Loss vs. edge angle at four different frequencies and for the three differentiable surface finishes using conductor lines ALN11 and ALN33.</i>	50
3.18	<i>Correlation coefficients, R, versus scales of observation for two different conductor lines. Correlation coefficient were determined from measured edge angle vs. relative</i>	51

	<i>length graphs at different scales of observation</i>	
3.19	<i>Correlation coefficient, R, versus scale of observation for the three different conductor lines. Correlation coefficients were determined from loss vs. relative length graphs at different scales of observation</i>	52
3.20	<i>Cartoon of microstrip circuit with the different topographies shown: conductor edge angle, conductor-ceramic interface and conductor edge profile.</i>	53
3.21	<i>3.21a, is a micrograph of the ALN33 silver conductor on Honed AlN substrate after firing, 3.21b, is the Ag mapped image of the same area, 3.21c, is the edge of the silver isolated by image manipulation.</i>	54
4.1	<i>Cross section illustration of PCB formed using thick-film print showing conductor angle of inclination.</i>	62
4.2	<i>Top view photograph of a 0.625mm thick AlN substrate with one of two sets of three transmission lines, nominal lengths: 10, 20, and 40mm. The serpentine line is used to measure bulk conductivity. The area selection for the conductor edge taper measurement are shown</i>	65
4.3	<i>Interferometer measurement on lapped surface sample. (a) - the height map (red is highest, blue is lowest), the red is the conductor material height measurement, the green-yellow the tapering/angle of the conductor edge and the blue area is the lapped ceramic surface. (b) – characteristic of ceramic and conductor to ceramic profile.</i>	66
4.4	<i>Cross section of microstrip circuit, x 50 magnification, across the width of the conductor at the edge. Shown is the AlN substrate with conductor ALN33 on Lapped (top), Vapor Honed (middle) and Chemically Etched (base) surface finish.</i>	67
4.5	<i>Edge angle mean results (with error bar) versus substrate process for ALN11 and ALN33: chemically etched, vapor honed and lapped surface finish.</i>	68
4.6	<i>Conductor edge angle mean results versus average roughness and length-scale fractal analysis for the two conductor types: ALN11 and ALN33.</i>	70
4.7	<i>Transmission loss of ALN 11 and ALN 33 fired conductors on chemically etched,</i>	71

	<i>vapor honed and lapped surface finishes as a function of frequency.</i>	
4.8	<i>Conductor edge angle mean results versus transmission loss at 20 and 10 GHz for the two conductor types: ALN11 and ALN33; with the coefficient of correlation R^2</i>	72
5.1	<i>The conductor and ceramic substrate, showing the conductor profile, of (a) an alumina substrate with silver alloy conductor, (b) AlN vapor honed substrate with ALN33, and (c) an LTCC substrate with silver alloy.</i>	79
5.2	<i>The fritless fired silver alloy ALN33 showing microstructure features such as grain boundaries and porosity.</i>	81

1.0 INTRODUCTION

1.1 MICROELECTRONICS AND MICROELECTRONIC PACKAGING

Microelectronic circuits exist in numerous applications; some examples are telecommunications systems, automobiles and medical devices - hybrid microelectronics - also known as microelectronic packaging, are used in all facets of the electronics industry, and are especially common within telecommunications. High-performance microelectronic packaging materials, and the processes required to make these materials into electronic circuits, were initially developed for applications in the computer and defense industries in the 1960s. Since then, these materials have been used to meet stringent design criteria for many other applications. Specific applications of this technology include: anti-collision radar for automotive, phased array radar for satellite systems, MRI scanners, Bluetooth, and even digital applications such as video cards that use high-speed interconnects.

Microelectronic packaging circuits have to be small and have low transmission loss. There are limited materials available that can be used in designs to meet both of these design drivers, and this is especially true for devices that have propagating microwave signals. The material choice is narrowed down to ceramic or ceramic composite materials for the electronic substrate, and precious metals such as silver or gold for the conductor. These materials are expensive when compared to organic Printed Circuit Boards (PCBs) but the improved performance outweighs the increase in cost.

This thesis takes a look at a major loss component of transmission loss – conductor loss – for ceramic PCBs using precious metal conductors for frequencies up to 20GHz. It is known that as the

conductor topography changes, the conductor loss changes, but there is little experimental data on this topic and little comparison of the different conductor topographies and their impact on conductor loss.

Organic PCBs, such as Rogers or FR4, have larger dielectric losses than ceramic substrates but are relatively inexpensive. Organic PCBs also have lower permittivities than ceramic PCBs, which forces the conductor to be wider for the same thickness substrate. Widening the conductor trace evens out the electric and magnetic fields, and reduces the conductor loss but the wider conductor takes up more space. For microelectronics design, the area of the circuit is usually limited; the area available is often a significant design driver.

The conductor loss of an organic PCB has a smaller percentage of the total loss, than ceramic PCBs, but it is still a significant loss component. Conductor loss for both organic PCBs and ceramic PCBs are influenced by the conductor topography; therefore, any findings that relate conductor topography to conductor loss on one of these material systems could be applied to the other material system.

Microelectronics packaging circuitry can be fabricated using several technologies; the fabrication method can influence the conductor topography. One of the fabrication methods is thick film; so named because the conductor trace is between 5 – 50 μm thick, by comparison thin film is 5nm - 0.2 μm . For thick-film technology, the paste or ink is deposited through a screen onto an insulating substrate, usually a ceramic or ceramic composite material. The ceramic substrate can be Alumina or AlN or more commonly Low Temperature Co-fired Ceramic (LTCC). These ceramic substrates are attractive because they have lower $\tan \delta$, also known as dielectric loss, than organic substrates; however, they are much more expensive. All of the ceramic substrate samples used in this study were fabricated using thick-film processing.

LTCC involves screen printing green ceramic sections with conductive patterns; several of these sections or layers collated, laminated and fired to produce a sintered monolithic substrate [1]. LTCC technology is often used for wireless and high-frequency applications for making hybrid integrated circuits, known as system-in-package (SiP) [2]. These circuits integrate components, such as capacitors and inductors, into the printed circuitry and add ICs, such as flip chips to the same package. LTCC hybrids have a smaller initial cost as compared with System-on-chip (SoC) [3], making them an attractive alternative for small scale integration devices.

The samples used in this study were fabricated using thick-film technology, therefore the conclusions made by this thesis directly relate to this type of PCB technology. However, this work could potentially apply to other PCB technologies such as thin-film and copper foil laminate boards; all of these PCB structures are sensitive to changes in conductor topography.

Further research is needed in the area of PCB characterization in relation to electronic parameterization and specification. The International Electronics Manufacturing Initiative (iNEMI) Research Priorities Report, for 2007, included the need for standardized test methods and figures of merit for printed electronics. Another section of this report stated that research was also needed to find low-cost solutions for carrying signal rates greater than 10Gb/s between components on a PCB.

1.2 BACKGROUND FOR PROBLEM STATEMENT I – ELECTRICAL LOSS DUE TO MATERIALS PROPERTIES

Electrical loss, also known as signal attenuation, is to be avoided - when a signal loses power, it often needs expensive amplification to reach its intended destination. There are four distinct high-frequency (GHz) loss categories (or causes of signal attenuation): radiative, reflected, conductor and

dielectric. Radiative and reflected losses are directly related to electrical design and can be accurately predicted by full-wave electromagnetic solvers. Dielectric and conductor losses depend on material and process parameters. Dielectric loss is the signal that is absorbed by the insulator material, the ceramic substrate. The conductor loss is the signal that is absorbed by the conductor, the metal strip; conductor loss can also be known as ohmic or resistance loss. The main focus of materials engineers has been to create materials with low dielectric losses.

Most high-frequency, high-performance electronic substrates have low dielectric loss to the point that conductor loss is the largest loss component [4]. For DC and low frequency signals the conductor loss is directly related to the conductivity (inverse of resistivity of the conductor). PCBs are fabricated with silver, copper and sometimes gold because all of these metals have relatively high conductivity. The high conductivity of these materials does result in small conductor loss for the DC-kHz frequency region. At frequencies above the kHz region electromagnetic phenomena induce a skin effect that exacerbates the conductor loss. The impact of the skin effect on conductor loss is influenced by conductor features or substrate surface topography. The specifics of these phenomena will be discussed in the next section, background for the problem statement.

Microelectronics circuits are designed using electromagnetic (EM) simulation in order to decrease design costs and quicken the process. Therefore, circuit design, for microwave frequencies, heavily depends on the accuracy of simulation tools that allow circuit prototypes to be created quickly and inexpensively. Although current EM simulation packages, such as SONNET®, CST® and HFSS®, can be good at predicting most electrical results such as matching of interfaces. They consistently underestimate the transmission loss, and therefore conductor loss, in an unpredictable manner. A summary of the commercial solvers currently available is given in Table I. Each software package uses a numerical method to solve either the electromagnetic fields or distribution of current density.

Table 1, Summary of commercially available simulation tools and their prediction of conductor loss	Description	Numerical Technique	Conductor loss Analysis
SONNET	2D current density planar solver	Moment Method (MoM)	The n-, two-, and one layer model used to predict conductor loss over a range of frequencies and the different physical effects at those frequencies. The model recognizes that edge current density can be a large contributing factor to conductor loss [Rautio]. This model was compared to experimental data. Arbitrary conductor geometry not modeled.
Computer Simulation Technology (CST)	3D electromagnetic solver	Finite Difference Time Domain (FDTD) and (FEM)	Some comparison with empirical method [5] for calculating ceramic-interface roughness contribution [41]. Future research – probabilistic approaches.
Ansoft, High frequency Structure Simulator	3D electromagnetic	Finite Element	Empirical method Hammerstad [5] for calculating the surface roughness

(HFSS)	solver	Method (FEM)	influence on conductor-ceramic interface is incorporated into Software.
Vector Fields, CONCERTO	3D and 2D solver	FDTD and MoM	No information on conductor loss analysis found.

It is not just analogue applications, in the GHz range, that are affected by conductor loss; fast-switching digital signals also degrade because these types of signals propagate as electromagnetic waves. Video cards have digital signals with rise times less than 50 pico seconds (ps); the Fourier series of this rise time ramp includes signal components greater than 8 GHz. Thus, even digital signals, which have fast switching times, can suffer from high-frequency loss. Digital engineers such as signal integrity engineers are increasingly using these EM simulation tools to predict loss characteristics in digital systems. Since digital switching times are decreasing, the loss caused by high frequency will also increase. A method or tool that can accurately predict the conductor loss for these systems will greatly improve the design process.

1.3 BACKGROUND FOR PROBLEM STATEMENT II - CONDUCTOR LOSS AND SKIN EFFECT

Even at DC, the geometry of a conductor determines the overall electrical resistance. The equation for the resistance of a material formed in a particular shape is:

$$R_{DC} = \frac{l}{\sigma * cross - section Area} \text{ Ohms/per unit length} \quad (1.1)$$

Applying this equation to a wire, where l is the total length of the wire, the area is πr^2 and, sigma, σ , is the material conductivity. If the radius of the wire is reduced, the resistance increases.

The geometry factor becomes more complicated as frequency increases. At microwave frequencies, 0.3GHz – 300GHz, the skin effect causes the signal, within the conductor, to concentrate at the conductor extremities and therefore becomes sensitive to the conductor topography at these extremities.

Skin effect is caused by alternating currents inducing magnetic fields internal to the conductor. The internal magnetic field is in addition to the magnetic fields between the signal and ground plane conductors; these fields will be discussed later in this thesis. These internal magnetic fields, shown in Fig 1.1 as H , create induced current loops within the conductor, shown in Fig. 1.1 as I_w . The current loops I_w produce their own magnetic fields, which oppose the initial magnetic fields; this effectively pushes the current carrying electrons toward the surface of the conductor. The skin effect becomes more pronounced as the frequency increases.

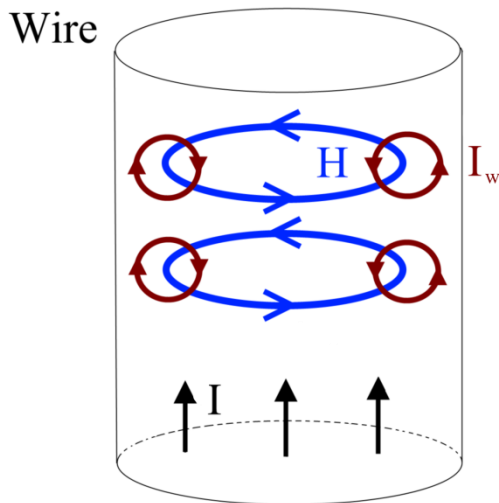


Fig. 1.1 Metal wire with AC signal at GHz frequencies showing current I, induced internal magnetic fields, H and current loops, I_w.

The equation for skin depth, δ , is given below, eq. 1.2. The skin effect depends on frequency, f , and material conductivity, σ .

$$\delta = \frac{1}{\sqrt{\pi\mu_0 f \sigma}} \text{ S/m} \quad (1.2)$$

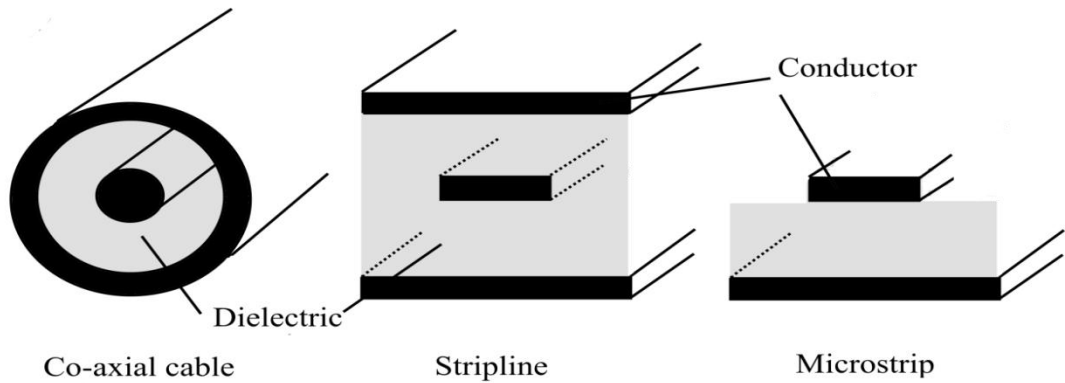
At frequencies greater than 10GHz, with materials of high conductivity such as silver or copper, the skin depth is in the order of a micron. At this scale, the shape of the conductor material at the conductor extremities influences the flow of the signal.

There are many different structures that can be used to transmit microwave frequency signals. These include: coaxial cable, stripline, microstrip, twisted pair, finline, slotline, double-ridged waveguide and circular waveguide. The cheapest and most common structure is microstrip, and it is the structure that has been used for this study. Three common transmission structures, including microstrip are shown in Fig. 1.2.

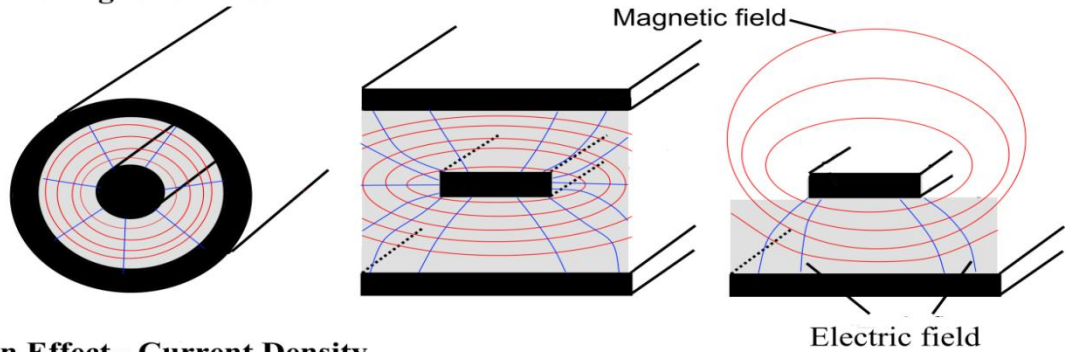
Three common transmission structures: Coaxial cable, Stripline and Microstrip are shown by Fig. 1.2. These structure have different geometries and therefore, different loss results. Coaxial cable is a wire, surrounded by a dielectric material, which can be air, surrounded by another conductor that is the groundplane. The signal is the potential difference between the groundplane and the wire. The wire is also known as the centerconductor. At frequencies in the GHz region the skin effect draws the current to the extremities of the centerconductor but since the centerconductor is a cylinder, the current density is evenly distributed around the circumference. The stripline structure is a layered structure, with the groundplane on both sides of the centerconductor. The dielectric layer, of ceramic material, separates each groundplane from the centerconductor. The stripline centerconductor has a rectangular cross-section that causes the field, and therefore current density, distribution to be higher at the edges and

sides. The microstrip structure has a single groundplane and single layer of dielectric material that separates the groundplane from the centerconductor. This geometry causes the fields and current densities to be concentrated on the underside and lower edges of the centerconductor.

Transmission Structures



Electromagnetic Fields



Skin Effect - Current Density

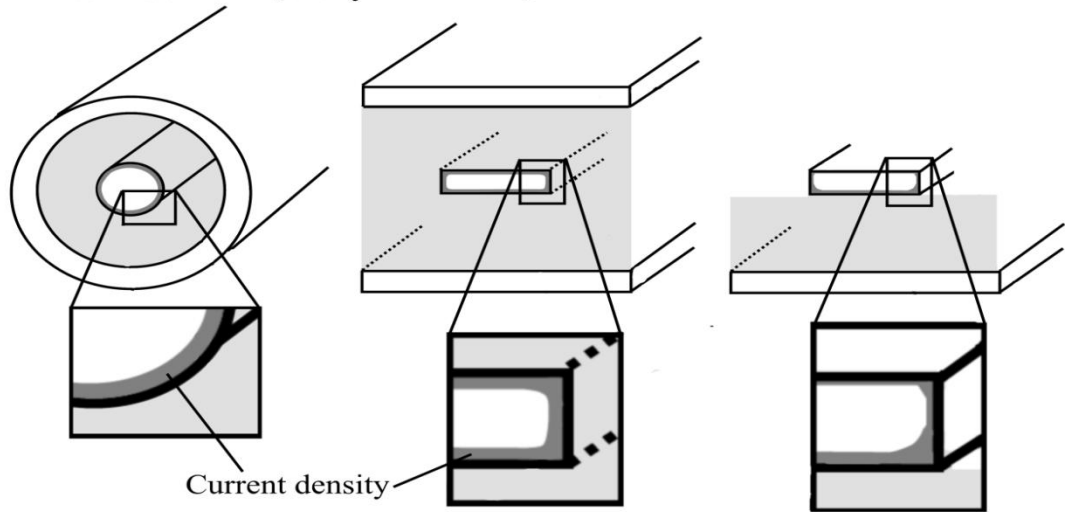


Fig. 1.2, An illustration of three transmission structures common for signals in the GHz frequency range, the distribution of the electric and magnetic fields, and the corresponding current density. The circuit structures are shown for comparison and are assumed to have similar conductivities, dielectric constants and operating at similar frequencies at similar scale.

A microstrip is supported by a dielectric layer so that most of the field is confined between the groundplane and the centerconductor, as shown in Fig 1.3 on the right hand side. This circuit structure is often called a printed circuit board (PCB) and can be made in several ways: thick-film, thin film or by laminated copper foils.

The distributed magnetic and electric fields change as a function of frequency, which changes the current density distribution as a function of frequency. At DC and low frequencies, the current density and resistance are evenly distributed across the conductor cross-section geometry, represented by eq. 1.1. As the frequency increases the current distribution starts to change due to the changing electric and magnetic fields. It is seen from Fig 1.2 that the current density concentrates at the edges and this effect is often assumed to happen at a medium frequency; in the order of 1-5 skin depths of the thickness of the conductor. The medium frequencies are also known as the transition frequency range. At high frequencies, where the conductor thickness is greater than five skin depths, the current density is assumed to be concentrated at the conductor surface of a skin depth, represented by eq. 1.2.

The resistance of the conductor, for a microstrip circuit, at frequencies in the high frequency or skin frequency region has been represented by:

$$R_{skin} = 0.3178 \left(\frac{1}{h_s} + \frac{1}{\omega_{eq0}} \cdot \left[1 + \frac{1.25}{\pi} \cdot \ln \left(\frac{2h_s}{t} \right) \right] \right) \sqrt{\frac{\pi f \mu_o}{\kappa}} \left(\frac{32 - \left(\frac{\omega_{eq0}}{h_s} \right)^2}{32 + \left(\frac{\omega_{eq0}}{h_s} \right)^2} \right) \quad (1.3)$$

Where t is the thickness of the conductor, h_s is the height of the substrate.

$$\text{With } \omega_{eq0} = \omega + \frac{t}{\pi} \cdot \ln \left\{ 1 + \frac{4 \cdot \exp\left(\frac{t}{h}\right)}{\frac{t}{h} \cdot \cot h^2 \left(\sqrt{6.517 \cdot \frac{\omega}{h_s}} \right)} \right\} \quad (1.4)$$

The resistance at GHz frequencies given by eq. 1.3 is far more complicated than the resistance at DC represented by eq. 1.1. The R_{skin} depends on the size of conductor parameters such as t and h_s , however, these parameters give a simplified representation of the cross sectional geometry of the conductor.

1.4 PROBLEM STATEMENT - CONDUCTOR TOPOGRAPHY INFLUENCE ON CONDUCTOR LOSS FOR A MICROSTRIP STRUCTURE

Thin and thick film fabrication can produce various cross section shapes that will influence the conductor loss result. For the screen printing process, the conductor paste shape is influenced by the ceramic substrate surface. The conductor starts in a viscous form and is pushed through a mesh screen, onto the ceramic substrate. The part is then fired, at approximately 850°C, and nominally square silver alloy conductor line is formed. There are several topographic components, of this silver alloy line, that contribute to conductor loss. The topographic or geometric components examined in this study include conductor-ceramic interface and the conductor strip edge. The focus of this work has been on isolating and measuring the impact of the conductor edge topography and conductor-ceramic interfaces as a function of frequencies for frequencies ranging from kHz to 20 GHz.

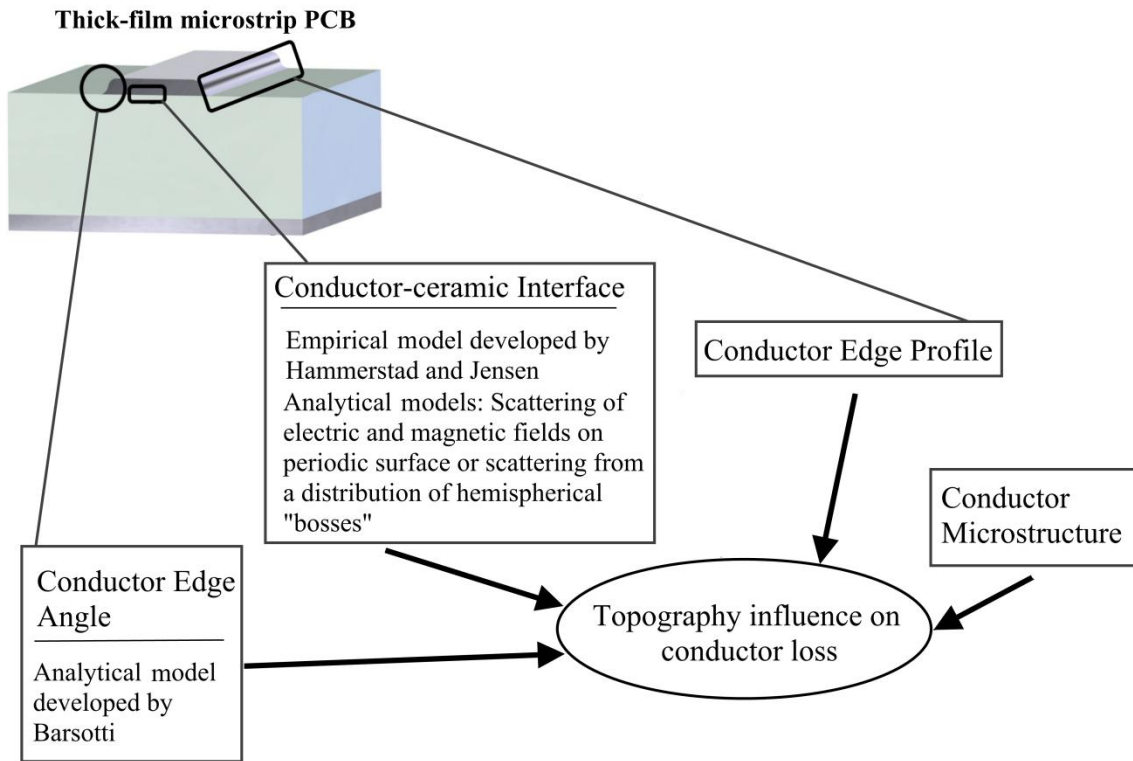


Fig. 1.3, an illustration noting the three conductor geometries that are thought to influence conductor loss.

Different mathematical models have been developed to predict the influence of certain geometries on conductor loss. An empirical model was developed by Hammerstad [5] to predict the increase in conductor loss, α_c due to surface roughness. The average surface roughness parameter, R_a was used to curve fit the increase in loss, eq. 1.5.

$$\alpha_c = \alpha_{smooth} \left\{ 1 + \frac{2}{\pi} \arctan \left(1.4 \left(\frac{R_a}{\delta_s} \right)^2 \right) \right\} \quad (1.5)$$

The empirical model uses familiar and conventional surface roughness parameterization that is often readily available but perhaps not the most suitable fit for this physical phenomenon. R_a is insensitive to the spatial distribution of the surface heights; two very high peaks will contribute the same

value whether the peaks are close to each other or separated over the measurement field, it also averages the absolute value without representing any anisotropic characteristic of the surface. Ra does not directly relate the surface roughness profile to the electrical path length at a particular frequency or scale. Additionally, the empirical method only considers the conductor-dielectric interface geometry influence. Comparisons between this model and actual data are presented later in this thesis.

Several analytical methods have been developed to predict the conductor-ceramic interface topography on conductor loss. Most of these methods represent the surface as either a periodic or Euclidean structure, such as a flat plane with hemispherical bosses. However, surfaces do not follow periodic or geometric rules. Most of these studies attempt to prove a mathematical model by comparing it to other mathematical models.

There has been one primary analytical method used to predict the conductor edge angle feature that has been developed and compared to experimental data. It is not known if this method reliably predicts conductor loss for angles less than 20° . In general there has been little research in this area, especially when compared to the amount of research on the conductor-ceramic feature.

Numerical methods require the problem region to be discretized, by meshing, and approximate solutions found at mesh nodes. However, it is difficult to mesh geometries with small scale detail and arbitrary shapes. The commercial solvers, which use numerical techniques, either do not address small scale geometry, such as surface roughness, or account for the additional conductor loss by including the Hammerstad empirical method within the software, Table 1.

1.5 RESEARCH OBJECTIVE

It is well known that conductor loss is the largest loss factor for microelectronic circuits operating in the GHz frequency range, but it is poorly understood and is not reliably predicted with current empirical, analytic, and numerical tools. There is little published measured data for conductor loss and the features that influence this loss. It is well known that surface roughness can have an adverse influence on conductor loss, and similarly, other geometric factors, such as conductor edge, also influence loss. However, these loss components have never been calculated or measured at the same time. There is little published data for surface roughness influence on conductor loss.

The objective of this research is to investigate the impact, by experimentation, of the conductor feature effects on conductor loss, specifically with respect to thick-film fabrication. The impact is observed and measured over a range of frequencies and skin depths. The surfaces of the ceramic substrates are altered by using different surface finishing techniques and the substrate surface roughness is characterized using conventional and length-scale fractal analysis. The differentiation of ceramic surfaces due to the different processing techniques is determined. The influence of the conductor features: conductor-ceramic interface and conductor-edge angle are quantified and tested against the conductor loss results. The conductor loss is tested over a frequency range from kHz frequencies, which will be similar to conductor loss at DC, to the skin frequencies, where there are at least five skin depths per conductor thickness.

1.6 PUBLICATIONS AND PRESENTATIONS

This work has been presented at various seminars and conferences, published in conference proceeding and submitted to journals. A summary of the significant publications and presentations is given below. The Journal publications can be found in Chapter III and IV, and some of the proceedings in Appendices A and B.

Journals

- T. Vincent, I. Bar-On, and B. Powers "The Influence of Electronic Substrate Surface Roughness on Radio-frequency Transmission Loss Utilizing Conventional and Length-scale Fractal Analysis" *Wear* (submitted April 2009)
- T. Vincent, I. Bar-On and Y. Itovich "Quantitative Conductor Edge Angle Influence on GHz Frequency Electrical Loss" *Transactions on Components and Packaging* (submitted February 2008)

Proceedings/Presentations

- T. Vincent and I. Bar-On, "Conductor Edge Definition Influence on High Frequency Electrical Loss," *Proceedings and Presentation, MS&T 2008, Pittsburg, Pennsylvania, October 5-9th, 2008.*
- T. Vincent and I. Bar-On, "Topography Influence of Ceramic Substrates on High Frequency Electrical Loss for Microelectronics Applications," *Conference Proceedings and Poster presentation hot topics, ICC, 2nd International Congress on Ceramics, Verona, Italy, 29th June – 4th July 2008.*
- T. Vincent, C.A. Brown, and I. Bar-On, "PCB Topographic Influence on GHz Frequency Loss," *Conference Presentation iMAPS New England Conference, MA. USA, May 6th 2008.*

- T. Vincent, I. Bar-On, C. A. Brown, Worcester Polytechnic, USA. Presented “Surface Roughness Influence on Insertion Loss with use of Length-scale Fractal Analysis at Radio-frequencies within Low Temperature Co-fired Ceramics (LTCC)” MS & T 2007, Detroit, Michigan, Sept. 16-20, 2007.
- T. Vincent, I. Bar-On, C. A. Brown "Examination of Surface Roughness Effect on Insertion loss at Microwave Frequencies within LTCC Structures" Conference Proceedings and Presentation iMAPS/ACerS 3rd International Conference and Exhibition on Ceramic Interconnect and Ceramic Microsystems Technologies (CICMT), April 23-26, 2007, Denver, Colorado USA, pp 138-144.

1.7 THESIS ORGANIZATION

The core of this thesis is divided into six chapters. This chapter, Chapter I, is an introduction that gives an overview of microelectronics and conductor loss. Chapter I also describes the problem statement, the research objectives and the thesis organization. Chapter II is a thorough review of the relevant literature from several subject areas necessary to cover this PhD study. Chapter III contains a paper that has been submitted to the journal *Wear* titled "The Influence of Substrate Surface Roughness on Electronic Telecommunication Transmission Loss Using Conventional Analyses and Length-scale Fractal Analysis" by T. Vincent, I. Bar-On, and B. Powers. Chapter IV contains a paper that has been submitted to the journal *IEEE Transactions on Components and Microwave Packaging* titled "Quantitative Cross-sectional Angle Impact on Conductor Loss". Chapter V offers suggestions for further work within this expansive area. Chapter VI provides the conclusions based on this research.

2.0 CHAPTER II

This dissertation includes two papers each with a referenced literature review section in chapters III and IV. The literature review for this study includes several areas of research and is brought together in this Chapter, Chapter 2, for clarity and thoroughness.

2.1 LITERATURE REVIEW

2.1.1 Conductor loss and Skin effect

The skin effect is the description given to the phenomenon where electromagnetic fields, and therefore the current density, decay rapidly with depth inside a good conductor. That is, the electric current tends to flow at the “skin” of the conductor. The skin effect causes the effective resistance to increase with the frequency of the alternating current as described in the introduction.

Maxwell [6] noticed that the resistance in a wire increased with frequency in 1873; he postulated that this could be caused by a departure from uniform current density. The concentration of current density at the surface of a conductor was first described in a paper by Lamb in 1883 [7], for the case of spherical conductors, and was generalized to conductors of any shape by Heaviside in 1885 [8]. Lord Rayleigh [9] gave the formula for skin effect in 1886 for the case of an infinitely wide strip. Hertz (1889) [10] and Thompson (1893) [11] discussed the subject from the experimental and mathematical viewpoint. Swinburne used the term “skin effect” in 1891. An extensive experimental study using a range of metals, sizes and cross-sectional forms was made by Kennelly (1915) [12], this is a common reference for skin effect in the literature. Kennelly measured the skin effect in materials to 5GHz.

The skin effect describes how the current density is concentrated at the conductor extremities. The depth of the current density from the surface of the conductor, where the current density magnitude is one;

to the internal of the conductor, where the current density magnitude has fallen to $1/e$; is described as the “depth of penetration” or “skin depth”. The skin depth is used to gauge the geometrical influences on the conductor loss.

If the thickness of a conductor is much greater than the skin depth, its behavior toward high-frequency alternating currents becomes a surface phenomenon rather than a volume phenomenon, Wheeler [13]. The transition between the volume and surface phenomena is complex; an analytical method of this transition was put forward by Djordević [14].

The analytical methods of Purcel [15], derived from Wheeler’s incremental inductance method are used to calculate conductor loss for microstrip applications. The attenuation for any lumped or distributed circuit is known if its inductance as a function of the geometrical conductor parameters can be calculated. However, the geometric parameters used for these calculations are simply the width, height and thickness of the conductor strip. Additionally, since the Purcel method uses an equivalent circuit representation – an inductor – the model is limited by the ability of an inductor to represent the loss phenomenon.

2.2.1 Conductor topography influence on conductor loss for a microstrip structure: Conductor - ceramic Interface topography

The interaction between electromagnetic waves and a rough surface was first analyzed by Rayleigh [17]. Rayleigh scattering is the scattering of an electromagnetic wave by particles much smaller than the electrical signal wavelength. In terms of plane wave travelling parallel to a surface; Rayleigh looked at the reflection and refraction of the wave, where the surface is periodic/corrugated (1945). He found that a deep corrugation, with high incidence angle, had the same effect as a shallow corrugation with a small incidence angle. Rayleigh’s approach has been developed and extended by other researchers.

It was recognized in 1948 that electrical loss of a copper wire at GHz frequencies had a relationship with the surface finish of the copper wire. Morgan [18] integrated Maxwell’s equations over periodic

surface shapes, such as rectangular and triangular grooves, transverse to the direction of induced current flow. The calculated loss increased by 60% when the dimensions of the surface scratches were comparable to the average skin depth. These classic papers looked at the problem from a theoretical standpoint only, with the surface set as a periodic structure. From this work a technique called the Rayleigh-Rice perturbation method was developed, again only valid for surfaces with small to moderate slopes. Sanderson [19] used the Rayleigh-Rice technique to compare calculated loss with experimental data; the results from this study had mixed correlation. The experiments were carried out on surfaces of high and relatively low conductivity materials: turned brass and steel and the surfaces of these samples were made periodic.

Another approach, not limited to surfaces with small slopes, is based on calculating the multiple scattered fields from a large number of small protuberances. Biot [20] and Wait [21] investigated how an electromagnetic wave would be scattered by a surface represented by hemispheric bosses.

Holloway and Kuester [22] looked at the specific problem of a planar conductor layer with a dielectric layer interface, essentially the Microstrip structure. They theoretically applied a thin cover layer to the rough surface in order to develop an equivalent boundary condition that can interpret electric and magnetic field densities. The result is an equivalent boundary condition that calculates the average electric and magnetic fields at an average smooth surface. The Holloway and Kuester model uses a periodic dielectric-conductor interface.

The microstructure of copper foils has been examined and a model formulated by Huray [23]; these foils are used for laminate PCB boards such as FR4. Huray examined the power lost due to a distribution of copper spheres or “snowballs” mimicking the material structure of electrodeposition on copper foils. The electrodeposition process purposely roughens the conductor surface to increase the adhesion between the conductor and insulator materials. The printed and fired thick film traces used for microelectronics have different microstructure compared to laminate copper foils. The fired thick-film pastes do not form spherical or ball like structures. The Huray/Hall analytical model for copper foils describes the surface as

flat with a distribution of hemispheres; the model is valid for scales where the skin depth is less than the peak surface height. Ceramic substrate surfaces used for microelectronics applications have a different surface structure.

For the last decade a group at the University of Washington [24, 25] has been simulating the surface roughness effect with various methods where the surface roughness is represented by probability distribution functions. The surface distribution function is inserted into analytical and numerical methods and the calculations compared.

The empirical equation generated by Hammerstad [5], derived from Morgan's work [18], is still in wide use. It calculates surface roughness effect on transmission loss as a function of average roughness and skin depth. It has not been found to determine this loss over a wide frequency range [4]. The transmission loss does not appear to follow a square root of frequency relationship [27, 28]. These studies altered the Hammerstad equation to curve fit the data. These papers, which include experiments, have focused on laminate printed circuit board (PCB) topography.

2.2.2 Conductor Topography: Conductor Edge Angle

By contrast to the ceramic-conductor interface roughness, the conductor edge inclination topography influence on conductor loss has had little research focus, especially in the last decade. Most conductor loss research has focused on the mathematical modeling of the conductor-ceramic interface roughness. Since the thick-film process can produce a wide variation of edge topographies it is of particular interest to study this topography effect within this material process system.

Most mathematical methods of calculating conductor loss ignore edge effects since they work on the premise that the conductor is infinitely thin [29]. The strip thickness of a microstrip circuit is much smaller than the width and this does not change the field except at the edges. The edge research to date has focused on analytical calculation techniques [30].

The increase in conductor loss due to the edge is caused by an increase in current density. It is thought that this occurs at frequencies between kHz and the skin frequencies [31] (when thickness is greater than five skin depth). It has been shown theoretically that the edge loss is increased further if the edge corner gets sharper [32]. Meixnier's paper focused on edge effects in waveguide structure. Waveguides are hollow metal pipes, either cylindrical or rectangular, and are much more expensive structures to make than microstrip, structures. Waveguides tend to be used for applications with high power or frequencies above 15GHz. Chryssomallis [33] used an analytical method to look at the difference of current density in rectangular and circular cross-section edges in a microstrip circuit.

A comprehensive mathematical study of conductor edge losses is given in an MS Thesis by Barsotti [34] to derive a conductor loss calculation process for CAD. As an extension to this thesis, a method used to mathematically model the edge inclination is given by Barsotti [35] using conductor loss calculations from the Lewin/Vainshein method [36, 37], who found the method independently, to equate the edge shape to a trapezoid. Barsotti uses trapezoids of 30°, 40° and 60° degree inclinations and it is seen that as the angle decreases the loss increases.

It has been noted that thick-film fabrication creates sharp edges and hypothesized that changing the shape would improve conductor loss [38]. The cross-sectional shapes of LTCC substrates are qualitatively observed and the electric fields simulated using Ansoft.

3.0 CHAPTER III

The Influence of Substrate Surface Roughness on Electronic Telecommunication Transmission Loss Using Conventional Analyses and Length-scale Fractal Analysis

Synopsis

The objective of this paper is to investigate the influence, by experimentation, of the conductor topography effects on conductor loss, for circuits made by thick-film fabrication. The impact is gauged over a range of conductor conductivities, frequencies and skin depths. The ceramic substrate has a range of surface roughnesses made by using different surface finishing techniques. The substrate surface roughness is characterized using conventional and length-scale fractal analysis. The distinct differentiation of ceramic surfaces due to the different processing techniques is determined. The influence of the conductor geometries, conductor-ceramic interface and conductor-edge angle, are tested against the conductor loss results. The conductor loss is tested over a frequency range from kHz frequencies, which will be similar to conductor loss at DC, to the skin frequencies, where there are at least five skin depths per conductor thickness.

Abstract— Two components of conductor topography can impact conductor loss for signals in the GHz frequency range: conductor-ceramic interface roughness and conductor edge angle. This study is an experimental investigation of the influence of these conductor topographies on conductor loss in microstrip circuits produced by thick-film technology. The aluminum nitride ceramic substrates have different surface roughnesses due to different surface finish processes. The substrate surfaces were characterized using conventional and length-scale fractal analysis. The conductor-ceramic interface was measured with a contact profilometer. The conductor edge angle and conductor edge profile were measured optically. It was found that there is a direct correlation between conductor loss and conductor edge angle, while there is an inverse correlation between loss and substrate roughness or relative length of the conductor-ceramic interface. There is also a negative correlation between conductor edge angle and surface roughness or relative length. The loss behavior can be explained by the interaction of the conductor paste with the surfaces during processing. The paste tends to spread more on the smoother surfaces and, thus creates an elongated edge of diminishing cross section and a small edge angle. This leads to greater conductor loss.

INTRODUCTION

Avoiding transmission loss is a significant design driver within the telecommunications field. It is undesirable for a signal to have high conductor loss, and therefore suffer from signal attenuation, since the signal then requires expensive amplification. For digital systems, with increasing bit/sec and pulse rise times in the pico second range, frequency dependant loss results in signal distortion and delay in interconnect applications; this leads to increased error rates [1, 2]. It is difficult to mitigate electromagnetic losses unless the mechanisms and impact of the loss components are fully understood.

The majority of prior work has focused on building mathematical models; there is a lack of published measured data, especially for microstrip topology and none has been found for microstrip made by thick-film fabrication. It was observed in 1948 that electrical loss of a copper wire at GHz frequencies would depend on the surface treatments to which the copper had been subjected [3]. Loss increased when the dimensions of the surface scratches were comparable to the average skin depth. Most classic papers looked at the problem from a theoretical standpoint with the surface set as a periodic structure [4, 5].

Experiments with mixed results were carried out on surfaces of high and relatively low conductivity materials: turned brass and steel, where the surfaces were made to be periodic. In all prior studies the multi-scale surface is represented by a geometric or periodic structure; however real surfaces do not follow periodic, geometric or stochastic rules. Real surfaces do have fractal properties [6], in that the length of the profiles and the steepness of the slopes on the surface increase, as the scale of observation decrease.

An empirical equation to estimate transmission loss was generated by Hammerstad [7], and is still in wide use. It calculates surface roughness effect on transmission loss as a function of average roughness and skin depth. It has not been found to determine this loss over a wide surface topography or frequency range [8], and transmission loss does not appear to follow a square root of frequency relationship [9, 10]. These respective studies altered the Hammerstad equation to curve fit the data. These papers, which include experiments, have focused on laminate printed circuit board (PCB) topography.

Fractal analysis has a broad range of application that gives a good fit for structures in nature [11]. Fractal electrodynamics is an emerging research area [12]. Scale-sensitive fractal analysis has the benefit of characterizing the surface over a range of scales [13] that could apply to different scales of interaction [14]. Length-scale fractal analysis is based on the principle from fractal geometry that the length of a rough profile depends on the scale of observation.

This study looks at the measurements of radio-frequency transmission loss of microstrip conductive lines with three different lengths, on substrates with four different surface finishes. Three of the substrate surfaces have statistically different surfaces over certain scale ranges using average roughness (Ra) and length-scale fractal analysis [13]. The conductor loss analyzed as a function of average roughness, apparent lengths of the profiles measured on the substrates over a range of scales and as a function of conductor edge angle.

The objective of this study is to develop, and test, an experimental method that considers all of the conductor topographies that influence conductor loss - rather than focusing on a single conductor topography component, that is assumed to be the influencing component.

THEORY

The surface roughness influence on conductor topography, and therefore conductor loss, can be separated into two features of interest: conductor-ceramic interface and conductor edge inclination. The conductor-ceramic interface will cause the electrical signal to travel a longer path following the contour of the ceramic at GHz frequencies; this has been pointed out in previous studies by [5, 15, and 16]. The printed conductor is thinner at the edges of the print; this topography is noted as the conductor edge angle. A large amount of conductor loss occurs at the edges [17] because current density increases at a conductor edge becoming larger as the corner gets sharper [18]. The degree of conductor edge angle can potentially be influenced by several factors; one possible influence is the surface roughness.

The conductor line has two distinct topographies that impact conductor loss: conductor-ceramic interface and conductor edge angle - both of these topographies can be influenced by the substrate surface roughness. The skin effect [19] forces the signal to follow the surface profile more faithfully, as frequency increases. Therefore, for the conductor-ceramic topography, positive correlations should be found between loss and increased surface roughness characterized by the path length. The skin effect also causes the signal to concentrate at the conductor edges. The edge shape is influenced by the substrate surface topography [20], as frequency increases, positive correlations should be found between loss and conductor edge angle and a negative correlation between loss and surface roughness. In this study the surface of the substrates are measured and parameterized using conventional methods and length-scale fractal analysis. Length-scale fractal analysis [13] calculates the path length as a function of scale of calculation. This shows that path, or profile, length tends to increase as the scale of calculation, or observation, decreases, and that the lengths can increase differently with decreasing scale for different surface preparations.

This paper describes an experimental study of transmission loss, specifically conductor loss, using microstrip ceramic substrates with different surface roughnesses. Conductor topography components, conductor edge angle or conductor-ceramic interface, are investigated to see which has a larger impact on

the conductor loss as frequency increases. The electrical samples were made using thick-film technology; a common fabrication method for microelectronics. This allowed the circuits to be fabricated on a substrate with negligible dielectric losses; therefore, the major transmission loss is the conductor loss.

Conductor Loss and the Skin Effect

Conductor loss is caused by power dissipation due to imperfect conductivity of the conductor line, the length of the propagation path, and the area available for current density. A microstrip topology is a thin, flat electrical conductor separated from the electrical ground plane by an insulating layer. Microstrip is a common configuration within the microelectronics industry. At GHz frequencies, this type of circuit has several loss components: reflected loss, dielectric loss and conductor loss. The total loss, in a two port system depicted in Fig. 3.1, is represented as the resultant signal divided by the incident signal, expressed in dB. The transmission loss is the total loss minus the reflected loss; this transmission loss is made up of the conductor loss and the dielectric loss components. For substrates with low dielectric loss at microwave frequencies, the transmission loss is dominated by the conductor loss [21]. The loss results given in this study are transmission losses; since the dielectric loss is so small, the changes in transmission loss are due to changes in conductor loss.

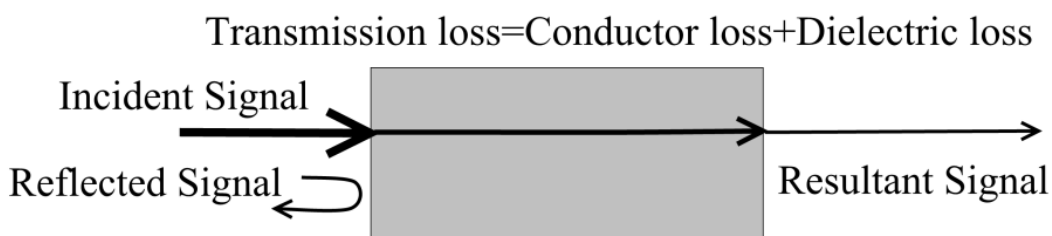


Fig. 3.1: Illustration of losses for microstrip topology at GHz frequencies

Skin effect is essentially, where the current in the propagating signal decays exponentially with the distance from the ceramic-conductor interface into the conductor. The skin effect is a function of operating frequency, f , and conductivity, σ , of the path trace as expressed by eq. 3.1. This is a well-known

phenomenon in microwave engineering and is central to our understanding of why surface roughness influences conductor loss. The material permeability is given by μ . The skin effect equation can be found in many radio-frequency design books [22]

$$\delta_s = \sqrt{\frac{1}{\pi f \sigma \mu}} \quad (3.1)$$

A single skin depth, (δ_s), is defined as the depth at which the current density has decreased to 37% of its surface value or the equivalent thickness of a conductor at frequency having the same resistance as the DC resistance (that uses the whole area of the conductor).

Conventional Surface roughness characterization

Ra and Rt have been frequently used as parameters to characterize the roughness of surface for electrical applications [2].

$$R_a = \frac{1}{N} \sum |z| \quad (3.2)$$

The conventional parameters Ra and Rt do not relate the surface roughness profile to the electrical path length at a particular frequency or scale. They are also insensitive to the spatial distribution of the surface heights. One significant peak could have the same influence on the Ra as two lesser peaks, which will contribute the same value whether the two peaks are close to each other or separated over the measurement field. A valley or a peak of same magnitude will have similar influence on the Ra values.

Skin Effect

A side view of a cross section of a simulated microstrip circuit, including roughness at the conductor-ceramic substrate interface is given in Fig. 3.2. This illustrates the skin effect phenomenon for several discrete frequencies: 100MHz, 1GHz, 10GHz and 30GHz. Note that in this configuration the skin effect forces the current density towards the conductor-ceramic interface rather than an actual free surface. For a frequency of 100MHz the electrical current density is evenly distributed across the full thickness of the conductor: 8 μ m in this example. As the frequency increases the current density concentrates towards the ceramic material; the concentration of this signal is shown by the skin depth. Since the skin effect

forces the current density to the periphery of the conductor, the cross sectional area decreases and the overall current density increases. The current density increase creates more heat and loss per unit length.

The skin depth of the current density is illustrated by a virtual band across the conductor. The band is represented as a darker shade, at each discrete frequency, as the frequency increases; hence it is darkest at 30GHz, shown in Fig. 3.2 and Fig. 3.3. One skin depth is the upper edge of the designated band to the ceramic substrate surface.

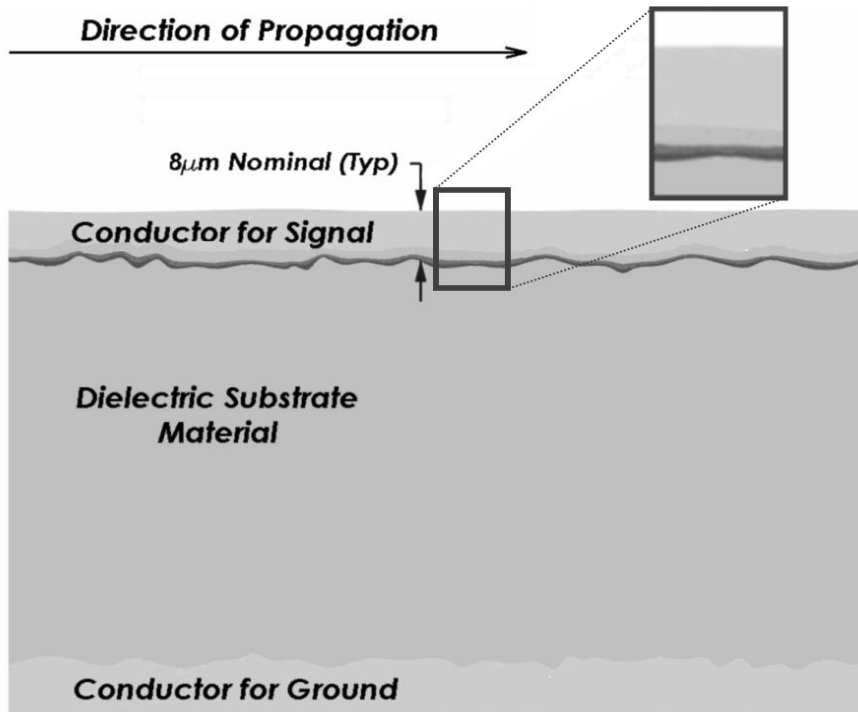


Fig 3.2a, diagram of skin depth phenomena in microstrip topology: thickness of a skin depth given for the bulk conductivity of silver. The illustration profile is approximately to scale for chemically etched surface peak-to-peak roughness.

Each shade represents one skin depth at a given frequency

Frequency	Thickness
100MHz	full conductor
1GHz	2µm
10GHz	0.64µm
30GHz	0.37µm

Fig 3.2b, legend of skin depth phenomena for given frequencies

The surface roughness causes the current to flow along a longer path increasing the conductor loss per unit length. The conductor loss increases at a rate of the square root of frequency due to the conductor area restriction. As the skin depth and surface roughness scales become similar this causes the loss to increase at a higher rate than the square root of frequency. Fig. 3.2 is approximately to scale for a chemically etched surface, this figure shows that, in this case, at frequencies above 10GHz the skin depth is comparable to the conventional parameters: average Ra and peak to peak Rt roughness, so that propagation path should lengthen as the current path begins to follow the rough interface of the ceramic. The conventional equation [7] used to estimate the additional loss caused by surface roughness; the resultant conductor loss, α_c is represented by:

$$\alpha_c = \alpha_{smooth} \left(1 + \frac{2}{\pi} \arctan \left(1.4 \left(\frac{R_a}{\delta_s} \right)^2 \right) \right) \quad (3.3)$$

Hammerstad formulated this equation, eq.3, to calculate the surface roughness contribution of conductor-ceramic interface loss. It was formulated to curve fit empirical data for conductor traces that have a thickness that is at a minimum five skin depths [7]. For a conductor line with a thickness less than one skin depth, the conductor loss depends entirely on the conductivity. When the conductor thickness is five skin depths, or greater, the overriding conductor topography loss component is caused by the skin effect [23]. When the conductor line thickness is between one and five skin depths, there is a transition stage. For the silver alloy, ALN33, specimen used in this study, five skin depths would be at a frequency of 7GHz. At this frequency, the measured transmission loss, versus Hammerstad calculation, are beginning to diverge, as shown in Fig. 3.3. Thus, the very frequency where eq.3.3 is supposed to start being able to calculate the surface roughness effect on conductor loss, it does the opposite.

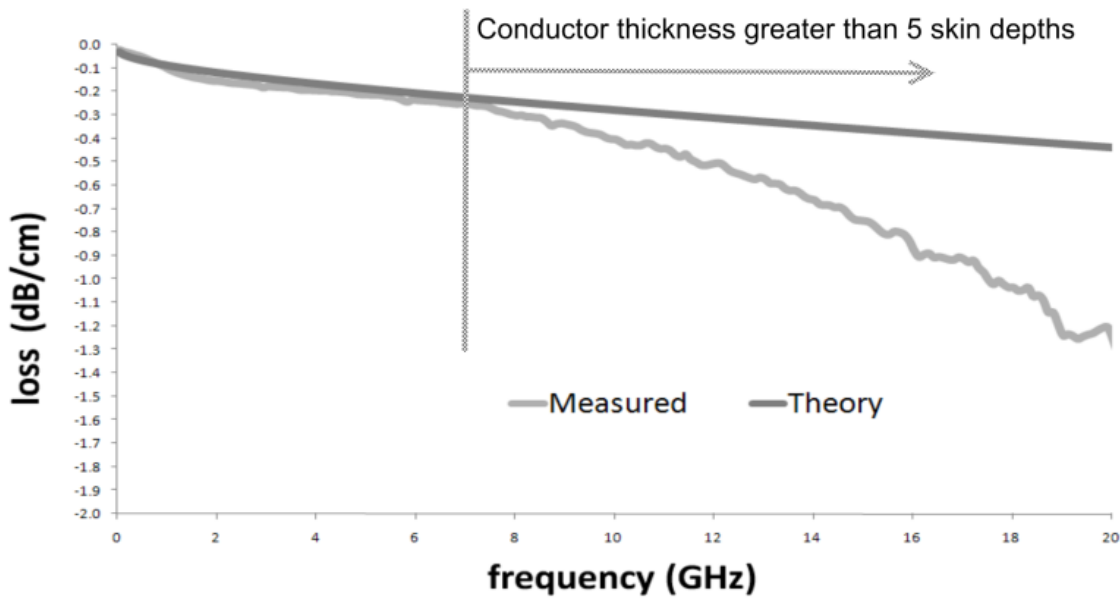


Fig. 3.3: Comparing measured conductor loss from a lapped surface with the theoretical loss derived from eq.3.3.

The skin effect phenomenon has a greater influence at higher frequencies and with conductor lines with higher conductivities. The set of experiments in this study uses a range of surface roughness, conductivities and frequencies.

The current density increases at the conductor edge, shown in Fig. 4 due to fringing fields. The mathematical solution states that current density increases at the conductor edge, becoming larger as the corner gets sharper [18]. Since the samples for this study are made by thick-film printing, the surface roughness influences the conductor edge topography [20] as well as the conductor-ceramic topography. The higher peaks or steeper slopes of the substrate surface impede the lateral movement of the conductor paste creating edges with larger cross-sectional edge angles.

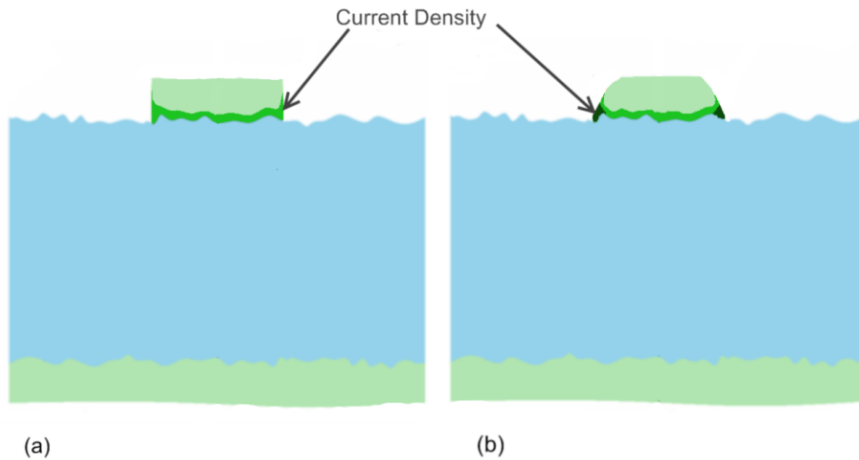


Fig. 3.4: Diagram of skin depth phenomena in microstrip topology, front cross-section view: a, is a given skin depth for a GHz frequency signal with square cross section edges, b, is a given skin depth for a GHz frequency signal with cross section edges at an angle, common for circuits made by thick-film processing.

An illustration of the skin depth current density, influenced by conductor edge topography, is shown in Fig. 3.4a and Fig. 3.4b. Fig. 3.4 is essentially the front view of Fig. 3.2. This figure demonstrates the increase in current density when the conductor edge is at an angle rather than perpendicular, as it is for thick-film circuits.

Characterization of surface roughness by length-scale analysis

Scale-sensitive fractal analysis [13] has been used to statistically discriminate rough surfaces and to find correlations with surface behavior for various applications [24, 14] including optical scattering [25]. Length-scale fractal analysis can be used to statistically discriminate surfaces where Ra measurement cannot [26]. Length-scale fractal analysis calculates the lengths of a profile as a function of scale by virtually stepping along the surface. The smaller the steps the closer the stepping pattern follows the actual surface profile and the longer the calculated profile length, giving a physical interpretation for conductor loss. The relative slope increases as the scale decreases.

The tiling or stepping sequence in length-scale analysis is demonstrated in Fig. 3.5. A series of progressively shorter step sizes is used to calculate the measured length of the profile as a function of scale. The step size is the scale of observation, or calculation. The relative length at a particular scale is the measured length at that scale divided by the nominal, or straight-line, length.

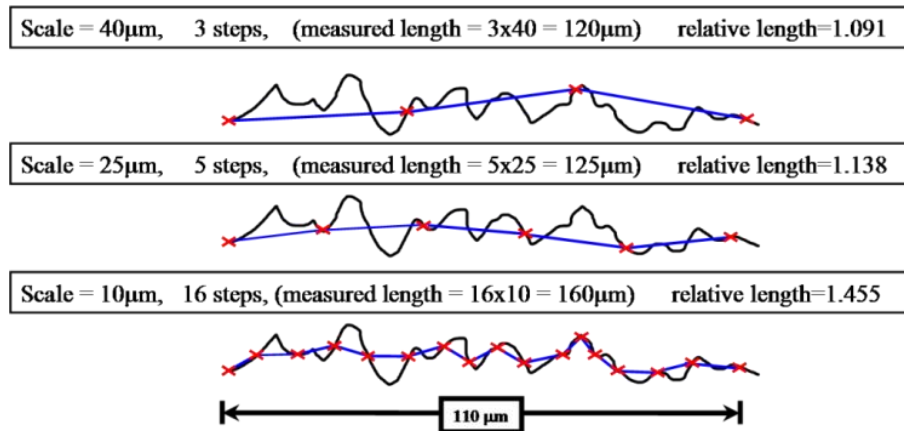


Fig. 3.5: An example length-scale analysis on a cartoon profile, showing the increase in measured length as the scale, or step length decreases. All the nominal lengths are 110µm.

EXPERIMENTAL PROCEDURES

Substrate Production and Profile Measurement

Aluminum nitride (AlN) is commonly used as an electronic substrate for the fabrication of thick film radio-frequency electronic components for high power applications. (Note that ‘AlN’ with a lower case ‘l’ is used to denote aluminum nitride, the ceramic substrate material). Four substrate surface roughnesses were created on AlN substrates using four different surface finish processes as described in Table 3.1. All the surfaces had previously been vapor honed.

Table 3.1: Surface finish processes description with average roughness result.		
Surface Finish Process	Process Descriptions	Ra (μm)
Lapped	Lapped using an oil-based abrasive; cleaned in ultrasonic bath and rinsed with alcohol (ACUMET).	0.184
Vapor Honed	Blasted with 220 grit aluminum oxide and water, then vapor honed for 2.5 minutes with 0.5mil of material removed.	0.559
Sintered	After vapor hone, placed in a furnace for a sintering cycle.	0.546
Chemically Etched	Held in an Anodex solution for 1 hour at 150 °C, then in an HCl solution for 1hour at 150 °C, followed by cold water rinse. This process is repeated twice.	1.091

Six profiles (height z as a function of position x) were measured on each surface finish with a Perthen (Mahr Federal) profiler using an unskidded stylus with a tip radius of $2\mu\text{m}$. The sampling interval was 69nm and the trace length $560\mu\text{m}$. The profiles were Gaussian filtered with wavelength cut off 0.08mm and characterized using arithmetic average roughness (Ra), and length-scale fractal analysis (ASME B46 2002). The measured profiles were analyzed using Map Premium software® (Digital Surf) and Sfrax (www.surfract.com). The mean and standard deviation of Ra values for each surface finish are given in Table 3.1. A total of twenty-four AlN substrates were to make the samples; six substrates were put through each surface finish process, as described in Table 3.1. Two specimens of each substrate finish were printed with each paste.

F-tests using the mean, standard deviation, and degrees of freedom [27] were performed on the roughness characterization parameters to determine the level of confidence in discriminating the substrates from each other based on their measured profiles.

The Conductor Edge Measurements

The conductor edge was measured for the ALN11 and ALN33 samples using an interferometric microscope. Details of the measurement method are given elsewhere [28]. The Interferometer measured an area large enough to include - a section of the ceramic surface to the conductor edge; the surface of the conductor from the conductor edge across the conductor, at an angle to the ceramic, until the surface of the conductor was parallel to the ceramic surface. The ceramic substrate was taken as a reference and an averaged line through the conductor edge, to at least 30% of the maximum conductor thickness was made. The angle between the referenced ceramic substrate and the conductor edge was noted for each surface roughness. For rougher surfaces, the edges are seen to have a larger cross section angle, where the conductor meets the ceramic substrate, shown in Fig. 3.4b. When this conductor edge angle is small, the current density is concentrated in a smaller area increasing the conductor loss. Therefore, as the angle increases, the current density reduces and the conductor loss is also reduced.

The Conductor Line Measurements

Thick-film screen-printing technology was used to make the microstrip circuits for this study. Six substrate plates were printed with microstrip circuits; two were printed with ALN 11 paste, two with ALN 33 and two with ALN 23 (Note that upper case “L”s in “ALN” are used to denote the conductor pastes on the AlN substrates.):

[29] ALN 11© [DuPont 2001] a silver conductor,

[30] ALN 33© [DuPont] a silver/palladium conductor (10:1)

[31] ALN 23© [DuPont] silver/platinum conductor (3:1)

There were two sets of microstrip circuits on each plate. Each microstrip circuit set consisted of three conductor lines of different lengths, the longest being 40 mm; the longest conductor line was used for the loss measurements. Every plate also had a serpentine line, as shown in Fig. 6 middle right. The serpentine line was used to measure bulk conductivity, represented as σ .

The total loss was measured using an Anritsu Vector Network Analyzer with (GGB industries) picoprobes®, to obtain S-parameters (signal parameters). S-parameters are used to describe the electrical behavior of an electrical device when undergoing steady state stimuli by small signals. The losses were measured on both circuits after calibrating with the picoprobe® substrate standard. The first circuit was used for analysis. The measurement of the second circuit was taken as validation of the first measurement. The loss measurements were viewed using SONNET software® and analyzed using Microsoft Excel. The frequency range extended from DC to 20GHz.

Transmission line equations [32] were used to calculate the reflected loss from the mismatch measurement. Reflected loss is caused by a mismatch between the input and output transition and the conductor line. This mismatch was measured for each of the circuits. Reflected losses are design dependant, and, therefore, the reflected loss is subtracted from the total loss to calculate the transmission loss. Three different conductor line lengths, shown in Fig. 3.6, were used to measure and corroborate the transmission losses for each of the lines.

The loss measurement and profile characterizations were compared using regression analyzes at each length-scale at selected frequencies, regressing the loss versus the relative length. The results of this analysis are plotted as the regression coefficient versus scale determined by the length-scale analysis.

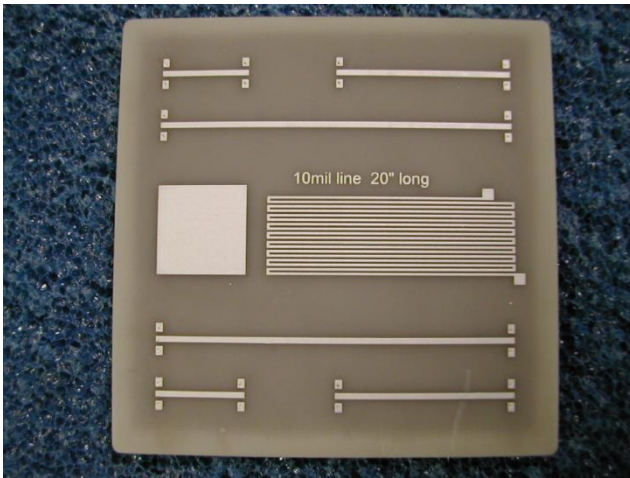


Fig. 3.6: Photograph of an AlN substrate with conductor with two sets of three conductor lines with nominal lengths: 10, 20, and 40mm. The serpentine line is used to measure bulk conductivity.

The conductivities of the three ALN microstrip conductor lines and pure silver are shown in Table 3.2. By using eq. 3.1 the skin depth is calculated for the bulk conductivity and frequency.

Conductor line	Measured DC Bulk Conductivity S/m	Skin Depth μm				
		100MHz	1 GHz	10 GHz	15 GHz	20 GHz
Silver*	6.2×10^7	6.35	2	0.64	0.52	0.45
ALN11	2.2×10^7	10.75	3.4	1.08	0.89	0.76
ALN33	6×10^6	19.56	6.18	1.96	1.6	1.38
ALN23	8×10^5	56.27	17.79	5.63	4.59	3.98

*Pure silver was not tested here, and appears in this table to provide a reference for comparison

RESULTS

Surface Roughness Characterization

Measurements were taken of the chemically etched; vapor honed and lapped substrate surfaces, shown in Fig. 3.7a, 3.7b, 3.7c, with an Olympus, LEXT OLS3100, scanning laser confocal microscope. The substrate surfaces are clearly seen to be different to one another.

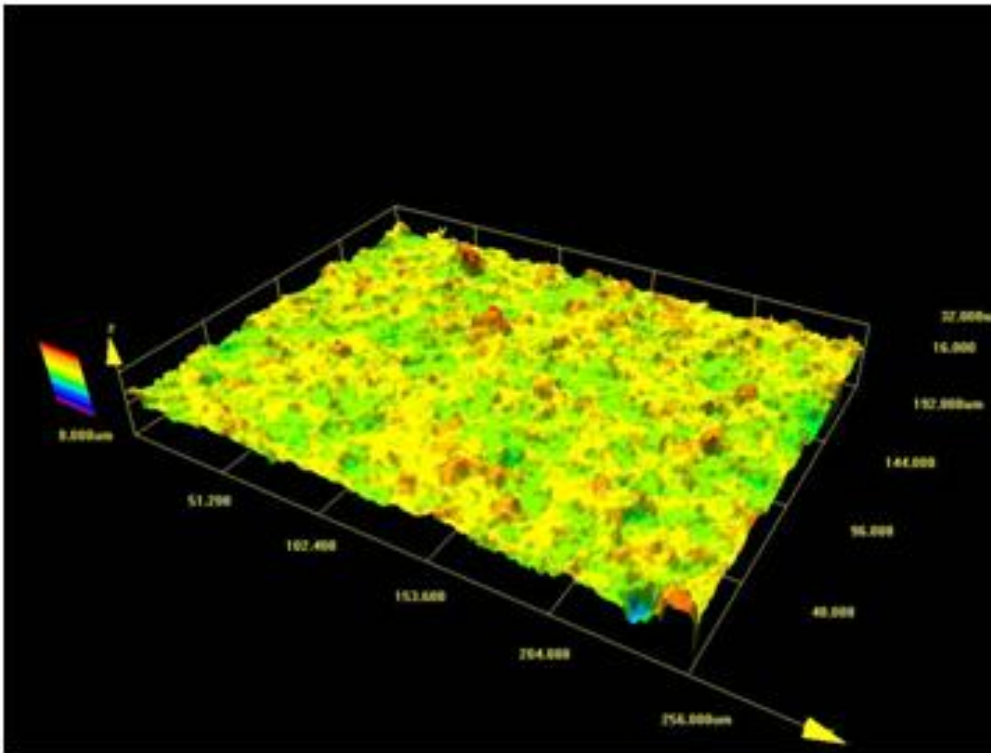


Fig. 3.7a: Height map measurement of chemically etched surface.

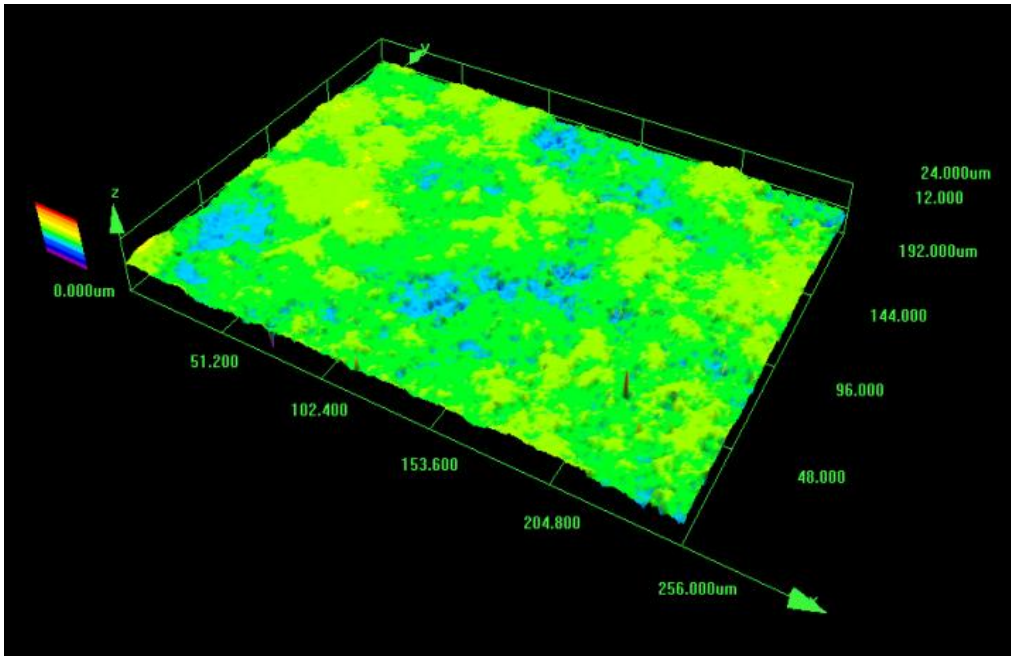


Fig. 3.7b: Height map measurement of honed surface

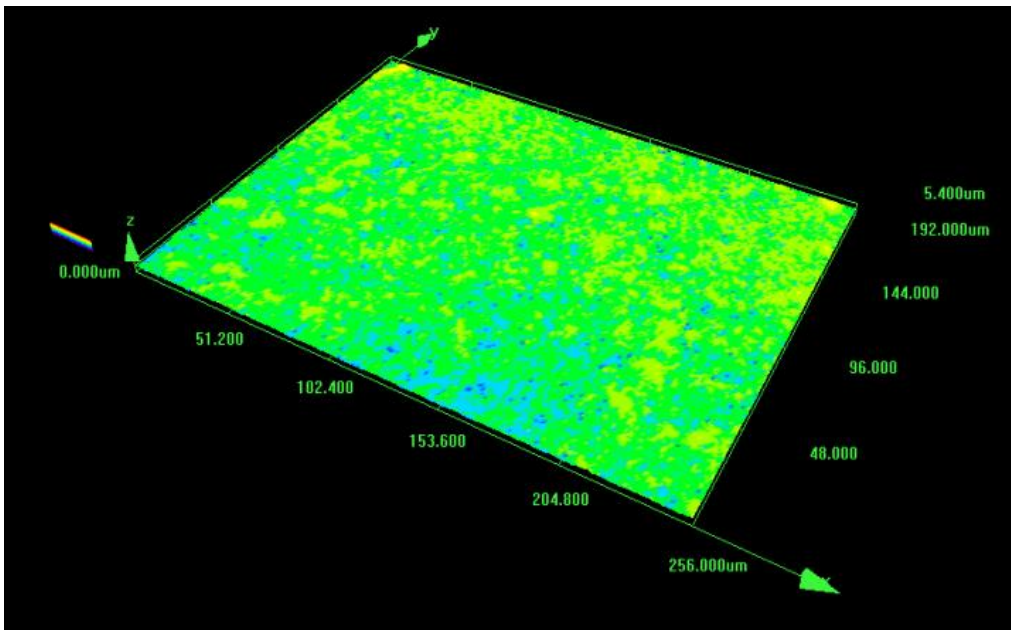


Fig. 3.7c: Height map measurement of lapped surface

The length-scale fractal analysis gives the relative lengths over a range of scales for the profiles measured from each of the substrate surface finishing processes, see Fig. 8. The x-axis represents the scale of calculation of the length, or step size in a virtual tiling exercise. The y-axis represents the relative length (calculated length divided by the nominal length).

Conventional average roughness and peak-to-peak results of surface profiles, from the four different substrate surface finishes, are shown in Table 3.3; with the mean average of six measurements, standard deviation, 95% confidence, and range. Student t-tests were made on all six data set combinations of pairs for Ra. All of the surface comparisons were discernable with zero probability of the null hypothesis except the vapor honed and sintered surface comparison.

Table 3.3: Roughness parameters, Ra and Rt for AlN surfaces with four finishing processes				
Surface Finish Process	Average Ra (μm)	Standard deviation of Ra (μm)	95% confidence interval (μm) of Ra	Rt(μm) range for six measurements
Lapped	0.184	0.027	0.0676 - 0.3020	0.94 – 1.73
Vapor Honed	0.559	0.059	0.4365 - 0.6805	2.85 – 5.23
Sintered	0.546	0.054	0.4249 - 0.6667	3.22 – 4.26
Chemically Etched	1.091	0.180	0.9690- 1.213	6.39 – 8.45

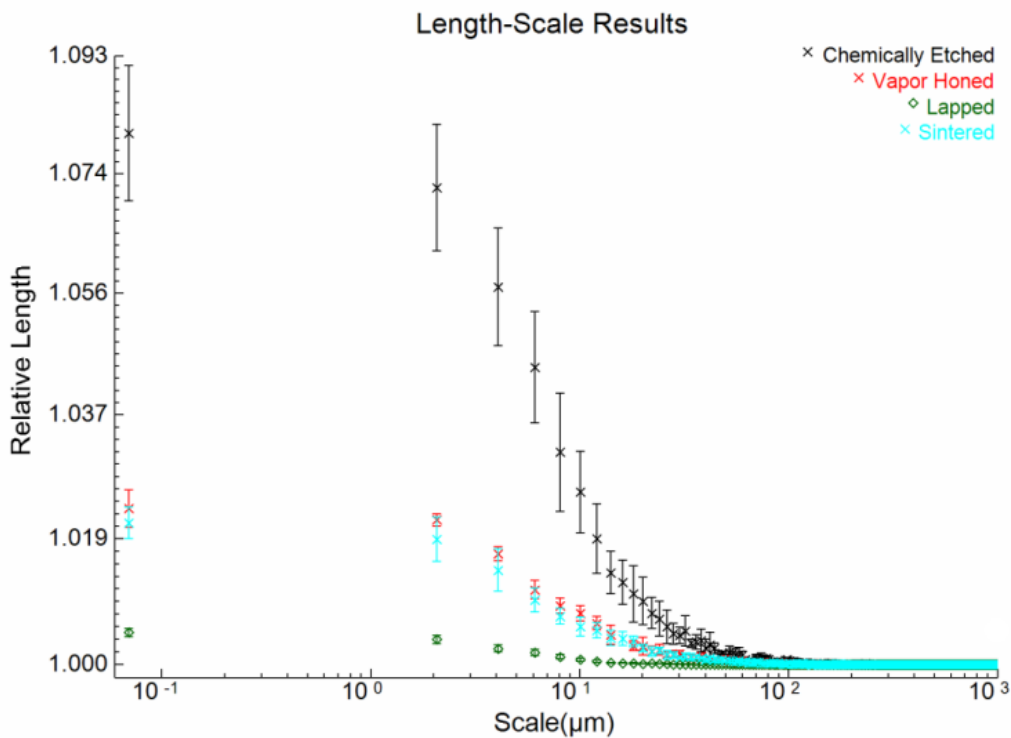


Fig. 3.8: Length-scale plots [ASME B46 2000] for the four surface treatments on the AlN substrates. The error bars represent +/- one standard deviation on the six profile measurement of each surface.

The relative lengths of the profiles measured from all four surface treatments are similar at scales above 100μm. The relative lengths increase rapidly with the decrease in scale between scales about 2μm and 20μm. The chemically etched surface clearly has a longer path length than all the other surfaces at scales below 50μm. The lapped surface clearly has a shorter path length than all the other surfaces at scales below 30μm.

The relative lengths, at all scales below 40μm, rank the roughness of the AlN substrate finishes in the same order as the Ra and the Rt roughness values.

The length-scale roughness characterizations of profiles from the four different substrate surface treatments are shown in Fig. 3.8 with the mean and variation of 6 measurements taken from 6 different areas of the substrate. F-tests [27] were performed on all six measurements. All of the surface comparisons were discernable, i.e., statistically different, for scales less than 60μm except the vapor honed

and sintered surface comparison. F-tests performed on the relative areas at each scale showed that, except for the vapor honed and the lapped surfaces, all the other binary combinations of the four surfaces were statistically different at scales below about $60\mu\text{m}$ with a level of confidence greater than 95%.

Transmission Loss versus Frequency for Four Surfaces

The conductor losses of the four AlN substrate surface finishes made with the highest conductivity line, ALN 11 ($2.19 \times 10^7 \text{S/m}$), are shown in Fig. 3.9. Note that the rank of the losses does not correspond to the average roughnesses (Ra) or to the relative lengths at any scale shown in Fig. 3.8.

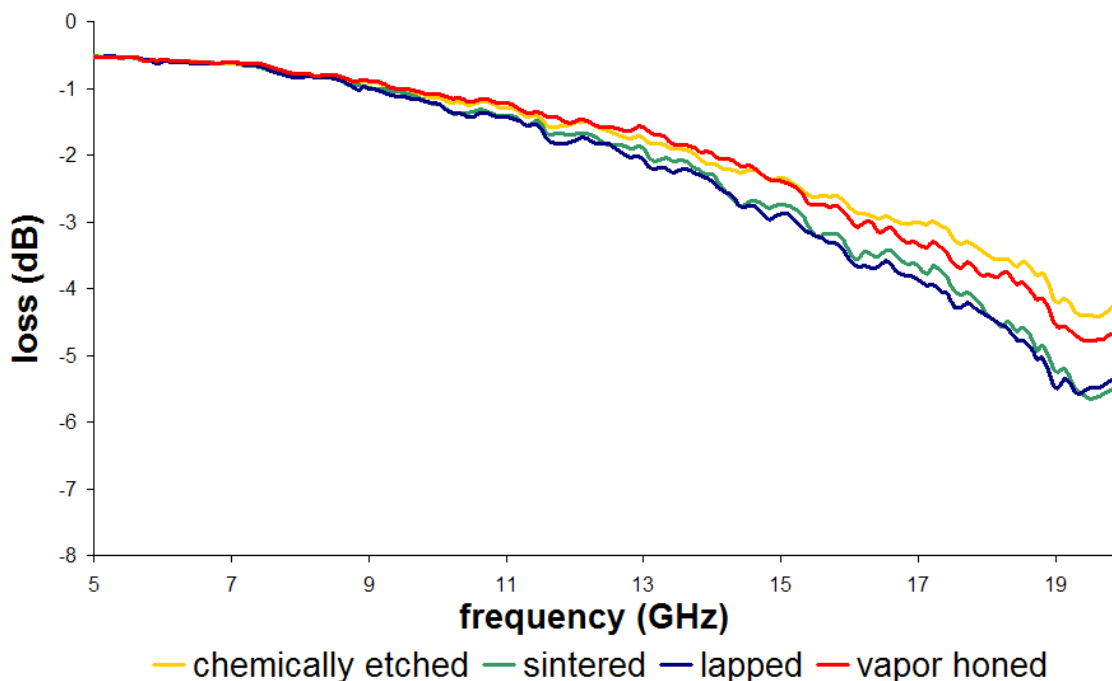


Fig. 3.9: ALN11 conductor losses versus frequency for all four substrates

The conductor losses for the four surfaces made with the intermediate conductivity line, ALN 33 ($6 \times 10^6 \text{S/m}$), are compared in Fig. 3.10. Note that the losses have an inverse rank compared to that by the average roughnesses or to the relative lengths, i.e., the roughest surface has the smallest loss.

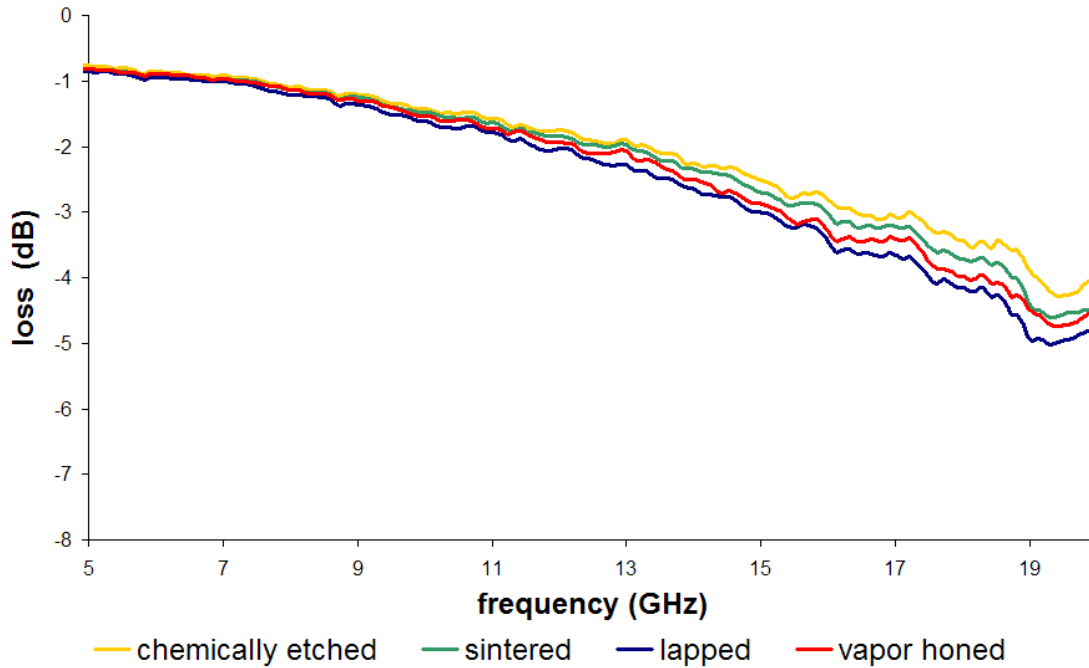


Fig. 3.10: ALN33 conductor losses versus frequency on all four substrates

For both the ALN 11 and ALN 33 lines all the conductor loss results are similar for all four AlN substrate surface finishes over the low frequency range but start to disperse around 9-11 GHz, where the average roughness (Ra) of the AlN substrates and skin depths (Table 3.1) are the same order of magnitude. The conductor lines on the chemically etched AlN substrate (Ra 1.091 μm) have the smallest losses and the conductor lines on the lapped AlN substrates (Ra 0.184 μm) have the greatest transmission loss.

The conductor losses for the ALN 23 line ($8 \times 10^5 \text{S/m}$), which has the lowest conductivity, on all four substrate finishes, is shown in Fig. 3.11. The loss results for the ALN23 are more similar than the loss results for the ALN33 and ALN11. The chemically etched AlN substrate, which has the greatest roughness, provides the greatest losses up to frequencies of approximately 18GHz. Above 20GHz this same surface has the smallest losses. The greatest loss occurs on the lapped AlN substrate, which is the smoothest.

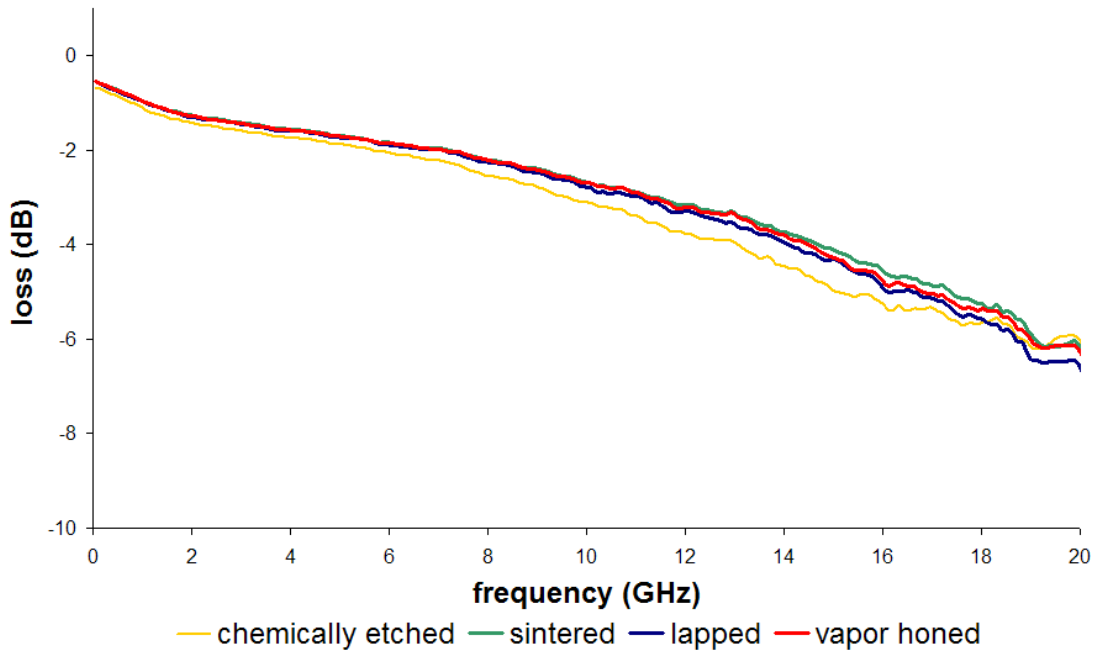


Fig. 3.11: ALN 23 conductor losses versus frequency on all four substrates

Correlation of Loss with Ra

Conductor loss in $-dB$, at four discrete frequencies, as a function of average roughness, R_a , is summarized in Fig. 3.12, for all four surface finishes and for all three conductor conductivities. At the lower frequencies (5GHz and 10 GHz) the loss does not depend on the frequency. At the highest frequency (20 GHz) the correlation between the loss and the roughness is negative: the smoothest surface has the greatest loss, while the roughest surface has the smallest loss. Identical behavior was observed for conductor loss as a function of R_t . For the intermediate frequencies this negative correlation can also be observed for the ALN11 and ALN33 conductor lines. The ALN23 behaves somewhat differently. This is due to the lower conductivity and thus, the larger skin depth for this conductor line.

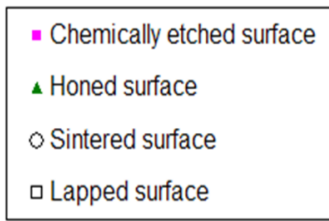


Fig 3.12a: Legend of four surface finishes

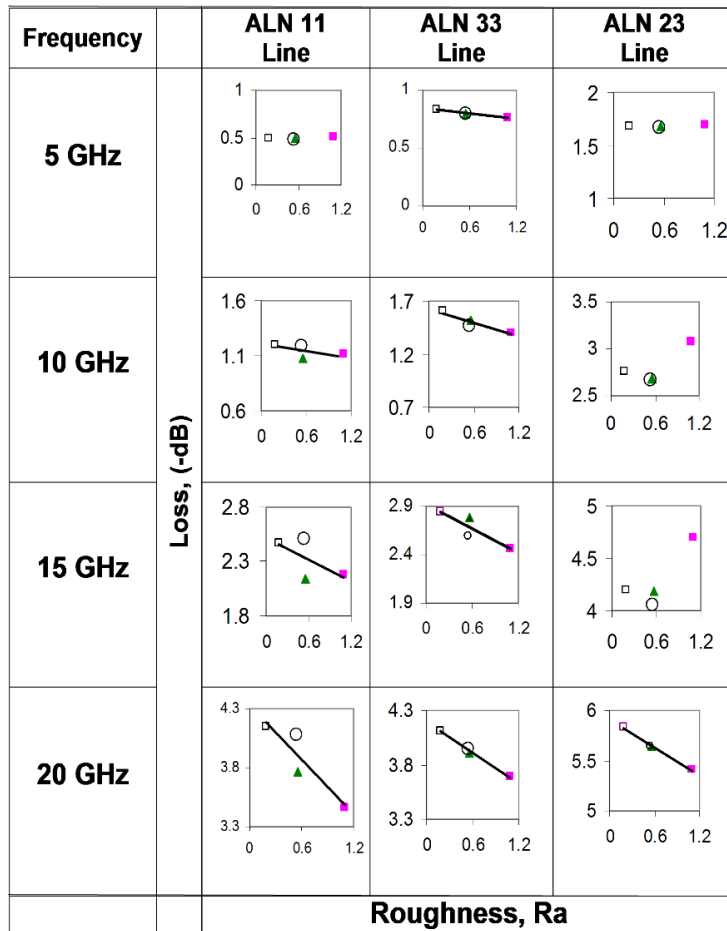


Fig 3.12b: Loss vs average roughness, Ra, or four surface finishes at four discrete frequencies.

Fig. 3.12: Loss vs. Average roughness

Correlation of Loss with Path Length (i.e., Relative Length) at three Scales and Four Discrete Frequencies

Conductor loss vs. relative length plots for discrete frequencies show trends that are similar to those observed for roughness, Ra. Figs. 3.13, 3.14, and 3.15 show conductor loss vs. relative length for ALN11, ALN33, and ALN 23, respectively. These figures show loss vs. relative length at four discrete frequencies

for three different scales of observation. The different symbols indicate the different surface finishes. For the two better conductors, ALN11 and ALN33, and the lower frequencies, 5 and 10 GHz, the loss values are very similar - for all surface finishes. For 15 and 20 GHz the loss results differ for the different surface finishes; the lapped surfaces exhibit the largest losses followed by the sintered, honed, and the chemically etched surfaces. This is the case for all scales of observation: as the scale of observation decreases the differentiation by length-scale between the different surfaces increases.

For the ALN23 line the behavior is similar with the exception that at 10 and 15 GHz the chemically etched surface, the surface with the greatest relative length, has the greatest loss amongst the four different surfaces, shown in , Fig. 3.15.

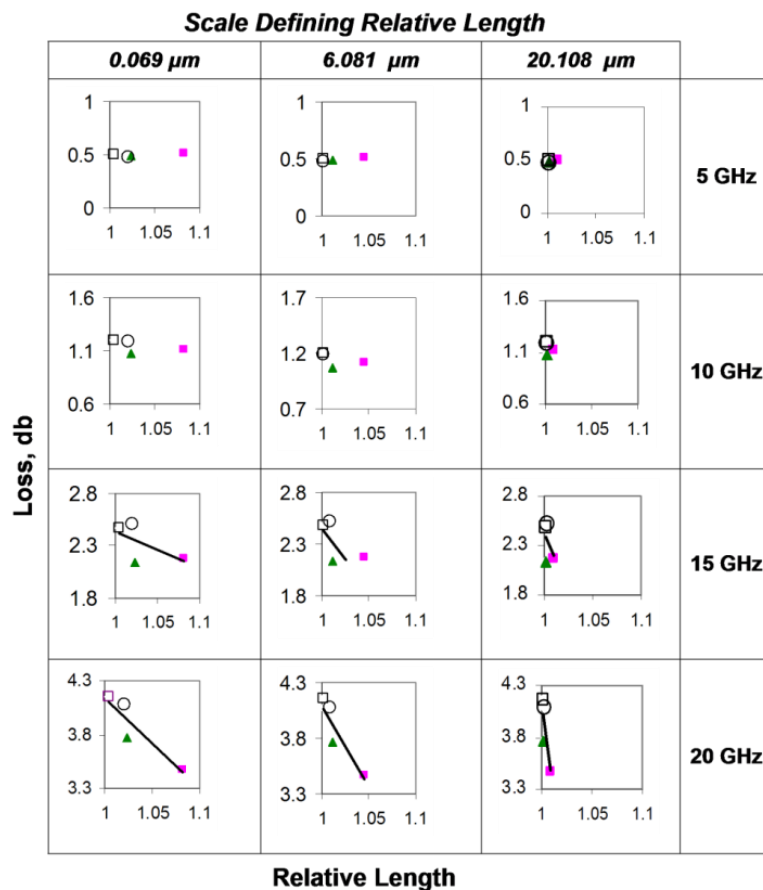


Fig. 3.13: Loss vs. relative length at four different frequencies and at three scales of observation for the four different surfaces finishes using conductor line ALN11.

Scale Defining Relative Length

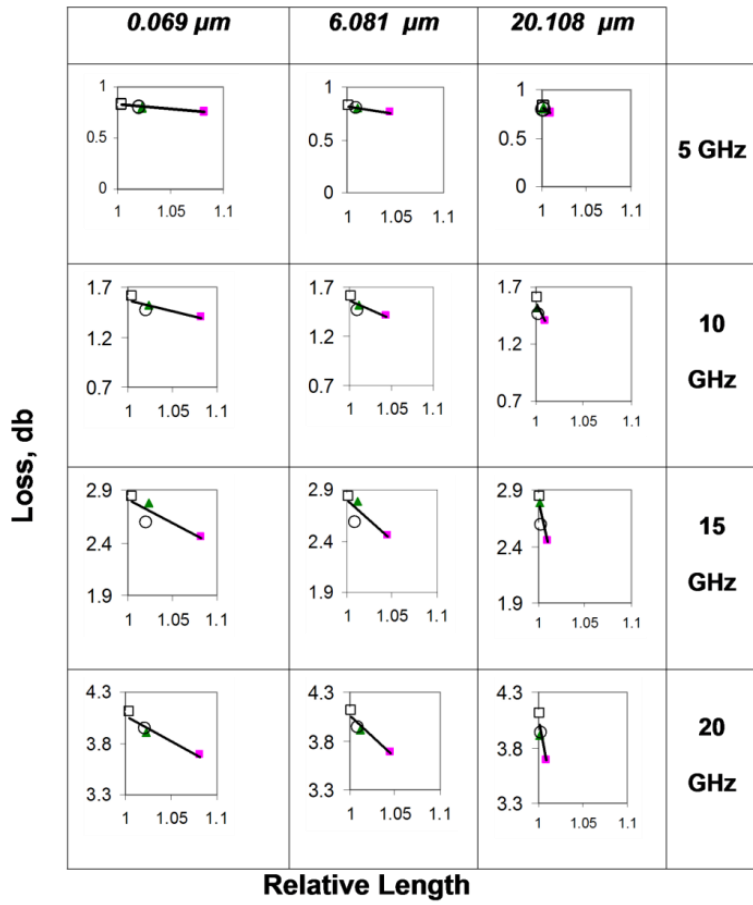


Fig. 3.14: Loss vs. relative length at four different frequencies and at three scales of observation for the four different surface finishes using conductor line ALN33.

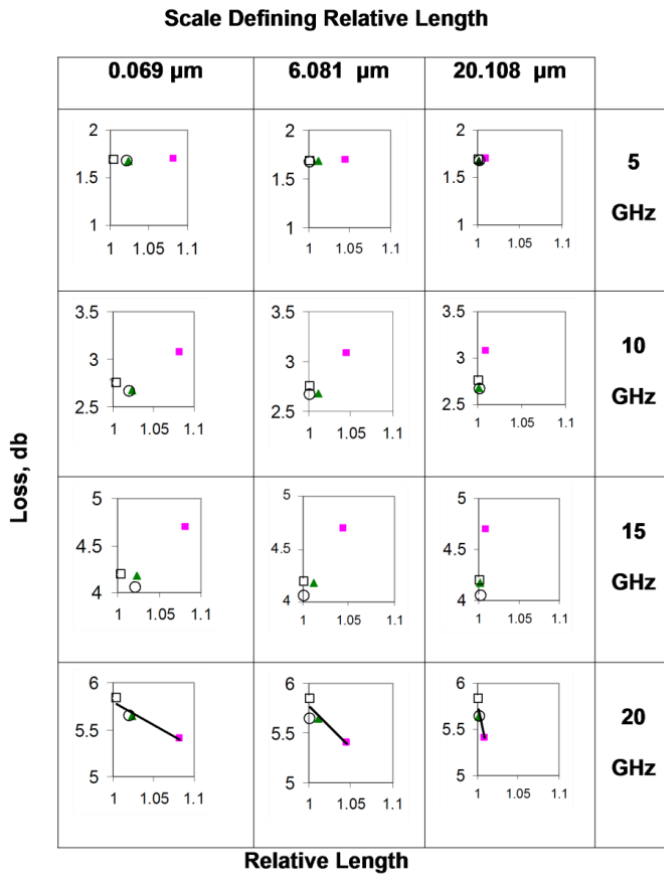


Fig. 3.15: Loss vs. relative length at four different frequencies and at three scales of observation for the four different surfaces finishes using conductor line ALN23.

Correlation of Loss with Conductor Edge Angle

Conductor edge angle in degrees, measured at different Length-scale, is summarized in Fig. 3.16 for two of the conductor lines, ALN11 and ALN33. For both conductors there is a positive correlation between conductor edge angle, and length scale, becoming more pronounced as the scale decreases. The same relationship is seen between conductor edge angle and average surface roughness. This suggests that the angle is influenced by the substrate surface roughness, the rougher surface measured by relative length at the appropriate scale, causing a greater contact angle [34]. In turn, the conductor angle in degrees, as a function of conductor loss for the different discrete frequencies, is summarized in Fig. 3.17 for two of the

conductor lines, ALN11 and ALN33. As the frequency increases a correlation between the conductor edge angle and loss appears and is distinct at 20GHz.

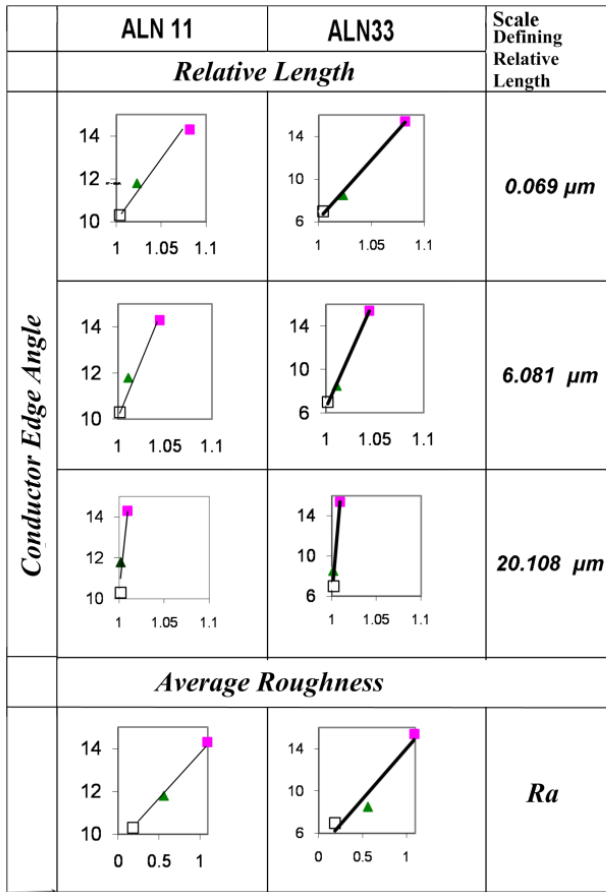


Fig. 3.16: Conductor edge angle vs. relative length at three scales of observation for the three differentiable surfaces finishes using conductor lines ALN11 and ALN33.

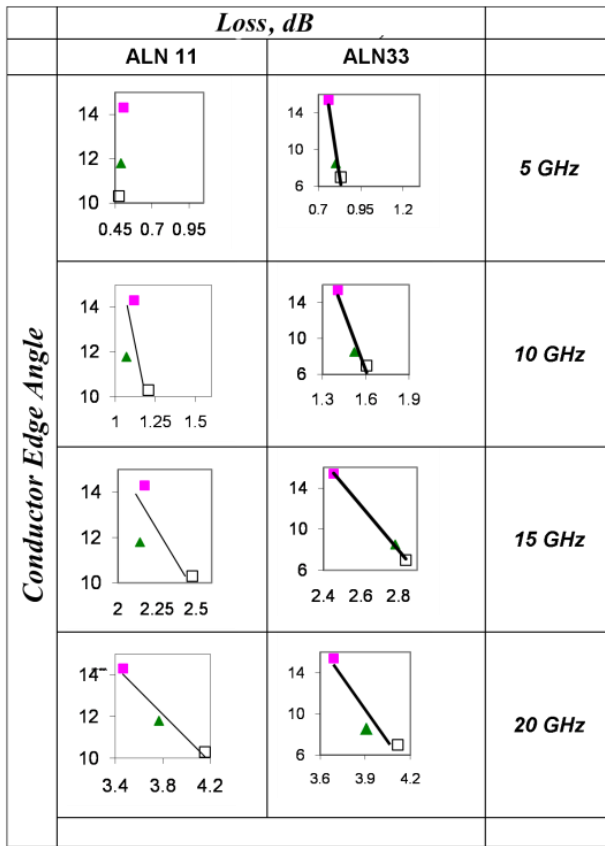


Fig. 3.17: Transmission Loss vs. edge angle at four different frequencies and for the three differentiable surfaces finishes using conductor lines ALN11 and ALN33.

DISCUSSION

The correlation between relative lengths and conductor edge angle becomes stronger as the scale of observation decreases, as shown in Fig. 3.18. The correlation coefficient R is plotted vs. scale of observation for a number of scales and for two conductors, for conductor edge angle measured. The correlation coefficients are determined from the graph in Fig. 3.16.

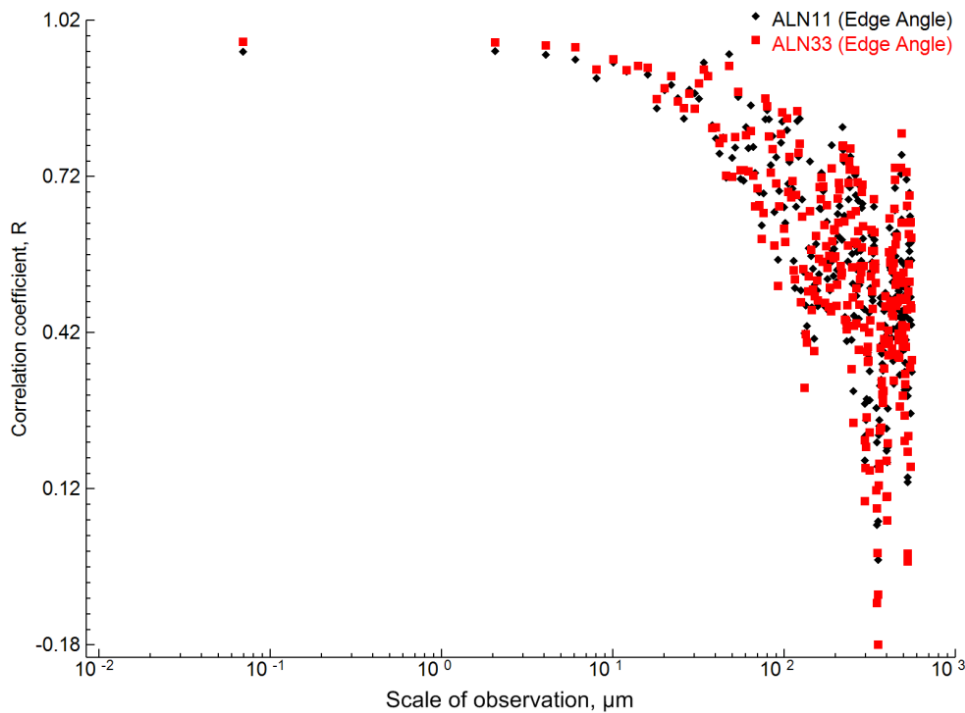


Fig. 3.18: Correlation coefficients, R , versus scales of observation for two different conductor lines. Correlation coefficients were determined from measured edge angle vs. relative length graphs at different scales of observation

The conductor edge angle, influenced by the surface roughness, has the dominant conductor topography impact on conductor loss, Fig. 3.18. The rougher surface, with larger slopes and peaks, created a larger conductor edge angle, Fig. 3.16; the contact angle was formed when the conductive paste settled during thick-film fabrication [20]. The larger angle evens the current density at the edges and lowers the loss [18]. Therefore, a larger edge angle lowers the loss, Fig. 3.18, and the larger edge angle is caused by greater surface roughness, Fig. 3.16.

From the literature [34] the dominant conductor topography component, influenced by the surface roughness, has been assumed to be the conductor-ceramic interface roughness but this paper shows that this assumption is not always true.

For all of the conductivities, Figs. 3.13-3.16, there is a strong correlation between conductor loss and surface roughness, R_a , or relative length for the 20 GHz case, however, the correlation is negative. That is, the smoother surfaces exhibit greater loss. This result shows that the loss rank is not due to

conductor-ceramic interface roughness - which would mean a longer path for the signal to travel, and thus greater loss. For the relative lengths the inverse correlation becomes more consistent and stronger as the scale of observation decreases as shown in Fig. 3.19. Here the correlation coefficient R is plotted vs. scale of observation for a number of scales and for the three conductors, all for 20GHz, where the skin effect is strongest. The correlation coefficients are determined from graphs like those shown in Figs. 3.13 – 3.15. Fig. 3.19 leads to two conclusions: as the scale of observation decreases, relative length increasingly becomes a better parameter for characterizing the surface, and, as the scale of observation decreases, the negative correlation between loss and relative length is stronger and more consistent. This shows that loss is related to surface characteristics, but it is not the increased path length that leads directly to increased loss at higher frequencies.

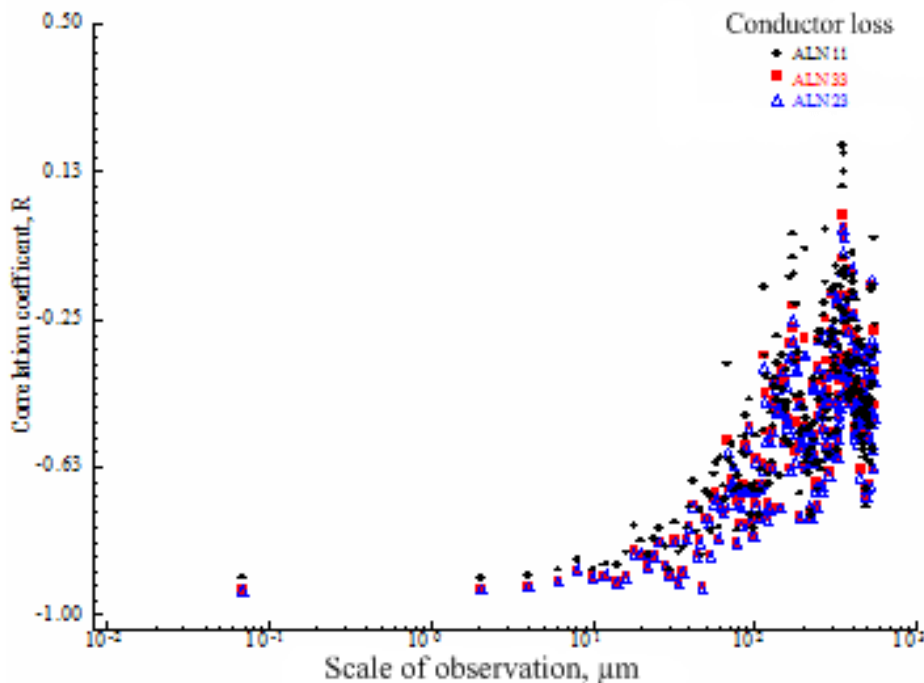


Fig. 3.19: Correlation coefficient, R , versus scale of observation for the three different conductor lines. Correlation coefficients were determined from loss vs. relative length graphs at different scales of observation

Another conductor topography that could potentially influence the loss is the conductor edge profile - in the direction of signal propagation (or the x-axis edge characteristic of the conductor). The conductor topographies correlated with loss in this study were the conductor-ceramic interface and the conductor edge angle (or the z-axis angle of the conductor at the edges of the silver conductor line).

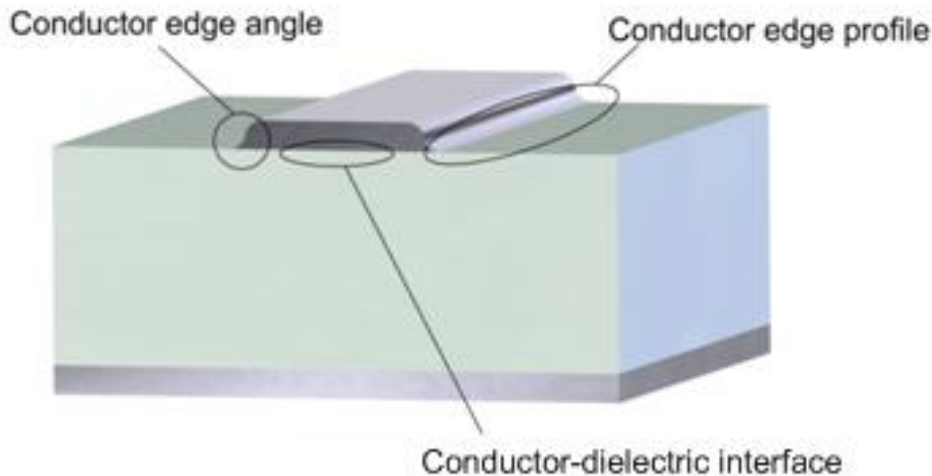


Fig. 3.20: Cartoon of microstrip circuit with the different topographies shown: conductor edge angle, conductor-ceramic interface and conductor edge profile.

From the micrograph in Fig. 3.21 (a) this edge profile is seen to be ragged. The conductor edge profiles were analyzed using a Kevex Energy Dispersive X-ray. The mapping of the Ag creates an image where the silver conductor edge profile is seen distinctly, Fig. 3.21 (b). Five of these edge profiles for each of the surface roughnesses for the ALN 11 and ALN 33 conductors were mapped and image manipulation used to isolate the edge profile as seen by Fig. 3.21 (c). A software program was written to measure the lengths of the edge profile image, for each of the surface roughness samples, but no discernable difference was seen between the lengths of the profile for different surfaces. This suggests that the x-axis edge profile characteristic is not responsible for the changes in loss seen between the different surface roughness samples.

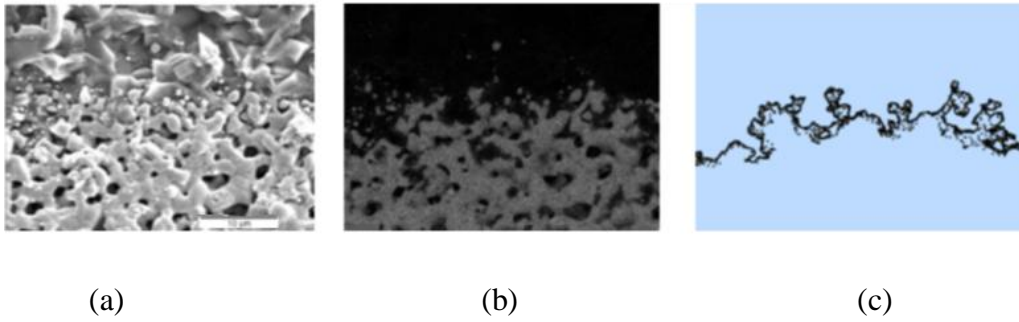


Fig. 3.21: a, is a micrograph of the ALN33 silver conductor on Honed AlN substrate after firing, b, is the Ag mapped image of the same area, c, is the edge of the silver isolated by image manipulation.

The three surface characterization methods used here, peak-to-valley roughness, R_t , arithmetic average roughness, R_a and the relative lengths as a function of scale, provide the same ranking of the surfaces with respect to the different treatments, and show similar abilities to discriminate. Apparently, for these surfaces, R_a and the relative length at the finer scales are highly correlated. Therefore, it should be expected that the two kinds of characterization parameters would provide similar correlations with the loss. The ability of different roughness characterization parameters to correlate with each other is dependent on the particular set of surfaces that are considered [35]. It cannot be expected that R_a and relative-length would both find similar correlations with loss on a different set of surfaces. In this application relative-length would appear to be a functional parameter as it seems to provide clear physical interpretations for conductor loss based on its assessment of path length and for inclinations on the surface.

Both conventional and length-scale methods of characterization clearly discriminate three of the four prepared surfaces as shown in Fig. 3.8 and Table 3.3. For the length-scale measurements the discrimination depends on the scale of observation, and is more distinct as the scale of observation is finer.

The conductor loss relationship to surface roughness depends on the conductor conductivity and the operating frequency. For frequencies below 10 GHz, conductor loss is not influenced by surface roughness, as characterized by R_a , R_t , or by relative-length. For frequencies of 20 GHz, conductor loss is distinctly dependent on surface roughness, as characterized by R_a , R_t , or relative-length for all three conductor lines. At 15 GHz the conductor loss is influenced by surface roughness for the higher

conductivity metal trace and does not depend on it for the lower conductivity conductor line. Conductor loss is greater for lower conductivity materials and at higher frequencies, albeit not following the prediction based on the Hammersted equation, eq. 3.3, Fig. 3.3. The ALN 23 conductor does not have the same loss rank as ALN 11 and ALN 33 until frequencies greater than 15 GHz; at frequency less than 15 GHz the skin effect is not present.

CONCLUSIONS:

- Microstrip configurations were produced on three clearly discernible surfaces of AlN substrates with conductors of low, medium and high conductivity.
- The substrate surfaces were characterized and ranked using conventional arithmetic average roughness, Ra, peak to valley roughness, Rt, and relative lengths as calculated from scale sensitive length-scale fractal analysis, giving the same ranking of surface treatments.
- Conductor loss was measured for frequencies ranging from DC to 20 GHz.
- At 20 GHz the loss shows an inverse correlation with roughness, Ra, and with relative lengths as calculated by length-scale fractal analysis, for low, medium and high conductivity conductor lines.
- These observations do not support the claim that greater conductor loss, at higher frequencies, is a direct result of increased path length at the ceramic-conductor interface. Rather that there is a strong negative correlation of conductor loss to surface roughness, shown by the length-scale relative length results.
- These observations indicate that the greater conductor loss, at higher frequencies, is a direct result of cross-section conductor edge angle. The edge inclination is shown to be formed by the surface roughness; the angle is larger for rougher surfaces.

- The dependence of loss on the surface roughness characteristics, for the different conductors, changes as a function of frequency.

ACKNOWLEDGEMENTS

The authors would like to thank Mahr Federal (Providence, RI, USA) for the donation of the Perthin SPK, Surftract for the use of Sfrax for length-scale profile analysis and scale based correlation testing, Digital Surface (Besançon, France) for the conventional profile analyses, Olympus for the use of the confocal microscope, Dr Brown in the Surface Metrology lab, at WPI, for his help and expertise. Barry Industries (Attleboro, MA, USA) for providing the AlN samples. The support of the Lady Davis foundation for Professor Bar-On's Lady Davis fellowship during part of this work is gratefully acknowledged.

REFERENCES

- [1] L. Proekt and A. C. Cangellaris, Investigation of Conductor Surface Roughness on Interconnect Frequency-Dependant Ohmic Loss, Electronic Components and Technology Conference, 2003, p. 1004.
- [2] M. Bayes, A. Horn, Effects of Conductor Surface Condition on Signal Integrity, Circuit World 2004 pp11-16.
- [3] S. P. Morgan, Effects of Surface Roughness on Eddy Current Losses at Microwave Frequencies, J. Appl. Phy., vol. 20, Apr. 1949, p. 352.
- [4] M. A. Biot, Some new Aspects of the Reflection of Electromagnetic Waves on a Rough Surface, J. Appl. Phys., vol. 28, no. 12, Dec. 1957, pp.1455-1463.
- [5] A. E. Sanderson, Effect of Surface Roughness on Propagation of the TEM mode, Advances in Microwaves. New York: Academic, 1971, vol. 7, p. 1.
- [6] L. DeChiffre, P. Lonardo, H. Trumphold, D.A Lucca, G. Goch, C.A. Brown, J. Raja, H.N. Hansen, Quantitative Characterization of Surface Texture, Annals of the CIRP, 49/2 (2000) 635-652.

- [7] E. Hammerstad, Ø. Jensen, Accurate Models for Microstrip Computer Aided Design, IEEE MTT-S May 1980 pp407-409.
- [8] T. S. Vincent, I Bar-On and C.A. Brown, Examination of Surface Roughness Effect on Insertion loss at Microwave Frequencies using Conventional Surface Roughness Parameters within LTCC Structures, ICIMT IMAPS/ACerS April 2007 proceedings p. 138.
- [9] G. Brist, S. Hall, Non-Classical Conductor Losses due to Copper Foil Roughness and Treatment, ECWC 10 Conference at IPC 05.
- [10] S. Hall, S. Tao Liang Heck, H. Shykind, Modeling requirements for transmission lines in multi-gigabit systems, D. Electrical Performance of Electronic Packaging. IEEE 13th Topical Meeting, 2004 p. 67-70.
- [11] B. B. Mandelbrot, The Fractal Geometry of Nature, Freeman, San Francisco, 1977.
- [12] G. Franceschetti, D. Riccio, Scattering, Natural Surfaces and Fractals, Academic Press 2007.
- [13] ASME B46.1, Surface Texture (Surface Roughness Waviness and Lay), an American National Standard, ch 10, American Society of Mechanical Engineers, New York, 2002.
- [14] C.A. Brown and S. Siegmann, Fundamental scales of adhesion and area-scale fractal analysis, International Journal of Machine Tools and Manufacture, 41 (2001) 1927-1933.
- [15] K. Kalyanasudaram and P. Nagy, A Simple Numerical Model of the Apparent Loss of Eddy Current Conductivity due to Surface Roughness, NDT&E International 37 (2004) p. 47.
- [16] S. Hall, S. G. Pytel, P. G. Huray, D. Hua, A. Moonshiram, G. A. Brist, and E. Sijercic, Multigigahertz Causal Transmission Line Modeling Methodology Using a 3-D Hemispherical Surface Roughness Approach, IEEE Transactions on Microwave Theory and Techniques, vol. 55, no. 12, December 2007 p. 2614-2624.
- [17] E. L. Barsotti, Effect of Strip Edge Shape on Microstrip Conductor Loss, MS Thesis University of Colorado 1990.
- [18] J. Meixner, The Behavior of Electromagnetic Fields at Edges, Inst. Math. Sci. Res. Rept. EM-72, New York University, New York, NY, 1954.

- [19] A. E. Kennelly, F. A. Laws, and P. H. Pierce, Experimental researches on skin effect in conductors, Trans. AIEE, vol. 34, pp. 1953-2018, 1915
- [20] T. Vincent and I. Bar-On, Conductor Edge Definition Influence on High Frequency Electrical Loss, Proceedings, MS&T 2008, Pittsburg, Pennsylvania, October 5-9th, 2008.
- [21] B. Young, T. Itoh, Loss Reduction in Superconductor Microstrip – like Transmission Line, Microwave Symposium Digest, May 1988, IEEE MTT-S.
- [22] W. H. Hayt, Engineering Electromagnetics, (4th Edition McGraw-Hill 1981) p. 398-413.
- [23] A. R. Djordjević and T. K. Sarkar, Closed-Form Formulas for Frequency Dependent Resistance and Inductance per Unit Length of Microstrip and strip Transmission Lines, IEEE MTT-S February 1994 p. 241.
- [24] P. Narayan, BC. Hancock, R. Hamel, T.S. Bergstrom, B.E. Childs and C.A. Brown, Differentiation of the Surface Topographies of Pharmaceutical excipient compacts, Materials Science & Engineering A 430 (2006) p. 79.
- [25] E. M. Shipulski, C.A. Brown, A scale-based Model of Reflectivity, Fractals Vol.2 No. 3 (1994) p. 413.
- [26] S. E. Jordan, C.A. Brown, Comparing Texture Characterization Parameters on Their Ability to Differentiate Ground Polyethylene Ski Bases, Wear 261 (2006) 398-409.
- [27] C. Lipson, Statistical Design and Analysis of Engineering Experiments, McGraw-Hill, Inc, New York (1973) p. 196-201.
- [28] T. Vincent, I. Bar-On and Y. Itovich “Quantitative Conductor Edge Angle Influence on GHz Frequency Electrical Loss”, unpublished (submitted to IEEE Transactions on Components and Packaging March 2009).
- [29] ALN11 Silver Conductor, DuPont Microcircuit Materials datasheet [www.dupont.com/mcm/MCMALN11\(07/2002\)](http://www.dupont.com/mcm/MCMALN11(07/2002))
- [30] ALN33 Silver/Palladium Conductor (10:1), DuPont Microcircuit Materials [www.dupont.com/mcm/MCMALN33\(06/2002\)](http://www.dupont.com/mcm/MCMALN33(06/2002))

- [31] ALN23 Silver/Platinum 3:1 Conductor, DuPont Microcircuit Materials www.dupont.com/mcm
MCMALN23(08/2002)
- [32] B. C. Wadell, Transmission Line Design Handbook, Artech House, 1991, p. 25.
- [33] R. N. Wenzel, Surface Roughness and Contact Angle, Ind. Eng. Chem. Vol.28 1936, pp988-994.
- [34] T. Laing, S. Hall, H. Heck and G. Brist, IEEE 2006 p. 1780.
- [35] B. Nowicki, Multiparameter representation of surface roughness, Wear69 (1985) p. 161.

4.0 CHAPTER IV

Quantitative Edge Cross-section Angle Impact on Conductor Loss

Synopsis

The objective of this paper is to investigate the impact, by experimentation, of the conductor-edge effects on conductor loss, for circuits made by thick-film fabrication. The methodology for measuring the conductor-edge angle, with an interferometer microscope, is explained. The impact of the conductor-edge angle is quantified over a range of conductor conductivities, frequencies and skin depths. The ceramic substrate has a range of surface roughnesses that have been characterized. The substrate surface roughness characterization is compared to conductor-edge angle measurement to determine the edge angle impact on conductor loss.

Abstract— This paper describes a method of forming different conductor edge cross-section angles by using thick-film screen printing on substrates of different surface roughness. The edge angle for each surface type is compared visually and measured using an interferometer microscope. The conductor edge angle is correlated to the respective transmission loss sample. The impact of different inclination angles on conductor loss is observed.

Index Terms— Conductor loss, edge angle, thick film, surface roughness, surface topography.

INTRODUCTION

Conductor loss is the largest transmission loss factor for telecommunications applications using ceramic substrates with low $\tan \delta$. A wide range of state of the art packaging applications utilize these forms of PCB circuitry. The inclination angle, Fig. 4.1, of the microstrip conductor edge influences the conductor loss at GHz frequencies with a lower angle causing larger losses.

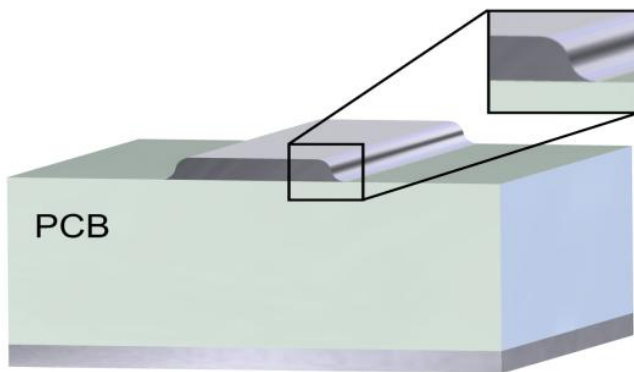


Fig. 4.1. Cross section illustration of PCB formed using thick-film print showing conductor angle of inclination.

It is well known that loss increases with the square root of frequency due to the skin effect. The skin effect causes this loss, at GHz frequencies, by restricting the electric current to the area close to the surface of the conductor. As the current becomes more confined, the resistance and therefore transmission

loss increases. In addition, current flowing on a good conductor tends to flow close to and parallel to a sharp edge therefore further restricting the current to the smaller edge area, increasing resistance further [1-3].

Most modeling methods of calculating conductor transmission loss ignore edge effects since they use the assumption that the conductor is infinitely thin or that the conductor has perfect conductivity. The strip thickness of a microstrip circuit is significantly less than the width and thus the infinitely thin assumption may well be justified [4-5]. Silver/copper has high conductivity and therefore perfect conductor assumptions are often used. However, the predicted fields of an infinitely thin strip or perfectly conducting material mathematically cause a current density singularity close to the conductor edge [6]. Modeling with finite thickness, especially since it is thin, a full-wave analysis can take an unreasonably long time.

The research in this area has focused on how to predict the edge losses by using numerical/analytical calculation [7-12]. The Barsotti [9] models shows that a sharper edge angle results in larger transmission losses but this model is not yet proven to predict the impact of small inclination angles.

There is little published measurement data on edge effects and it is unknown what impact the low inclination angles would have on transmission loss performance. This study measures the transmission loss of microstrip topology with a range of conductor edge angles below 20° . The edges are formed by varying the surfaces topography. The microstrip edge inclinations are measured quantitatively and correlated to the transmission loss.

EXPERIMENTAL METHOD

Thick film screen printing technology was used to make the microstrip circuits for this study. Prior to printing, the surface of the Aluminum Nitride or AlN substrates had been treated with three

different surface finishing techniques: lapping, vapor honing and chemical etching, a description of these processes is given in Table 4.1.

Table 4.1, AlN Surface finishing process			
Process	Description	Ra	Length-scale
Chemically etched	Held in an Anodex solution for 1 hour at 150 °C, then in an HCl solution for 1hour at 150 °C, followed by cold water rinse. This process is repeated twice.	1.09µm	1.0818
Vapor Honed	Blasted with 220 grit aluminum oxide and water, then vapor honed for 2.5 minutes with 0.5mil of material removed.	0.559µm	1.023
Lapped	Lapped using an oil-based abrasive; cleaned in ultrasonic bath and rinsed with alcohol (ACUMET).	0.184µm	1.004

Surface finish process descriptions for AlN substrate to form different surface topographies

The substrate surfaces of the AlN substrate have been characterized previously [13]. Length-scale [14] fractal analysis was used with a sampling interval of 69nm. Several measurements were taken in order to measure the surface area and surface slope relative to scale. The average roughness, Ra, is a conventional parameter used for measuring surface roughness and is included, however, it does not effectively measure surface area and slope characteristics.

Four substrate plates, of each surface finish, were printed with microstrip circuits; two were printed with ALN 11 paste, and two with ALN 33.

ALN 11© [15] is a silver conductor, with measured bulk conductivity of 2.2×10^7 S/m

ALN 33© [16] is a silver/palladium conductor (10:1), with measured bulk conductivity of $6 \times 10^6 \text{S/m}$.

The ceramic substrate is aluminum nitride and the standard notation is used: AlN. This should not be confused with the conductor nomenclature - ALN 11 or “high conductivity conductor” and ALN 33 or “medium conductivity conductor”. All the samples were printed in a clean room environment, with the same screen (325F 2N wire diameter $22.86\mu\text{m}$), same process parameters, at the same time. As a standard part of thick-film process, once printed the samples were left “to settle” for a controlled period of 15 minutes. The print used a trailing edge squeegee with rectangular cross-section and a speed of 0.0127m/s .

There were two sets of microstrip circuits on each plate. Each microstrip circuit set consisted of three signal traces of different lengths, shown in Fig. 4.2, the longest being 40mm, which is used for the transmission loss measurements. Every plate also had a serpentine line, as shown top right. The serpentine line was used to measure bulk conductivity, σ .

Measurements of conductor loss and surface texture are described elsewhere [13, 17].

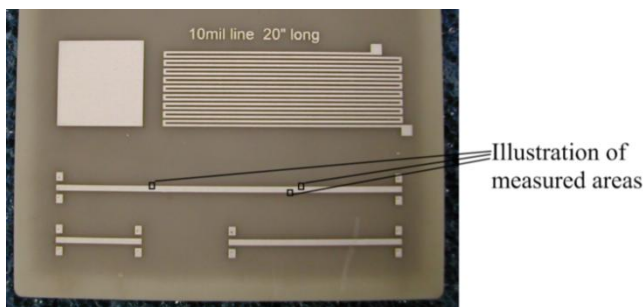


Fig. 4.2. Top view photograph of a 0.625mm thick AlN substrate with one of two sets of three transmission lines, nominal lengths: 10, 20, and 40mm. The serpentine line is used to measure bulk conductivity. The area selection for the conductor edge taper measurement are shown

The transmission line samples were measured using an interferometer microscope (Wyko NT110) at the Technion, Israel Institute of Technology. An area of $588\mu\text{m} \times 447\mu\text{m}$ was measured in three places along the transmission line. One of the measurements was taken on the opposing edge, Fig. 4.2. Within each area the profile was taken three times: at each side on the area and the middle. The profile taken was an average of 37 pixels each pixel has a length of $0.795\mu\text{m}$.

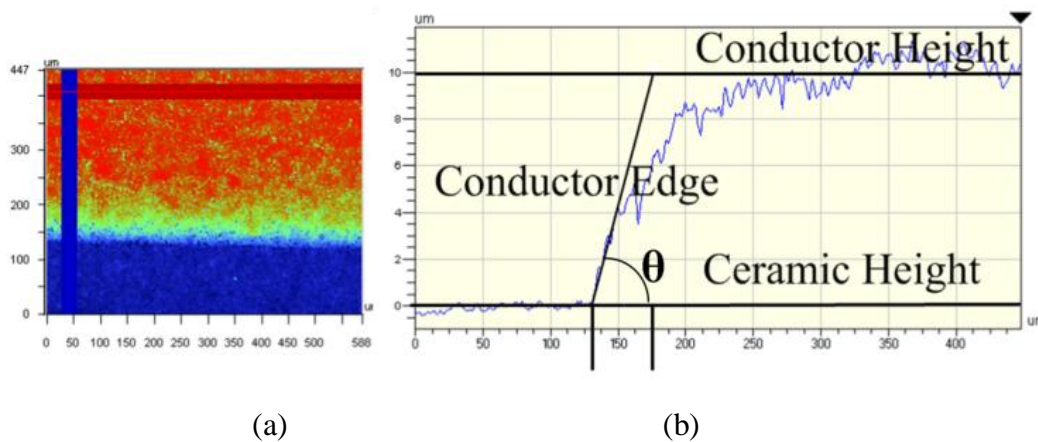


Fig. 4.3. Interferometer measurement on lapped surface sample. (a) - the height map (red is highest, blue is lowest), the red is the conductor material height measurement, the green-yellow the tapering/angle of the conductor edge and the blue area is the lapped ceramic surface. (b) - characteristic of ceramic and conductor to ceramic profile.

The profile measures the surface location in parallel with the y-axis shown as the line parallel to the y-axis on the height map, Fig. 4.3(a). The profile height map gives the ceramic level, inclination information and conductor level. The tapered/inclination angle of the conductor edge is taken from the conductor-ceramic contact area and a line averaged through the profile result for at least the first 30% of the surface location on the z-axis. The y-axis is a finer scale than the x-axis for Fig. 4.3(b); therefore the measured angle, represented, appears larger than it is.

RESULTS

Cross sections of the fired conductor edges are shown in Fig. 4.4 for each surface finish type.

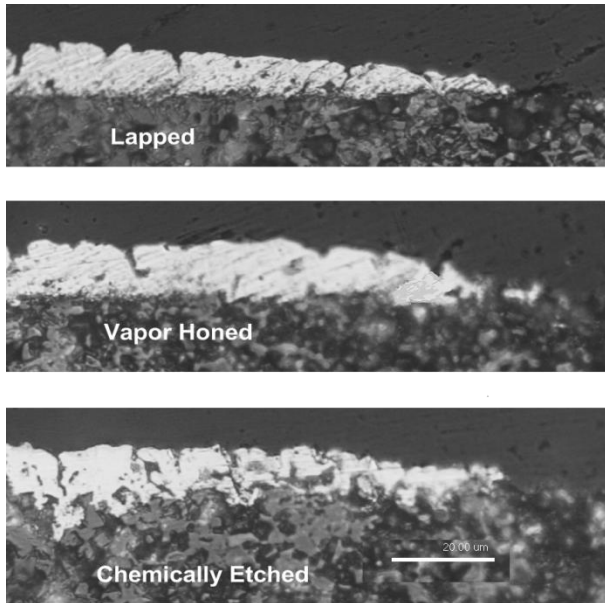


Fig. 4.4. Cross section of microstrip circuit, x50 magnification, across the width of the conductor at the edge. Shown is the AlN substrate with conductor ALN33 on Lapped (top), Vapor Honed (middle) and Chemically Etched (base) surface finish.

The edges of the ALN33 conductor visually change characteristic depending on the surface finish, as shown by Fig. 4.4. The lapped substrate sample has a more tapered edge than the chemically etched substrate.

The conductor edges measurements from the interferometer microscope are shown in Fig. 4.5.

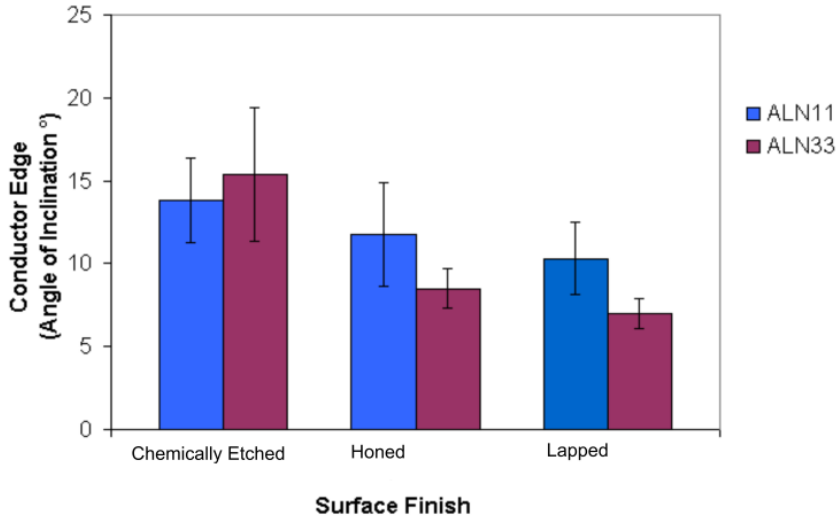


Fig. 4.5. Edge angle mean results (with error bar) versus substrate process for ALN11 and ALN33: chemically etched, vapor honed and lapped surface finish.

The conductor edge inclination angles for the different surfaces results for ALN 11 and ALN33 conductors are given in Fig. 5. For both ALN11 and ALN33 the chemically etched surface sample has the largest inclination angle, the honed sample has the medium inclination angle and the lapped has the smallest inclination angle. The ALN33 conductor exhibits greater differentiation between the surface samples. The ALN33 and ALN11 samples have a similar chemically etched edge measurement at around 14-15°. The honed ALN33 sample measures 8.5° compared to the ALN11 honed sample that measures 11.8°. The ALN33 and ALN11 lapped samples also have a significant differentiation with 7° and, 10° respectively. The roughest substrate is finished with chemical etching, the medium surface roughness is finished with a vapor hone process and the smoothest surface is finished by lapping.

Table 4.2: T-test results		
Test	ALN11	ALN33
Chemically etched versus Honed	0.29	0.01
Honed versus Lapped	0.38	0.02
Chemically etched versus Lapped	0.02	0.002

Student t-test results for each combination of measured conductor edge angles for both ALN 11 and ALN33.

Student t-tests were performed on all six data set combinations for the inclination/taper angle of the conductor. All of the measurement comparisons were discernable for the ALN 33 conductor with 0.02 or less probability of the null hypothesis. The null hypothesis assumes that there is no difference between the two sets of data. For the ALN 11 conductor the chemically etched versus lapped case also supports that the two sets of data are different, with 0.02 probability that they are from the same set. However, the other cases have weaker results with the chemically etched versus honed result of 0.38 probability and honed versus lapped with 0.29 probability.

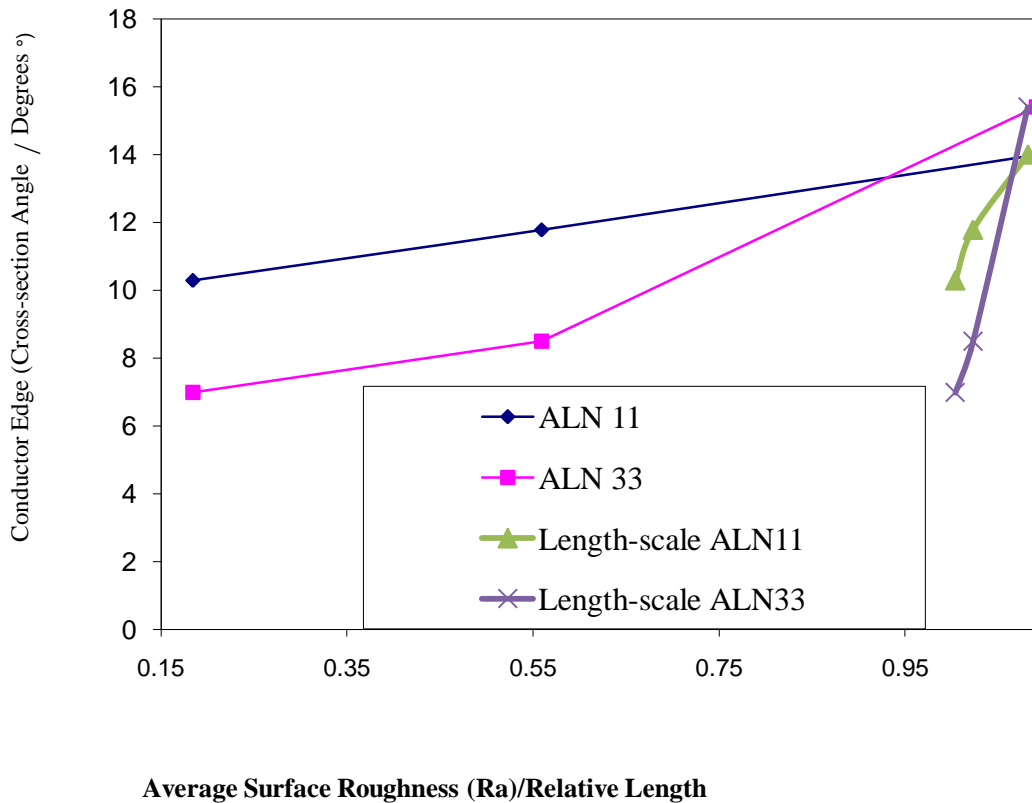


Fig. 4.6. Conductor edge angle mean results versus average roughness and length-scale fractal analysis for the two conductor types: ALN11 and ALN33.

As the average roughness increases the conductor edge inclination angle increases for both conductor types as shown by Fig. 4.6. As the length-scale (and therefore surface slope) increases the inclination angle increases for both conductor types. The length-scale measurement method has shows greater differentiation than the average roughness.

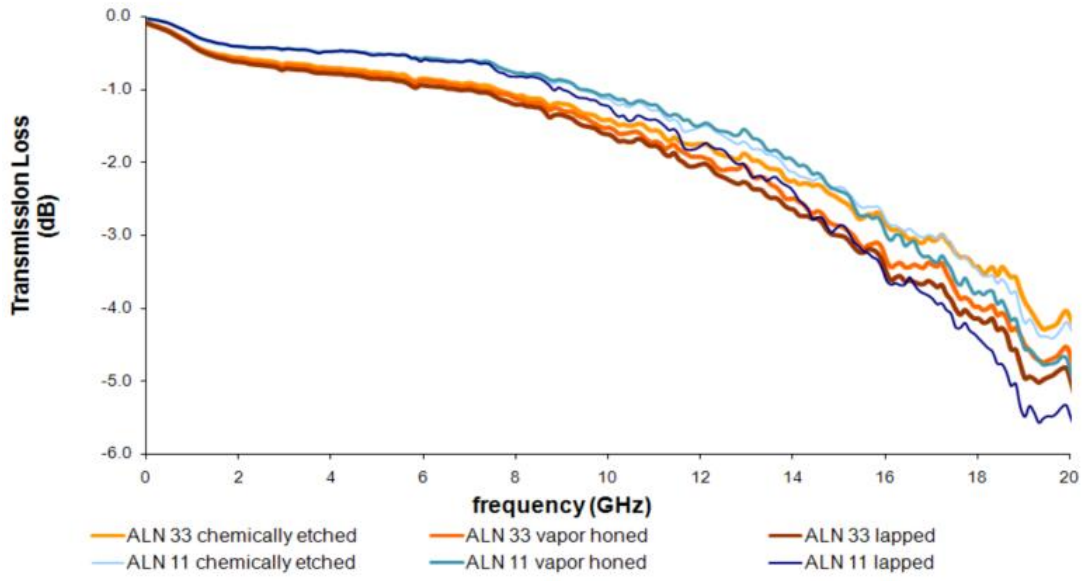


Fig. 4.7. Transmission loss of ALN 11 and ALN 33 fired conductors on chemically etched, vapor honed and lapped surface finishes as a function of frequency.

Transmission loss of the strip made with ALN 33, medium conductivity, and ALN11, high conductivity, are shown as a function of frequency in Fig. 4.7. At frequencies greater than 5GHz the loss results, of both conductors, begin to diverge depending on the surface finish. At frequencies greater than 15GHz the loss results are distinctly different. The chemically etched surface has the lowest loss for each conductor. At 20GHz the lapped surface has the highest loss for each conductor.

DISCUSSION

The loss measurements correlate with the edge inclination topography; as the edge angle increases, the transmission loss decreases Fig 4.8; this is the same trend in behavior that Barsotti predicted [8]. It can be concluded that the loss differences seen here are from edge topology effects.

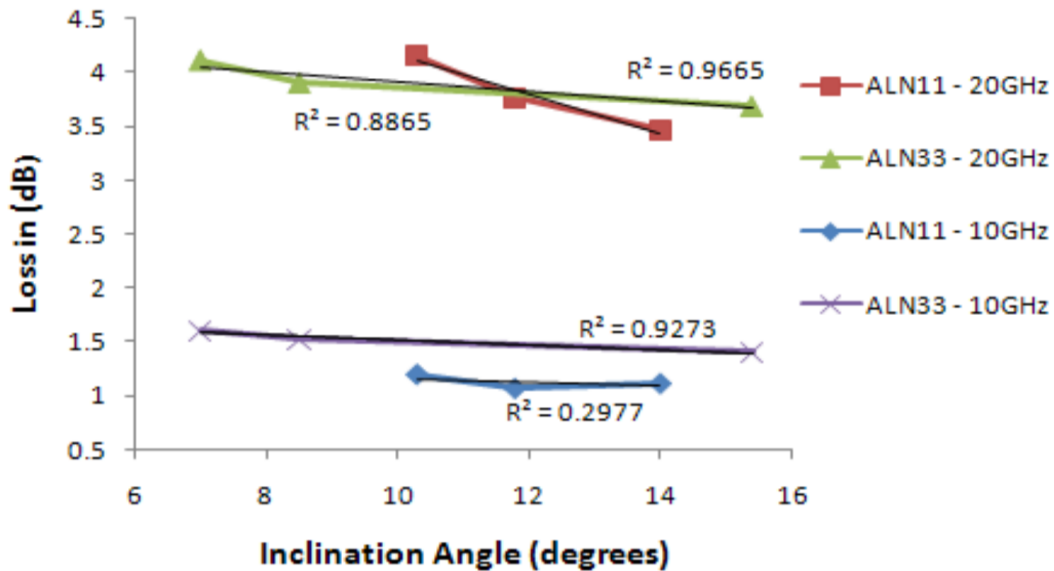


Fig. 4.8 Conductor edge angle mean results versus transmission loss at 20 and 10 GHz for the two conductor types: ALN11 and ALN33; with the coefficient of correlation R^2

The high conductivity conductor, ALN11, has a low range of cross-section angles and this is not seen to have a marked effect on loss at 10GHz, as shown by Fig. 4.8. However at 20GHz this has a significant effect with an angle increase of 4° causing a decrease of 0.7dB in loss. The medium conductivity conductor has a decrease in loss of 0.5dB with

an angle increase of 9° . It makes sense that the impact of edge loss would be more pronounced in the higher conductivity material since it relates to the skin effect.

When the edges are compared, the lapped surface conductor has a sharper edge, Fig. 4.5, implying that the lapped surface, which has a smaller surface roughness, has a greater lateral paste flow across the surface. The increased surface roughness/inclination and therefore surface area of the chemically etched surface, causes greater adhesion/inclination friction of the paste and less lateral motion of the conductor.

If the average cross-section area of the lapped and chemically etched sample conductors are compared; the conductor area of the last $20\mu\text{m}$ closest to the edge, where the current density is highest, is smaller in the lapped sample compared to the chemically etched sample. The smaller conductor area constrains the current and increases the current density and therefore loss.

The edge topographies of the high conductivity trace, ALN11, and the medium conductivity trace, ALN33, conductors show a difference in edge topography depending on the surface finish. This is especially true for the ALN33 conductor, most likely due to a difference in paste rheology. It is possible that a larger difference in surface characteristic would create a larger difference in the edges for ALN11 and ALN33 conductors, however, the range of surface topographies used is typical of ceramic substrates in the microelectronics industry.

It is a possibility that the edges could be varied by changing the conductor paste rheology instead of the surface characteristic. This can be done by altering another process parameter such as paste viscosity, printing speed/pressure and screen parameters, for example, mesh number/wire diameter. Environment changes such as temperature or humidity can have a significant effect on paste rheology.

Conventional theory states that an increased surface roughness or ceramic-conductor interface non-uniformity result in increased loss [18]. However, these results show that the roughest surface, the chemically etched surface finish, has the smallest loss and the smoothest surface, the lapped surface, has the greatest loss. This shows that the loss differences, seen in this case, are caused by the conductor inclination angle, which has a larger impact on the loss results than the ceramic-conductor interface non-uniformity.

CONCLUSION

Edge topography has been measured for two thick-film paste systems, with high and medium conductivities, on substrates with three substrate surface topographies formed by different surface treatments. It has been shown quantitatively that the substrate with a chemically etched surface finish has the roughest surface and the largest conductor cross-section angle. The lapped surface substrate has the smoothest surface and the lowest conductor edge inclination.

For frequencies greater than 15GHz the greater mean edge angle results in a lower transmission loss with an angle increase of 4° causing a decrease of 0.7dB in loss at 20GHz on a 40mm transmission line. The differences in ranking of transmission losses between the AlN substrates is a result of the conductor edge topography and not a result of the conductor/substrate interface roughness.

For thick-film processing applications, especially with edges $< 20^\circ$, the edge topography loss may be considered a significant portion of the conductor/transmission loss.

ACKNOWLEDGMENT

The authors would like to thank the Surface Metrology Laboratory at WPI, and to acknowledge the use of the interferometer microscope and the help of the Shamban Tribology laboratory Technion, Israel. The support of the Lady Davis Foundation for part of this work is gratefully acknowledged.

REFERENCES

- [1] J. C. Rautio, "An Investigation of Microstrip Conductor Loss," *IEEE Microwave Magazine* December 2000, pp60-67.
- [2] J. C. Rautio, V. Demir, "Microstrip Conductor Loss Models for Electromagnetic Analysis," *IEEE Transactions on Microwave Theory and Techniques*. Vol. 51, No. 3, March 2003 pp915-921.
- [3] J. D. Kraus, D. A. Fleisch, *Electromagnetics with Applications*, 5th Edition McGraw-Hill International Editions, 1999, Ch 2.
- [4] M. Kobayashi, "Longitudinal and Transverse Current Distributions on Microstriplines and their Closed form Expression," *IEEE Trans. Micr. Theory Tech.*, vol. 33, pp. 784-788, 1985.
- [5] E. F. Kuester and D.C. Chang, *Theory of Guided Waveguides and Transmission Lines*. University of Colorado Electromagnetics Laboratory, 1990.
- [6] R. Mittra and S. W. Lee, *Analytical Techniques in the Theory of Guided Waves*, New York, The Macmillan Company, 1976.
- [7] J. Meixner, "The Behavior of Electromagnetic Fields at Edges," *IEEE Transactions on Antennas and Propagation*, Vol. 20, July 1972.

- [8] J. Geisel, K-H Muth, and W. Heinrich “The Behavior of Electromagnetic Field at Edges or Media with Finite Conductivity,” *IEEE Transactions on Microwave Theory and Techniques*. Vol. 40, 1992.
- [9] E. L. Barsotti, J. M. Kuester, J. M. Dunn, “Strip Edge Effects on Conductor Loss Calculations using the Lewin/Vainshstein Method,” *Electronic letters* 5th July 1990, Vol. 26 No. 14 p 983-985.
- [10] L. Lewin, “A Method of Avoiding the Edge Current Divergence in Perturbation Loss Calculations,” *IEEE Transactions MTT-32*, No. 7 July 1984.
- [11] L. A. Vainstein, S. M. Zhurav, “Strong Skin Effect at the Edges of Metal Plates,” in Russian, *Pis'ma Zh. Tekh. Fiz.*, 1986, 12, pp.723-729; English translation in *Sov. Tech. Phys. Lett.*, 1986, 12, (6), pp. 298-299.
- [12] S. Safavi-Naeini, R. Faraji-Dana, Y. L. Chow, “Studies of Edge Current Densities in Regular and Superconducting Microstrip Lines of Finite Thickness,” *IEE Proceedings-H*, Vol.140, No. 5, October 1993.
- [13] T. Vincent and I. Bar-On, “Conductor Edge Definition Influence on High Frequency Electrical Loss,” Proceedings, *MS&T 2008*, Pittsburg, Pennsylvania, October 5-9th, 2008.
- [14] ASME B46.1, Surface Texture (Surface Roughness, Waviness and Lay), an America national standard, ch.10. American Society of Mechanical Engineers, New York, 2002.
- [15] ALN11 Silver Conductor, *DuPont Microcircuit Materials datasheet* [www.dupont.com/mcm MCMALN11\(07/2002\)](http://www.dupont.com/mcm/MCMALN11(07/2002))
- [16] ALN33 Silver/Palladium Conductor (10:1), *DuPont Microcircuit Materials data sheet* [www.dupont.com/mcm MCMALN33\(06/2002\)](http://www.dupont.com/mcm MCMALN33(06/2002))

- [17] T. Vincent, C. A. Brown, I. Bar-On, and B. Powers, “The Influence of Electronic Substrate Surface Roughness on Radio-frequency Transmission Loss Utilizing Conventional and Length-scale Fractal Analysis”, unpublished.
- [18] S. Hall, S. G. Pytel, P. G. Huray, D. Hua, A. Moonshiram, G. A. Brist, and E. Sijercic, “Multigigahertz Causal Transmission Line Modeling Methodology Using a 3-D Hemispherical Surface Roughness Approach”, in *IEEE Transactions on Microwave Theory and Techniques*, vol. 55, no. 12, December 2007.

5.0 CHAPTER V: FURTHER WORK

Math Modeling

Electromagnetic simulation programs are essential tools in the design of telecommunication systems. The long term goal of this study is to take the knowledge gleaned from these experiments to assist in making better, more accurate mathematical models. Rather than taking the surface roughness feature of the substrate to determine high frequency loss, the edge angle and perhaps other features should also be taken into consideration. This study has shown that surface roughness can indirectly decrease high frequency loss but that is the opposite result of most numerical and empirical tools currently available.

With the advent of modern laser optical microscopes, the field of surface metrology has many more characterization and parameterization tools at its disposal than it did thirty years ago. In the 1980s Hammerstad used average roughness in an equation, in order to curve fit to measured loss data. There are many parameters or possible algorithms that could better describe the surface roughness influence on conductor loss. In particular the length-scale or area-scale parameterization is a promising parameter for the characterization of conductor loss since it measures roughness at different scales and can therefore be used to calculate loss over broad frequency ranges.

Edge profile

If the profile of conductors on different substrates are compared; distinct differences in the profiles can clearly be seen, Fig. 5.1. The differences of these profiles may influence the

conductor loss by changing the mean average of the conductor edge-angle. The edge profile of the thick-film samples made with AlN substrates, were measured for the study described in chapter III. Despite a distinct different in surface roughness, there was no difference detected between the edge profiles of these different samples although there was some variation in edge angle detected; the mean average results were used for correlation with conductor loss.

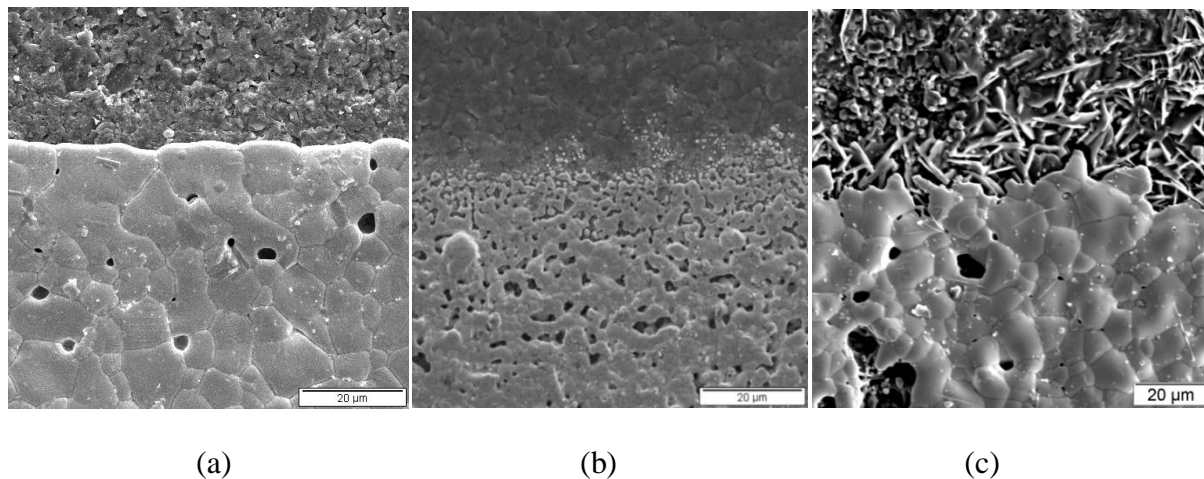


Fig. 5.1 the conductor and ceramic substrate, showing the conductor profile, of (a) an alumina substrate with silver alloy conductor, (b) AlN vapor honed substrate with ALN33, and (c) an LTCC substrate with silver alloy.

The methodology used to measure the edges could be used in other studies to observe influences of edge profile on conductor loss but it has yet to be proven.

Microstructure

Silver is a commonly used conductor for the fabrication of microelectronics circuits. The conductors used for this study were all silver alloys. The primary reason for using silver is of

course its comparatively low cost - it is dramatically cheaper than gold. Another apparent benefit of silver is the theoretical conductivity is 1.5 times that of gold.

Silver and gold tend to behave differently under the same or similar processing conditions, such as thick-film processing, this can result in different material and microstructural properties. Silver thick film materials generally do not sinter as densely as gold and hence the thick film conductivity is often worse [40]. Glass frit is often used as a fluxing agent to help increase the density of silver but this can cause the fired film to be glass heavy at the lower surface. The pastes used in this study were all fritless. Also, it is suggested that the edge definition of silver prints is frequently poorer than gold.

Any shape or feature that inhibits the flow of electrons, by increasing the electron path, will increase the conductor loss. Even microstructure defects such as grain boundaries and porosity, shown in Fig. 5.2, can have an influence on the conductor loss [39]. Thus it might be beneficial to include microstructural considerations and their impact on conductor loss.

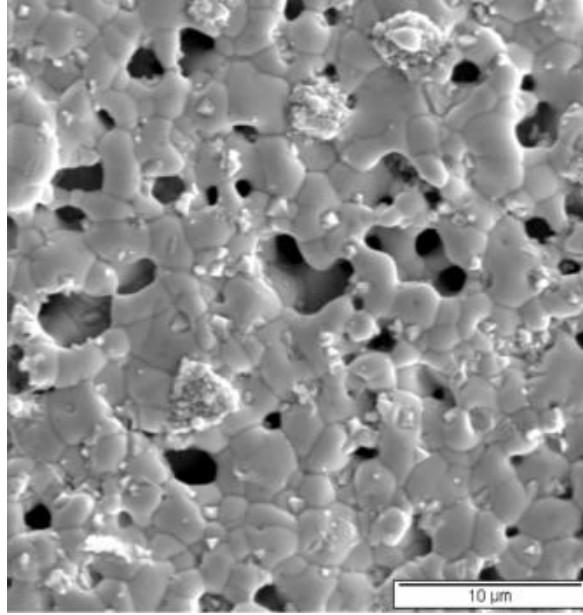


Fig. 5.2 the fritless fired silver alloy ALN33 showing microstructure features such as grain boundaries and porosity.

6.0 CHAPTER VII: CONCLUSION

- Microstrip configurations were produced, by thick-film fabrication, on three clearly discernible surfaces of AlN substrates with conductors of low, medium and high conductivity.
- The substrate surfaces were characterized and ranked using conventional average roughness, Ra, peak to valley roughness, Rt, and relative lengths as calculated from scale sensitive length-scale fractal analysis, giving the same ranking of surface treatments.
- The conductor-edge angles were measured using interferometer microscope.
- Conductor loss was measured for frequencies ranging from kHz to 20 GHz.
- The dependence of loss on the surface roughness characteristics, for the different conductors, changes as a function of frequency.
- The edge inclination is shown to be formed by the surface roughness; the angle is larger for rougher surfaces.
- At 20 GHz the loss shows an inverse correlation with roughness, Ra, and with relative lengths as calculated by length-scale fractal analysis, for low, medium and high conductivity conductor lines.
- These observations do not support the claim that greater conductor loss, at higher frequencies, is a direct result of increased path length at the ceramic-conductor interface. Rather that there is a strong negative correlation of conductor loss to surface roughness.

- The experiments show that the greater conductor loss, at higher frequencies, is a direct result of smaller conductor-edge angle.

REFERENCES FOR THESIS (EXCLUDING CHAPTERS III AND IV)

- [1] J. E. Sergent and C. A. Harper, *Hybrid Microelectronics Handbook*, 2nd Edition, Electronic packaging and interconnection series, McGraw Hill Inc, 2005.
- [2] D. Y. Kim, J. K. Mun, D. S. Jun, and H. Kim, "Investigation of Ultralow loss Interconnection Technique for LTCC based System-in-Package (SIP) Technology at 60GHz", *Mater. Res. Soc. Symp. Proc.* vol. 969, 2007.
- [3] R. H. Reuss, B. R. Chalamala, "Microelectronics Packaging and Integration", *MRS bulletin* January 2003, pp. 11-20.
- [4] T. Vincent, I. Bar-On, C. A. Brown "Examination of Surface Roughness Effect on Insertion loss at Microwave Frequencies within LTCC Structures" Conference Proceedings and Presentation iMAPS/ACerS 3rd International Conference and Exhibition on Ceramic Interconnect and Ceramic Microsystems Technologies (CICMT), April 23-26, 2007, Denver, Colorado USA, pp. 138-144.
- [5] E. Hammerstad, Ø. Jensen, "Accurate Models for Microstrip Computer Aided Design", *IEEE MTT-S* May 1980 pp. 407-409.
- [6] J. C. Maxwell, "Electricity and Magnetism", vol. 2, section 690, p. 322, 1973.
- [7] H. Lamb, "Oscillatory current flow in spherical conductors", *Philosophical Transactions, Royal Society*, 1883.
- [8] O. Heaviside, "Effective Resistance and Inductance of a Round Wire", *The Electrician*, 1884, p. 583; 1885, p. 489. *Electrical Papers*. Vol. I, pp. 353- 429; Vol. II, pp. 50, 97.
- [9] Rayleigh, "Notes, chiefly historical, on some fundamental propositions in optics", *Phil. Mag.*, vol. 21, p. 381; 1886.
- [10] H. Hertz, *Electric Waves*, p. 160; *Wied. Ann.*, 1899, p. 395.

- [11] J. J. Thompson, *Notes on recent researches in electricity and magnetism*, Oxford Univ. Press, p.xvi, 1893.
- [12] A. E. Kennelly, F. A Laws, and P. H. Pierce, “Experimental researches on skin effect in conductors”, *Trans. AIEE*, vol. 34, pp. 1953-2018, 1915
- [13] H. A. Wheeler, “Formulas for the skin effect”, *Proc. IRE*, vol. 30, September, 1942, pp. 414-424.
- [14] A. R. Djordjević and T. K. Sarkar, “Closed-Form Formulas for Frequency Dependent Resistance and Inductance per Unit Length of Microstrip and strip Transmission Lines”, *IEEE MTT-S February 1994* p. 241.
- [15] R. A. Purcel, D. J. Massé, C. P. Hartwig, “Losses in Microstrip”, *IEE Trans. MTT-16*, No. 6, 1968, pp. 342-350.
- [17] Rayleigh, *Theory of Sound*, Volume II, Macmillan, London, 1929, pp. 89-96.
- [18] S. P. Morgan “Effects of Surface Roughness on Eddy Current Losses at Microwave Frequencies,” *J. Appl. Phys.*, vol. 20, Apr. 1949, pp. 352-362.
- [19] A. E. Sanderson, *Effect of Surface Roughness on Propagation of the TEM mode, Advances in Microwaves*. New York: Academic, 1971, vol. 7, p. 1.
- [20] M. A. Biot, “Some new Aspects of the Reflection of Electromagnetic Waves on a Rough Surface”, *J. Appl. Phys.*, vol. 28, no. 12, Dec. 1957, pp.1455-1463.
- [21] J. R. Wait, “Guiding of Electromagnetic Waves by Uniformly Rough Surfaces”, part II, *IRE Trans. Antennas Propag.*, 7, 1959, S163-S168.
- [22] C. L. Holloway, E. F. Kuester “Impedance-Type Boundary Conditions for a Periodic Interface Between a Dielectric and a Highly Conducting Medium” *IEEE Transactions on Antennas and Propagation*, 2000, pp. 1660-1672.

- [23] P. G. Huray, S. Hall, S. Pytel, F. Oluwafemi, R. Mellitz, D. Hua, and P. Ye, "Fundamentals of 3-D snowball model for surface roughness power losses", SPI 2007, pp. 121-124.
- [24] L. Tsang, X. Gu, and H. Braunish, "Effects of Random Rough Surface on Absorption by Conductors at Microwave Frequencies" IEEE Microw. Wireless Compon. Lett., vol. 16, no. 4, Apr. 2006, pp. 221-223.
- [25] X. Gu, L. Tsang, H. Braunisch, and P. Xu, "Modeling Effects of Random Rough Interface on Power Absorption Between Dielectric and Conductive Medium in 3-D Problem" IEEE Transactions on MTT vol.55, no. 3 March 2007.
- [27] G. Brist, S. Hall, "Non-Classical Conductor Losses due to Copper Foil Roughness and Treatment", ECWC 10 Conference at IPC 05.
- [28] T. Laing, S. Hall, H. Heck G. Brist "A Practical Method for Modeling PCB Transmission Lines with Conductor Surface Roughness and Wideband Dielectric Properties" IEEE 2006 pp. 1780-1783.
- [29] B. A. Auld and W. Strauss "Internal magnetic field analysis and synthesis for prescribed magnetoelastic delay characteristics," J. Appl. Phys., vol. 37, p. 983, 1966
- [30] S. Safavi-Naeini, R. Faraji-Dana, Y. L. Chow, "Studies of Edge Current Densities in Regular and Superconducting Microstrip Lines of Finite Thickness," IEE Proceedings-H, vol.140, No. 5, October 1993.
- [31] J. C. Rautio, V. Demir, "Microstrip Conductor Loss Models for Electromagnetic Analysis," IEEE Transactions on Microwave Theory and Techniques. vol. 51, No. 3, March 2003 pp. 915-921.
- [32] J. Meixner, "The Behavior of Electromagnetic Fields at Edges," IEEE Transactions on Antennas and Propagation, vol. 20, July 1972.

- [33] M. Chrissomallis, K. Siakavara, J. N. Sahalos, "A study of open thick microstrip: the hybrid quasi-static approximation", *Can. J. Phys.* 67, 747, 1989, pp. 747-752.
- [34] E. L. Barsotti, Effect of Strip Edge Shape on Microstrip Conductor Loss, MS Thesis University of Colorado 1990.
- [35] E. L. Barsotti, J. M. Kuester, J. M. Dunn, "Strip Edge Effects on Conductor Loss Calculations using the Lewin/Vainshstein Method," *Electronic letters* 5th July 1990, vol. 26 No. 14 pp. 983-985.
- [36] L. Lewin, "A Method of Avoiding the Edge Current Divergence in Perturbation Loss Calculations," *IEEE Transactions MTT-32*, No. 7 July 1984.
- [37] L. A. Vainstein, S. M. Zhurav, "Strong Skin Effect at the Edges of Metal Plates," in Russian, *Pis'ma Zh. Tekh. Fiz.*, 1986, 12, pp.723-729; English translation in *Sov. Tech. Phys. Lett.*, 1986, 12, (6), pp. 298-299.
- [38] M. H. Lim, J. D. van Wyk, Z. Liang, "Impact of Conductor Cross-sectional Shape on Component Losses and System Performance", *Proc. 2nd Int. Ceram. Interconnect Ceram. Microsyst. Conf.*, Apr. 25-27, 2006, pp. 1-8.
- [39] A.F. Mayadas and M. Shatzkes. "Electrical-Resistivity Model for Polycrystalline Films: the Case of Arbitrary Reflection at External Surfaces" *Phy. Rev. B*1, 1382 (1970).
- [40] K. Pitt, C. Free, Z. Tian, M. Jakubowska, "A method for the prediction of microwave properties of thick film conductors from physical measurements and d.c. conductivity", *Journal of Mat. Sci: Materials in Electronics* vol. 12, 2001 pp. 491-495.
- [41] A. C. Scogma "Modeling Conductor Surface Roughness" printed circuit design and fabrication October 2008, pp.33-35

7.0 APPENDIX A

**PROCEEDINGS, IMAPS, DENVER 2007: EXAMINATION OF SURFACE
ROUGHNESS EFFECT ON INSERTION LOSS AT MICROWAVE
FREQUENCIES USING CONVENTIONAL SURFACE ROUGHNESS
PARAMETERS WITHIN LTCC STRUCTURES**

Tracey Vincent, Isa Bar-On and Christopher Brown

Abstract

The effect of surface roughness on electrical insertion loss at microwave frequencies has been evaluated on LTCC substrates. This involved the selection of suitable measurement instruments and examination of the data by using conventional roughness formula. Application of laser scanning microscopy (SLM) and interferometric microscopy on two samples of varying roughness, pertaining to different LTCC tape systems, were examined and compared. Taking other loss factors into account, the impact of surface roughness effect on overall Radio Frequency loss performance is shown. Comparisons between determined conductor loss and theoretical conductor loss, using the established conductor loss surface roughness correction formula, are shown. The utilization of S_a and S_q (root mean square) surface roughness parameters is discussed.

Low Temperature Co-fired Ceramic is used extensively for high frequency applications. LTCC technology is a way of producing multilayer circuits with the help of a tape lamination and fire process. LTCC tape systems are supplied in a range of dielectric loss tangents and surface roughness; 2 tape systems with different surface roughness and loss tangent are used for this study. These 2 tape systems have different compositions and use different processes.

INTRODUCTION

Insertion loss is a significant design driver within the microwave industry. This paper will show how surface roughness relates to conductor loss and in turn how the conductor loss factor can contribute to overall insertion loss.

Tape systems with lower dielectric loss factors have been developed, now attention is turning to conductor loss effect in this medium.

There has been recent effort in the PCB manufacturing [1-2] industry to examine surface roughness effect on insertion loss. Laing et al [3] show the surface roughness loss factor versus frequency with various surface roughnesses using the Rq parameter. There is no doubt within this industry sector that surface roughness can significantly impact insertion loss at frequency.

The objective of this investigation is to investigate the surface roughness effect on insertion loss. Part of this aim is to show the shortcomings of conventional surface parameters of surface metrology. Surfaces are often seen as Euclidian or at best with linearly periodic characteristics. It would be of benefit to microwave design engineers to comprehend the nature and complexity of surfaces especially when considering surface roughness.

Method

Loss Measurement

Insertion Loss is essentially power out divided by power in expressed in dB. The overall insertion loss is a combination of the rejected signal and attenuated signal.

The rejected signal or reflected loss was considered when measuring the samples. Reflected loss is caused by mismatch between the input/output transition and the conductor path itself.

The overall loss was measured using a Vector Network Analyzer (VNA) to obtain s-parameters. Transmission line equations were used to calculate the reflected loss. Samples

compromising 3 different microstrip lengths were used to extrapolate and corroborate the attenuated signal per centimeter. The reflected loss is then subtracted from the overall measured loss to attain the attenuated signal. The frequency range extends to 30GHz.

Loss Calculation

The loss of interest is part of the attenuated signal. The phase, and amplitude, of the attenuated signal is represented by the propagation constant γ [4]:

$$\gamma = \alpha + j\beta \quad (1)$$

The attenuation constant α for microstrip structures can be broken into 3 loss factors: dielectric loss, radiative loss and metal or conductor loss:

$$\alpha = \alpha_d + \alpha_r + \alpha_c \quad (2)$$

Dielectric loss represents the power dissipated in the dielectric material. The dielectric loss tangent, $\tan \delta$, was measured using split-post [5] and split cylinder [6] techniques; the dielectric constant, or relative permittivity ϵ_r , was monitored with a ring-resonator [7] for every firing. Once dielectric loss tangent was found, dielectric loss equations from Schneider [8] were used to calculate dielectric loss attenuation. Since microstrip topologies require the electromagnetic wave to propagate through air and dielectric material this results in an effective permittivity ϵ_{eff} .

$$\alpha_d = 27.3 \frac{\epsilon_{eff} - 1}{\epsilon_r - 1} \frac{\epsilon_r \tan \delta}{\epsilon_{eff} \lambda} \quad (3)$$

Once the dielectric loss is found (eq. 3) then it is subtracted from the determined attenuated signal.

The radiative loss factor for the topologies considered is comparatively small; it is assumed zero for stripline structures and is design dependant within microstrip. The microstrip samples have been designed to mitigate radiative loss, that is avoid discontinuities and substrate thickness is minimized so that it is a fraction of the quarter wavelength at 30GHz.

Conductor loss is caused by the power dissipated due to the conducting surfaces of the line. The insertion loss of a microstrip line over a low-loss dielectric substrate at microwave frequencies is dominated by the conductor loss.

Skin effect is essentially where the signal exponentially decays from the propagating edge into the conductor. This is a well-known phenomenon in microwave engineering and is central to our understanding of how surface roughness effects conductor loss.

The signal level of 37% intensity is 1 skin depth. As the frequency increases δ_s decreases and the signal will conduct closer to the outer edge of the conductor where the EM wave is propagating. Figure 1 illustrates the skin effect in a microstrip topology.

$$\delta_s = \sqrt{\frac{1}{\pi f \sigma \mu_o \mu_r}} \quad (4)$$

Where σ represents bulk conductivity; the bulk conductivity was measured for both tape systems.

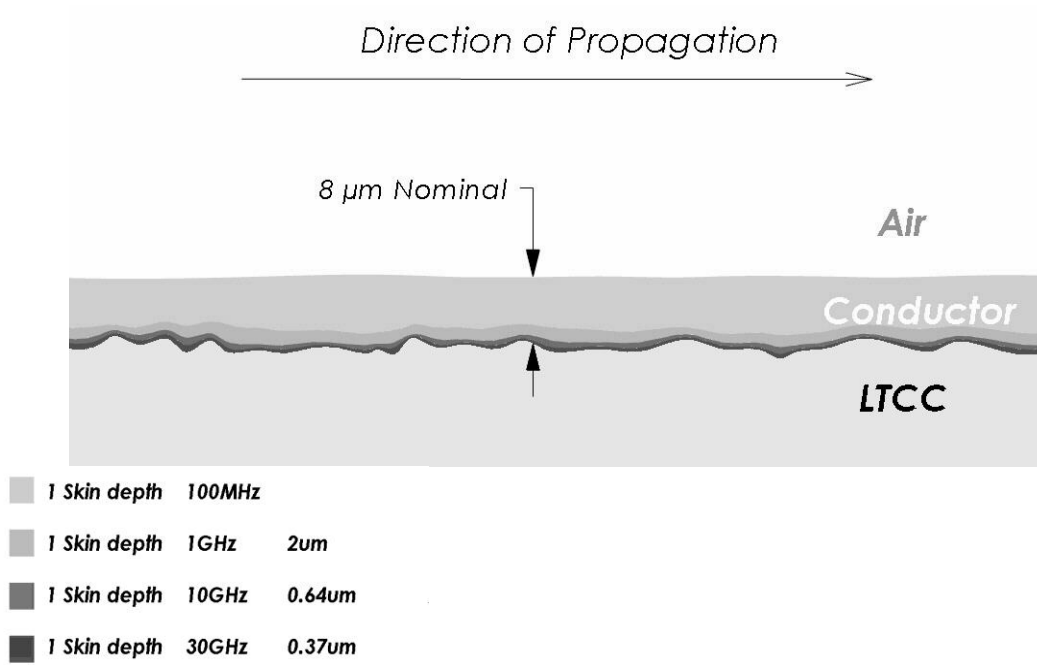


Figure 1: Skin effect representation shown for a range of frequencies using silver conductivity of 62893081 mhos/m.

The equation that been established for surface roughness effect on conductor loss attenuation [9] is represented by:

$$\alpha_c = \alpha_{smooth} \left\{ \left(1 + \frac{2}{\pi} \arctan \left(1.4 \left(\frac{S_a}{\delta_s} \right)^2 \right) \right) \right\} \quad (5)$$

Surface Texture Measurements

An interferometric and scanning laser microscope (SLM) were used to measure the surface roughness data. Two LTCC tape systems with different roughness are used to examine the roughness-loss relationship. These samples with differing roughness are from different tape systems. The samples consist of a transmission line printed a microstrip topology on LTCC.

Six regions of 250x250 μ m were measured; the measured textures were analyzed using Map Premium software (Digital Surf).

Surface Texture Characterization

The conventional parameters S_a and S_q were used to compare conductor loss at microwave frequencies with measured conductor loss. S_a is the areal average of the absolute values of the surface height deviations measured from the best fitting plane.

$$S_a = \iint_a |Z(x, y)| dx dy \quad (6)$$

S_q , the root mean square (rms) roughness is very similar to S_a ; the surface heights are “squared” prior to being integrated.

$$S_q = \sqrt{\iint_a (Z(x, y))^2 dx dy} \quad (7)$$

S_a and S_q value are insensitive to the spatial distribution of the surface heights; two very high peaks will contribute the same value whether the peaks are close to each other or separated over the measurement field. A deep valley or a high peak of same magnitude will result in the same S_a or S_q value.

Sa and Sq will average the absolute value without representing any anisotropic characteristic of the surface. Since the signal propagates along a specific axis, this may be a source of error. Although there is no evidence to suggest the surface is anisotropic.

The conventional parameters Sa and Sq do not directly relate the surface roughness profile to the electrical path length at a particular frequency or scale.

Results

Table 1 summarizes the measured parameters Sa (eq. 6), Sq (eq.7), and $\tan\delta$ (eq. 3) and bulk conductivity σ (eq. 4).

Table 1 – Summary of Measured Roughness, Dielectric Loss Tangent and Bulk Conductivity Parameters

	Sa	Sq
Tape system1	1.56 μm	1.98 μm
Tape system2	1.18 μm	1.6 μm
	Tanδ at 20GHz	
Tape system1	0.00154	
Tape system2	0.006	
	Bulk Conductivity σ	
Tape system1	2.22 x 10 ⁷ S/m	
Tape system2	1.39 x 10 ⁷ S/m	

Figure 2 shows measured attenuated losses for LTCC tape system 1. The attenuated loss is broken into the conductor and dielectric loss factors following the method described in loss calculation section. The conductor loss is significantly larger over the frequency ranges shown.

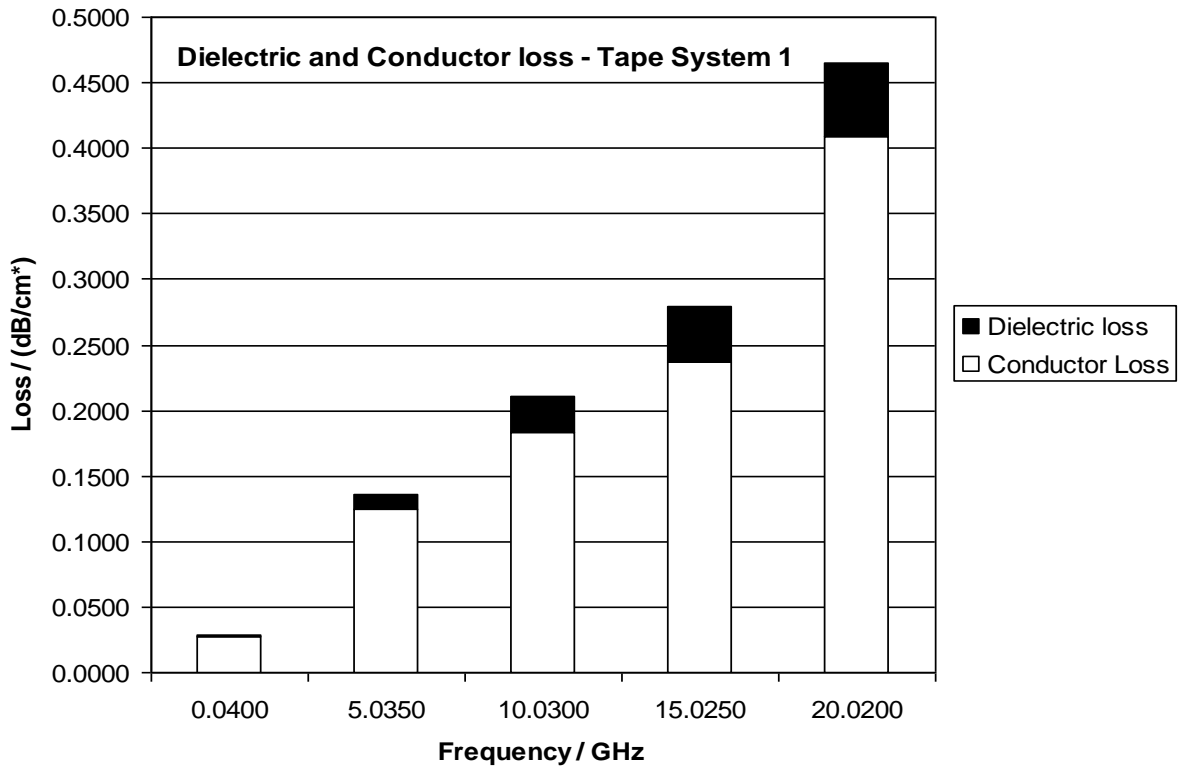


Figure 2: Measured Attenuated Loss for LTCC Tape System 1

Figure 3 shows the total losses including the reflected loss for this specific configuration in the same tape system. Even including the reflected losses, it can be seen that conductor loss is still the largest loss factor.

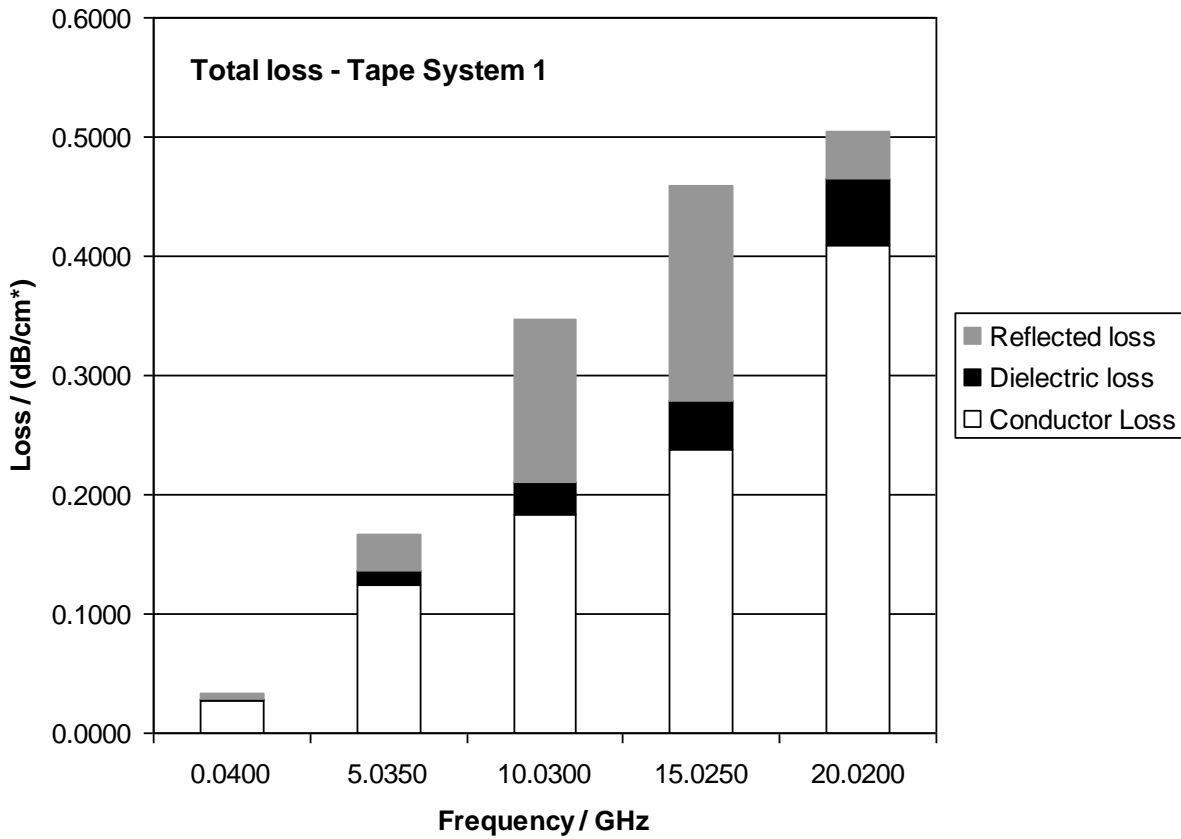


Figure 3: Measured Total Loss for LTCC Tape System 1

Figure 4 shows measured attenuated losses for LTCC tape system 2. The attenuated loss is broken into the conductor and dielectric loss factors using the method described above. The conductor loss is significantly larger over the frequency ranges shown. Both dielectric and conductor losses are larger than for tape system 1 with the dielectric loss taking up a larger fraction for the higher frequency ranges.

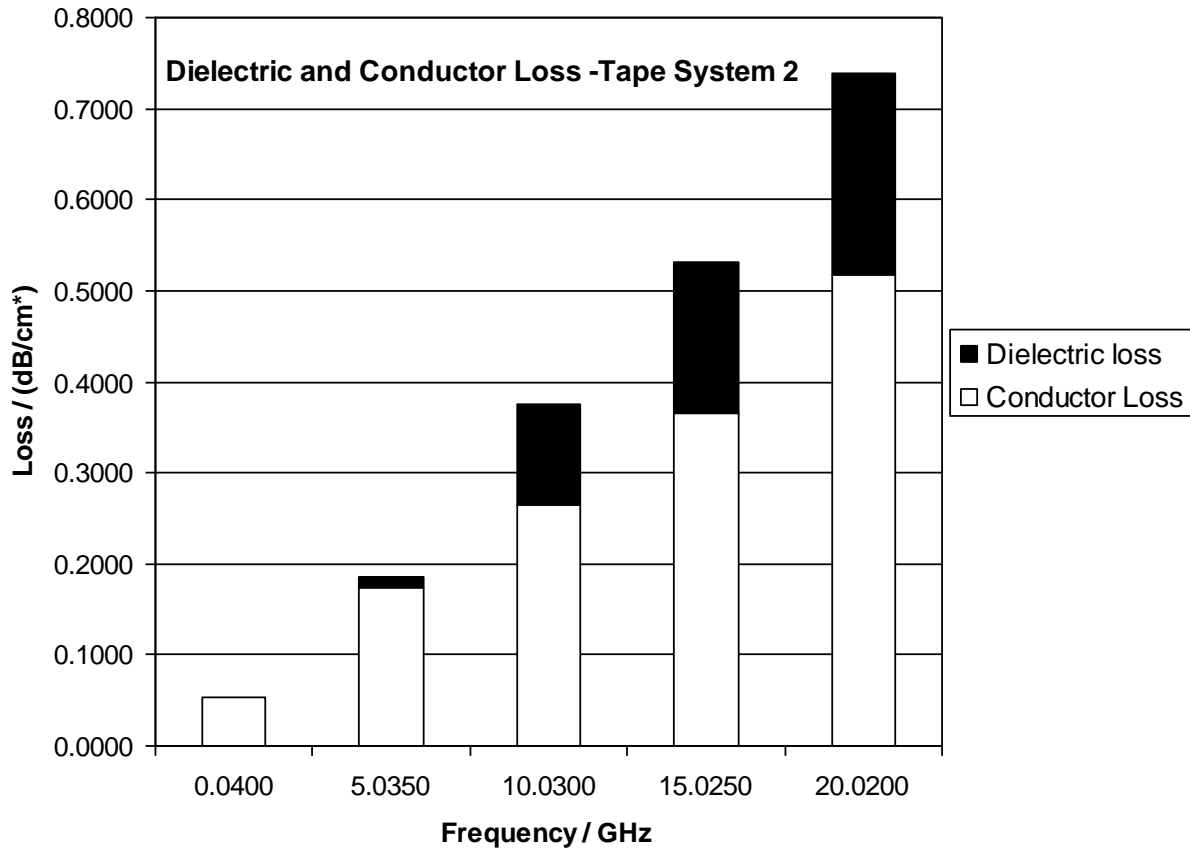


Figure 4: Measured Attenuated Loss for LTCC Tape System 2

Figure 5 includes reflected losses with conductor and dielectric losses for tape system 2. Conductor loss is still the largest loss factor. Due to improved return losses the reflected loss constitutes a lower fraction of the loss in general when compared to Tape System 1.

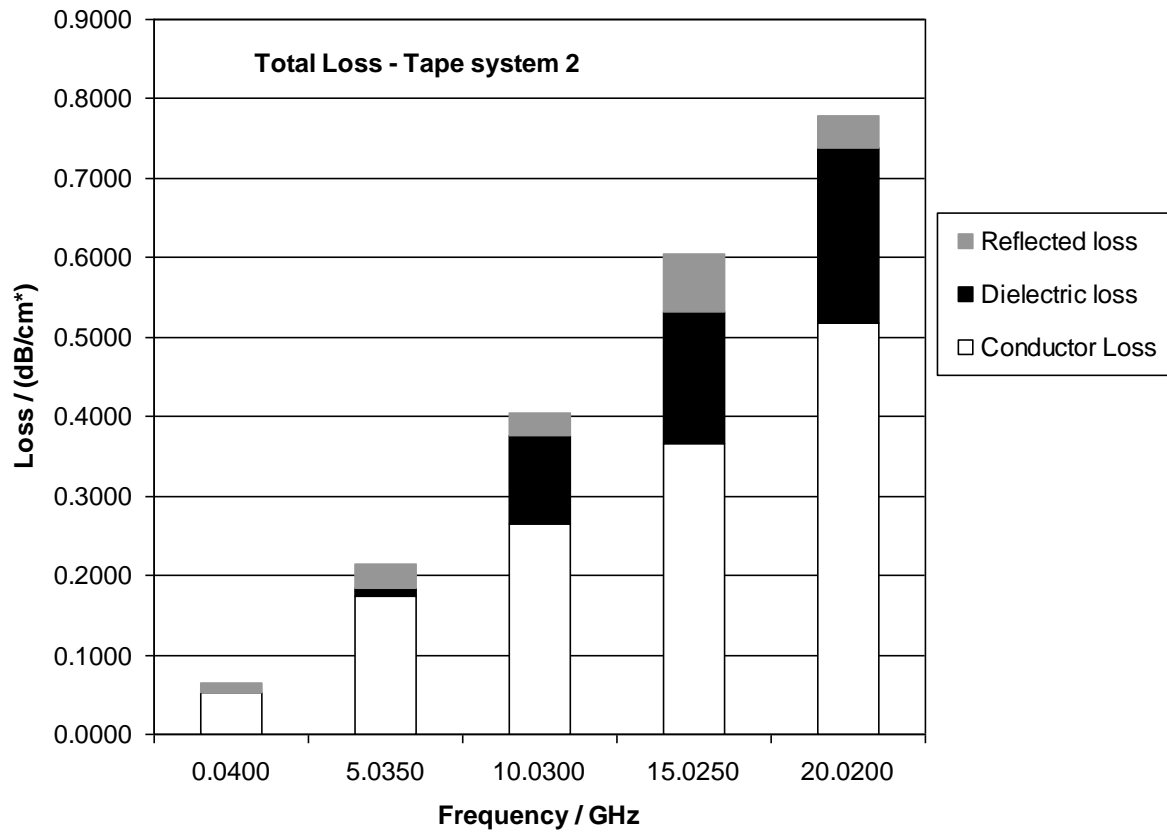


Figure 5: Measured total loss for LTCC tape system2

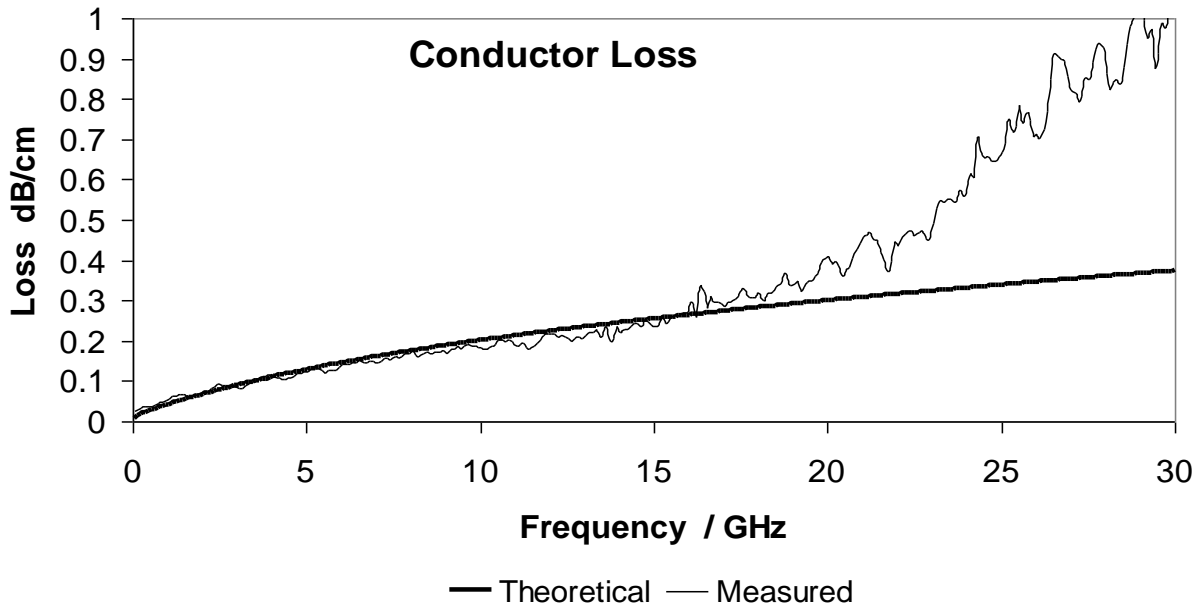


Figure 6: Measured Conductor Loss versus Theoretical Conductor Loss for Tape System 1

Figure 6 represents the determined conductor loss by the method explained in the loss calculation section derived from measurement of the total loss versus the conductor loss that is theoretically calculated by equation 5 using the data collected for tape system 1.

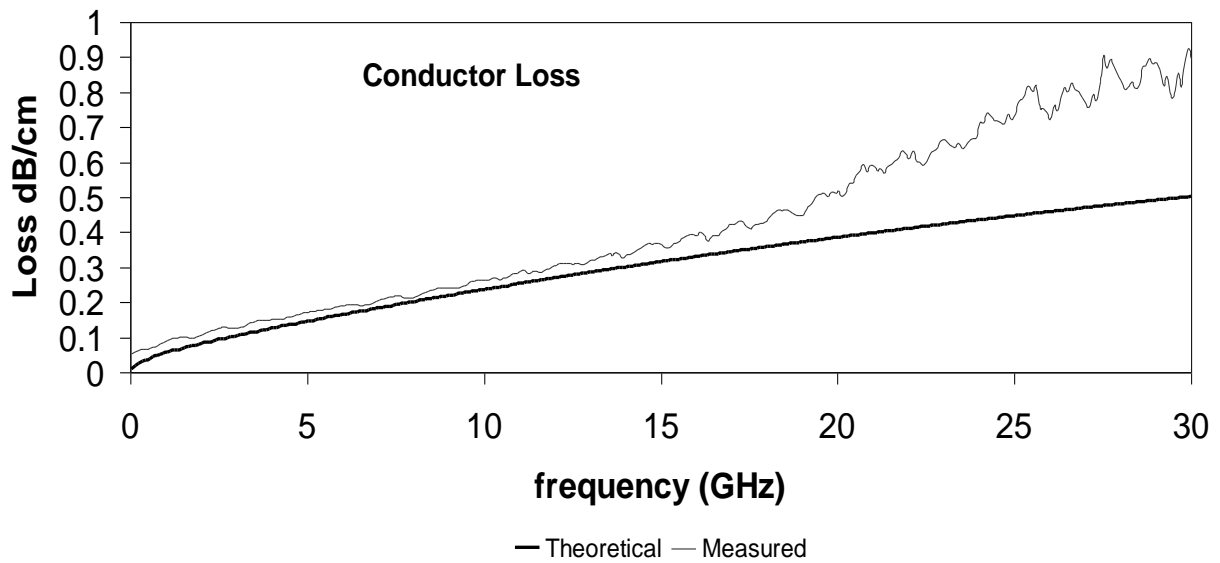


Figure 7: Measured Conductor Loss versus Theoretical Conductor Loss for Tape System 2.

Figure 7 represents the determined conductor loss by the method explained in the loss calculation section versus the conductor loss calculated by equation 5 using the data collected for tape system 2.

Discussion

The total loss increases with frequency and both the dielectric and conductor loss factors increase as frequency increases. The conductor loss remains the largest loss factor in this topology for both tape systems.

It is often assumed that surface roughness does not have a large effect on insertion loss for RF frequencies. This assumption could be precarious especially if engineering materials continue to improve in terms of dielectric loss tangent with no thought given to surface roughness effects. Trace conductivity also has to be considered when examining attenuation loss.

Tape system 2 has a lower conductivity that results in higher conductor loss than tape system 1 for the frequency range used in this study.

Equation 5 was formulated by Hammerstad and Jensen [9] to curve fit empirical data for conductor traces where there is a minimum of 5 skin depths. It can be seen in Figure 6 and Figure 7 that the measured conductor loss matches well with the theoretical conductor loss from low GHz to approx 20GHz. Above 20GHz the measured conductor loss deviates from the theoretical conductor loss calculation.

Surfaces have irregular complex textures and are self-similar over limited ranges of scale; length scale fractal analysis is a useful tool for surface scale length parameterization. It is thought that a surface specific length measurement may provide a useful correlation when calculating conductor loss at frequencies above 20GHz. Conventional surface parameters have their limitations and the field of surface metrology has become increasingly sophisticated since 1980. Further study using length scale fractal analysis [10] is underway.

The reflected loss has been included since it can be a major contributing loss factor. However, it should be noted that reflected loss is highly design dependant. This is can be seen by comparing Figure 3 with Figure 5.

Conclusions

Surface roughness and insertion losses have been determined for two different LTCC systems, the results show that the conductor loss factor is a high fraction of total loss and is therefore a major loss factor for this topology and frequency range.

The established Hammerstad and Jensen conductor surface roughness correction formula has been found to curve fit the determined conductor loss to 20GHz. However above 20GHz the determined conductor loss does not match the calculated conductor loss profile.

Acknowledgements

The authors would like to acknowledge Mike Ehlert and Ron Schmidt from Barry Industries for their helpful insights.

References

- [1] M. Bayes, A. Horn “Effects of Conductor Surface Condition on Signal Integrity” Circuit World 2004 pp11-16.
- [2] G. Brist, S. Hall “Non-Classical Conductor Losses due to Copper Foil Roughness and Treatment” ECWC 10 Conference at IPC 05.
- [3] T. Laing, S. Hall, H. Heck G. Brist “A Practical Method for Modeling PCB Transmission Lines with Conductor Surface Roughness and Wideband Dielectric Properties” IEEE 2006 pp1780-1783.
- [4] F. A. Benson, T.M. Benson “Fields Waves and Transmission Lines” Chapman and Hall 1991 pp31-49

- [5] J. Krupka, R. G. Geyer, J Baker-Jarvis and J. Ceremuga, "Measurements of the Complex Permittivity of Microwave Circuit Board Substrates Using Split Dielectric Resonator and Reentrant Cavity Techniques", 1996 DMMA Conference, pp. 21-24, 1996.
- [6] M. D Janezic, E. Kuester, J Baker-Jarvis "Broadband Complex Permittivity Measurements of Dielectric Substrates using a Split-Cylinder Resonator," IEEE MTT-International Microwave Symposium Digest, pp.1817-1820, June 2004.
- [7] K. Chang, L-H Hsieh "Microwave Ring Circuits and Related Structures" Wiley-Interscience 2nd edition pp139-152 2004.
- [8] M. V. Schneider, "Dielectric Losses in Integrated Microwave Circuits", Bell Syst. Techn. J., September 1969 pp2325-2333.
- [9] E. Hammerstad, Ø. Jensen "Accurate Models for Microstrip Computer Aided Design" IEEE MTT-S May 1980 pp407-409.
- [10] ASME B46.1, Surface Texture (Surface Roughness Waviness and Lay), an American National Standard, ch 10, American Society of Mechanical Engineers, New York, 2002.

8.0 APPENDIX B

**PROCEEDINGS, MS&T, PITTSBURG 2008: CONDUCTOR EDGE DEFINITION
INFLUENCE ON HIGH FREQUENCY ELECTRICAL LOSS**

T. VINCENT AND I. BAR-ON

Abstract

This study tests the theory that the edge definition of a thick-film print conductor can alter high frequency loss characteristic. High frequency loss degrades both GHz analogue and fast switching digital signals. A telecommunication electronic system contains transmission lines consisting of a conductor strip, which carries signals in the form of electromagnetic (EM) waves. This strip of conductor on the surface of a ceramic substrate is as a guide to the EM signal and results in conductor loss. Conductor loss is the largest loss factor for GHz frequency applications. As the frequency increases, the current concentrates closer to the conductor extremities especially at the conductor edge. The ceramic surface, in particular surface roughness, can influence the topography of the conductor strip when the conductor is formed by thick-film processing. Using AlN with known surface characteristics, the edge definition for several conductors is measured and correlated to loss over a range of frequencies.

Introduction

This paper tests the theory that the conductor edge topography is the primary topography influence on conductor loss results for printed circuit boards manufactured by thick-film processes. Most conductor loss research has focused on the influence of surface roughness topography; the consensus being that increased surface roughness increases conductor loss [1]. However, for microelectronics fabricated by thick-film technology it shall be shown that increased surface roughness can change the conductor edge topography to result in reduced conductor loss.

Most classic methods of calculating conductor loss ignore edge effects since they work on the premise that the conductor is infinitely thin. The strip thickness of a microstrip circuit is much smaller than the width and this does not change the field except at the edges. The edge research that has been made has focused on the numerical/analytical calculation techniques [2]. There is little published measurement data on edge effects.

Microstrip topology test samples of thick-film conductor printed on AlN substrates were fabricated and the transmission loss measured. The ceramic surfaces are characterized using length-scale fractal analysis and edge topography differences observed. The edge topographies are ranked and compared to the loss rank.

Theoretical Development

The transmission loss of a microstrip line over a low-loss dielectric substrate at microwave frequencies is dominated by the conductor loss [3]. Conductor loss is the power that is absorbed by the conductor material as the electrical signal propagates along the signal trace.

The skin effect is a well known phenomenon, where the current density becomes concentrated at the conductor extremities as frequency increases. In a microstrip topology, the most common type of circuit, the signal decays exponentially from the dielectric-conductor interface into the conductor. Therefore the current density is concentrated at the insulator surface and at the conductor edges. At GHz frequencies the skin effect is so pronounced that, for

a good conductor such as silver, the current flow is contained within a fraction of a micron from the substrate surface and edge and therefore is influenced by the surface/edge topography.

The current density is increased at the conductor edge, shown by Figure 1 due to fringing fields [4]. The two current carrying conductors will exert a magnetic force on one another. The magnetic force/field loops around each conductor; therefore the orthogonal electric field is vertical underneath the current strip and horizontal at the edge; this is also known as fringing field. The vertical and horizontal electric fields add; increasing the current density at the edge. It has been noted that a large amount of conductor loss occurs at the edges [5]. The mathematical solution states that current density increases at the conductor edge, becoming larger as the corner gets sharper [6].

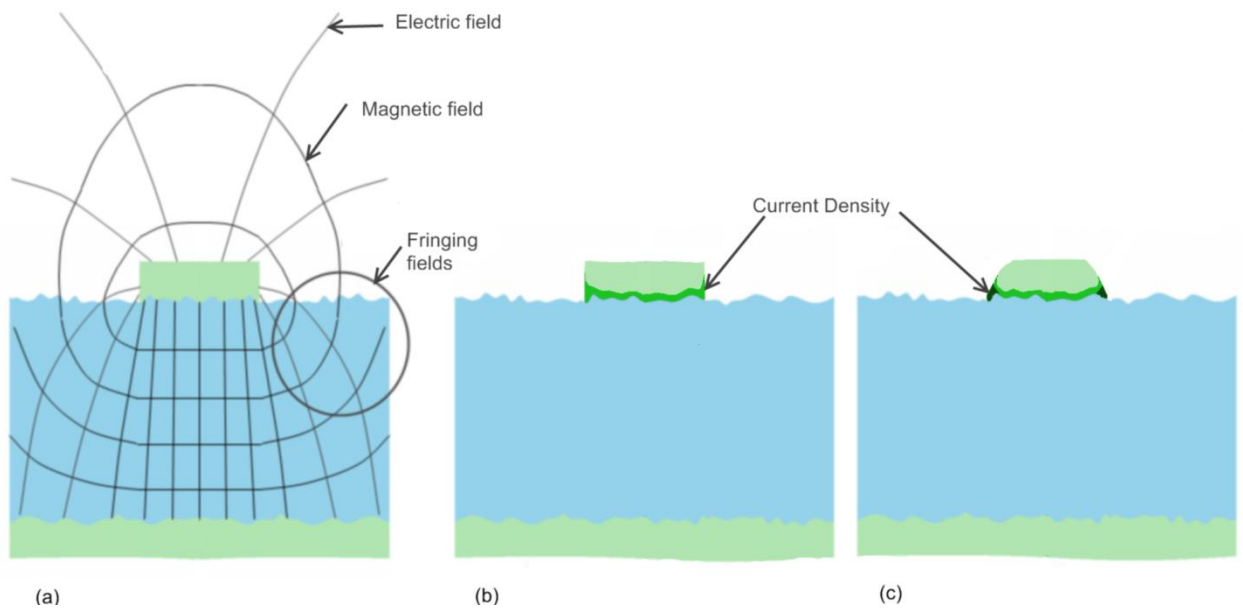


Figure 1 Cross-sectional front view of conductor (a) Shows the magnetic and electric fields (b) Is an illustration of the skin depth, the current is concentrated in the darker green shaded area; this conductor strip edge is wedge shape (c) Is an illustration of the skin depth, the current being concentrated in the darker green shaded area, the darker the shade the higher the current density; the conductor has a tapered edge.

When circuits are fabricated by thick-film printing, the conductor paste/ink is transferred through the screen to the substrate; this is a complex phenomenon and relates to the rheology of the ink [7]. The ink is required to flow through the openings of the screen and wet the surface of the substrate. This essentially involves lubrication theory [8] where the flow of fluids in one dimension is significantly smaller than the others. Data from shear testing suggests that the ink acts as a Bingham plastic [9]; that is, the ink acts as a combination of Newtonian and shear – thinning, pseudoplastic, material; this is not known quantitatively.

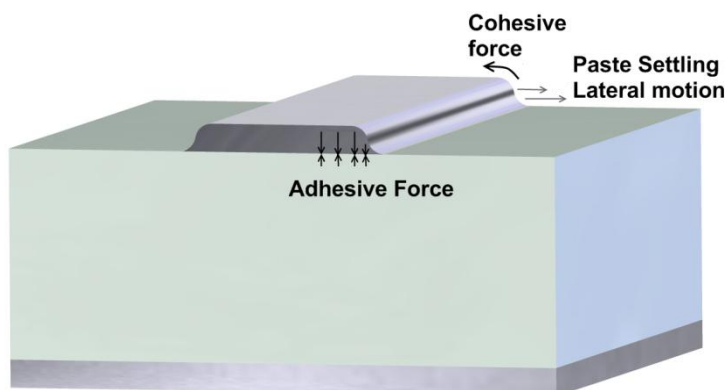


Figure 2 Illustration of settling mechanism for thick-film print conductors.

After printing, the trace is left to settle, allowing the lateral motion of the paste across the substrate to come to a complete stop. The adhesive forces between the atoms in the liquid and the substrate with the surface inclination will compete against the cohesive forces within the liquid, as shown by Figure 2. Hence, the amount of lateral motion will depend on the surface inclination/adhesive force between the printed ink and substrate surface [10]. Greater surface roughness will mean greater area and higher angle of inclination, which in turn causes greater local adhesion [11] and resistance force, this leads to less lateral motion. The thick-film print

fired conductor has a non-uniform thickness across the width, where the conductor gets thinner at the edges of the print.

Many parameters can be used to characterize surfaces. Length-scale fractal analysis calculates the lengths of a profile as a function of scale by virtually stepping along the surface [12]. The smaller the steps the closer the stepping pattern follows the actual surface profile and the longer the calculated profile length.

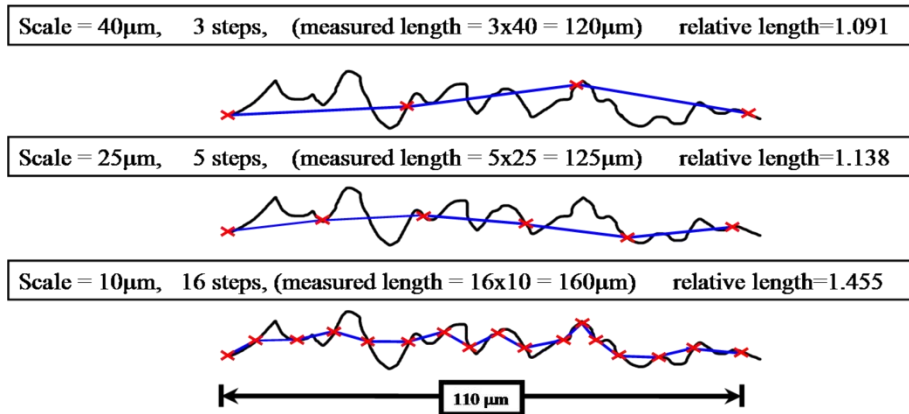


Figure 3 An example length-scale analysis illustration, showing how as the scale, or step length, decreases the measured length increases. The nominal lengths are all 110µm.

The tiling or stepping sequence in length-scale analysis is demonstrated in figure 3. A series of progressively shorter step sizes are used to calculate the measured lengths of the profile as a function of scale. The step size is the scale of observation, or calculation. The relative length at a particular scale is the measured length at that scale divided by the nominal, or straight-line, length.

Experimental Method

Thick film screen printing technology was used to make the microstrip circuits for this study. Four substrate plates were printed with microstrip circuits; two were printed with ALN 11 paste, and two with ALN 33.

ALN 11© [13] is a silver conductor, with measured bulk conductivity of $2.2 \times 10^7 \text{S/m}$

ALN 33© [14] is a silver/palladium conductor (10:1), with measured bulk conductivity of $6 \times 10^6 \text{S/m}$.

All circuits were printed in a clean room environment, with the same screen, same process parameters, at the same time. There were two sets of microstrip circuits on each plate. Each microstrip circuit set consisted of three signal traces of different lengths, the longest being 40mm, which is used for the loss measurements. Every plate also had a serpentine line, as shown in figure 5 middle right. The serpentine was used to measure bulk conductivity, σ .

The total loss was measured using an Anritsu Vector Network Analyzer with (GGB industries) picoprobes®, to obtain S-parameters (signal parameters). S-parameters are used to describe the electrical behavior of an electrical device when undergoing various steady state stimuli by small signals. The losses were measured on both circuits after calibrating with the picoprobe® substrate standard. The first circuit was used for analysis. The measurement of the second circuit was taken as validation of the first measurement. The loss measurements were

viewed using SONNET software® and analyzed using Microsoft Excel. The frequency range extends from DC to 20GHz.

Transmission line equations [15] were used to calculate the reflected loss from the mismatch measurement. Reflected loss is caused by a mismatch between the input and output transition and the conductor path itself. This mismatch was measured for each of the circuits. Reflected losses are design dependant, and, therefore, the reflected loss is subtracted from the total loss to calculate the transmission loss. Three different microstrip lengths were used to measure and corroborate the transmission losses for each of the lines.

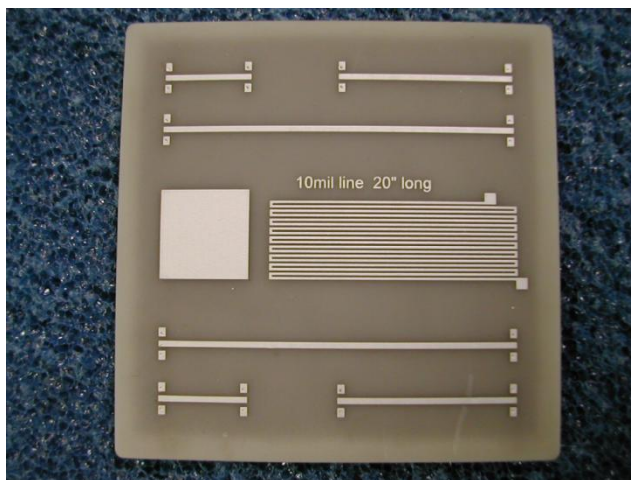


Figure 4 Top view photograph of an AlN substrate with conductor with two sets of three transmission lines with nominal lengths: 10, 20, and 40mm. The serpentine line is used to measure bulk conductivity.

The surface of the AlN substrates were treated with three different surface finishing techniques: lapping, honing and chemical etching. These techniques are detailed in Table 1. Six profiles (height z as a function of position x) were measured on each surface finish with a Perthen (Mahr Federal) profiler using an unskidded stylus with a tip radius of $2\mu\text{m}$. The

sampling interval was 69nm and the trace length 560 μ m. The profiles were Gaussian filtered with wavelength cut off 0.08mm, and length-scale fractal analysis performed (ASME B46 2002). The measured profiles were analyzed using Map Premium software® (Digital Surf) and Sfrax (www.surfract.com).

Table 1 Surface Finish Process

Surface Finish	Process
Lapped	Lapped using an oil-based abrasive; cleaned in ultrasonic bath and rinsed with alcohol (ACUMET).
Vapor Honed	Blasted with 220 grit aluminum oxide and water, then vapor honed for 2.5 minutes with 0.5mil of material removed.
Chemically Etched	Held in an Anodex solution for 1 hour at 150 °C, then in an HCl solution for 1hour at 150 °C, followed by cold water rinse. This process is repeated twice.

Sections of these samples, a sample is shown by figure 4, were cross sectioned to examine the edge topography. The diced parts were mounted in Buehler Epothin epoxy Resin and manually polished following the [16] precious metals procedure. To preserve the edge, the conductors were plated with Nickel [17], using electrolytic plating method. The cross sections were viewed with a Nikon Epiphot optical microscope, images taken with a Nikon Digital Sight DS-U1 camera using ACT-2U software. A minimum of four edges of each conductor, per surface finish, were viewed.

Results and Discussion

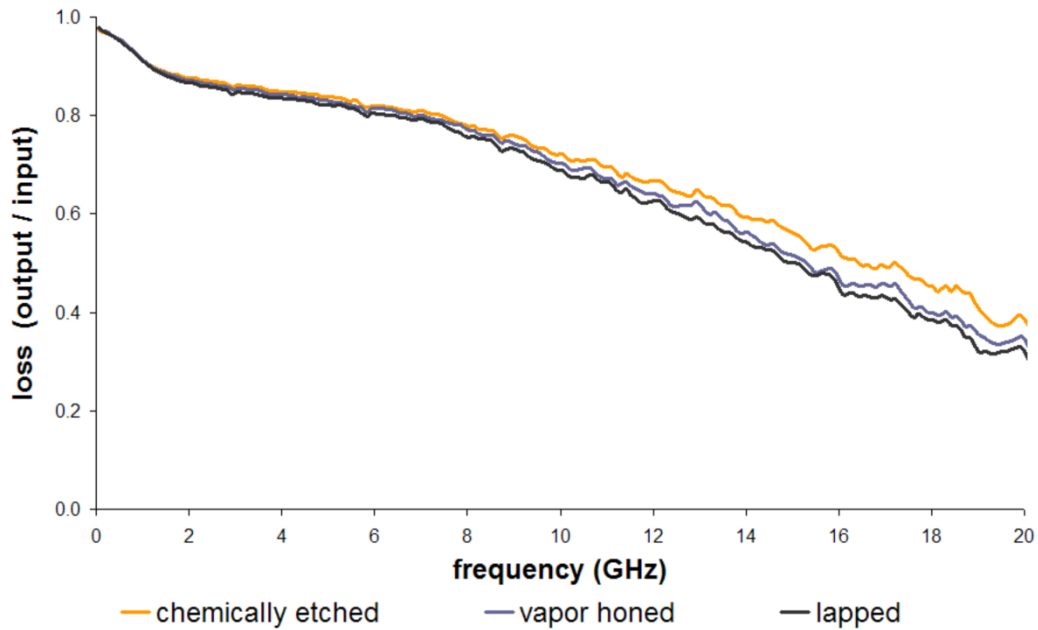


Figure 5 Electrical loss of 40mm ALN33 conductor line on chemically etched, vapor honed and lapped surface.

As the frequency increases the loss result, from the fired ALN33 conductor, from each of the samples, with different surface finish, begin to diverge at frequencies greater than 5GHz, figure 5. The chemically etched surface has the lowest loss. The lapped surface has the highest loss.

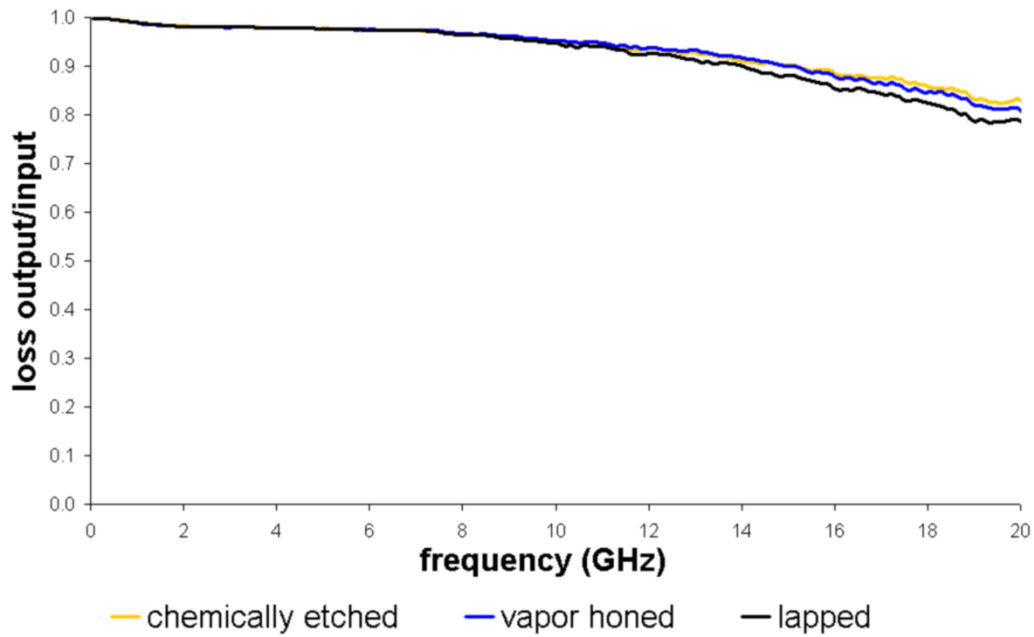


Figure 6 Electrical loss of 40mm ALN11 conductor line on chemically etched, vapor honed and lapped surface.

As the frequency increases the loss result, from the fired ALN11 conductor, from each of the samples, with different surface finish, begin to diverge at frequencies greater than 12GHz, figure 6. The chemically etched surface has the lowest loss. The lapped surface has the highest loss.

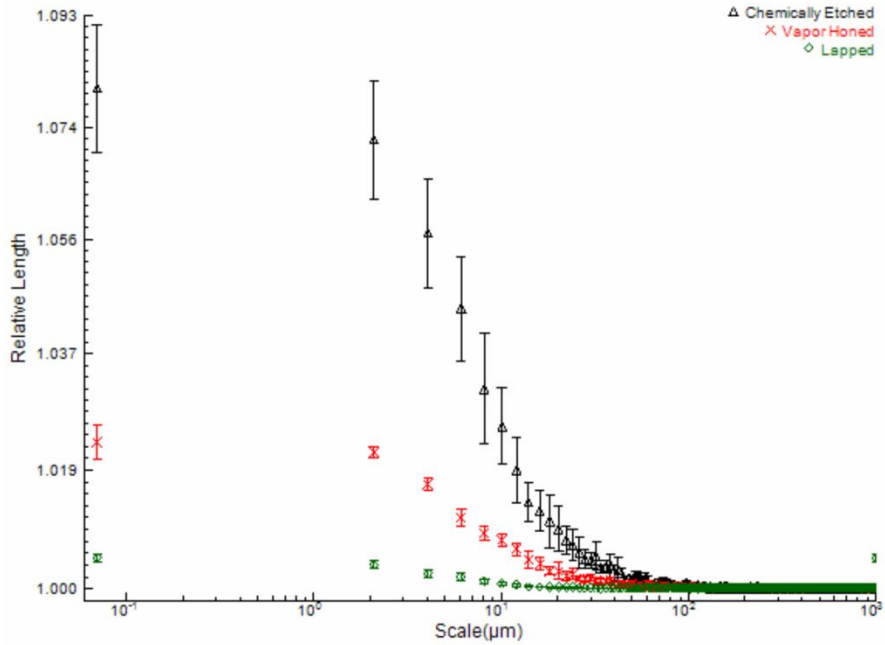


Figure 7 Length-scale Fractal Analysis for AlN with Chemically etched, Vapor Honed and Lapped Surface finish.

The length-scale roughness characterizations of profiles from the four different substrate surface treatments are shown in figure 7 with the mean and variation of 6 measurements taken from 6 different areas of the substrate. F-tests [18] were performed on all six measurements. All of the surface comparisons were discernable, i.e., statistically different, for scales less than 60 μm with a level of confidence greater than 95%.

The relative lengths of the profiles measured from all three surface treatments are similar at scales above 100 μm . The relative lengths increase rapidly with the decrease in scale between scales 2 μm and 20 μm . The chemically etched surface clearly has a longer length than all the other surfaces at scales below 50 μm . The lapped surface clearly has a shorter length than all the other surfaces at scales below 30 μm . The surfaces were isotropic therefore; the increase in length corresponds with an increase in surface area.

Conventional theory states that an increased surface roughness results in increased loss but the roughest surface, the chemically etched surface finish, has the lowest loss and the smoothest surface, the lapped surface, has the highest loss, shown by figures 5 and 6.

It is known that the edge topography also has an influence on the loss result. The edge topographies of both the ALN11 and ALN33 conductors show a marked difference in edge topography depending on the surface finish.

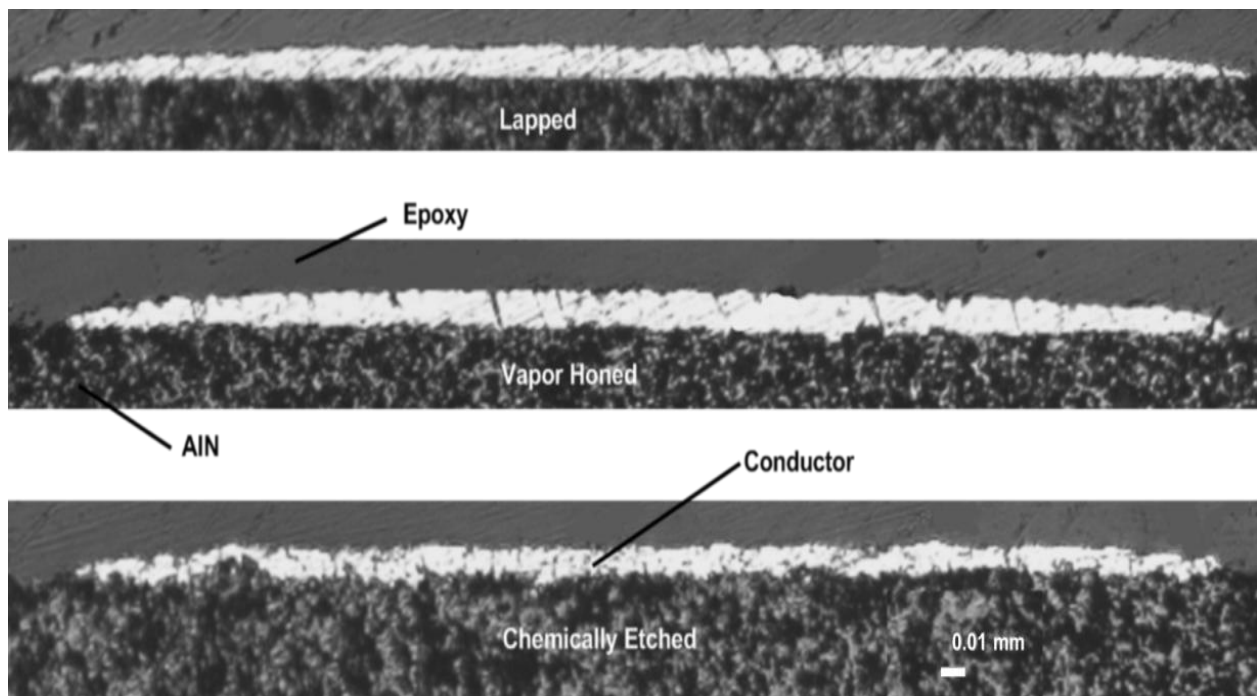


Figure 8 Cross section of microstrip circuit, x10 magnification, taken across the width of the conductor. Shown is the AlN substrate with conductor ALN33 on Lapped (top), Vapor Honed (middle) and Chemically Etched (base) surface finish.

It can be seen from figure 8 that the width of the lapped conductor strip is approximately 0.1mm wider than the width of the conductor strip on the chemically etched substrate. The conductor edges shape is also different.

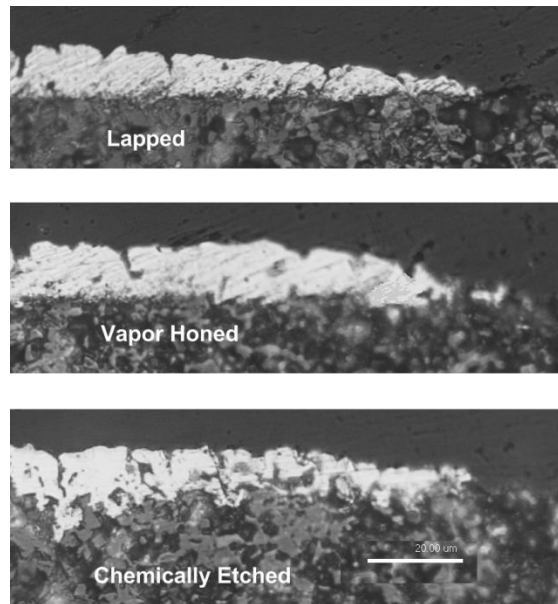


Figure 9 cross section of microstrip circuit, x50 magnification, across the width of the conductor at the edge. Shown is the AlN substrate with conductor ALN33 on Lapped (top), Vapor Honed (middle) and Chemically Etched (base) surface finish.

The edges of the ALN33 conductor change topography depending on the surface finish as shown by figure 9. The chemically etched surface has a conductor with an abrupt edge compared to the lapped surface with a tapered edge.

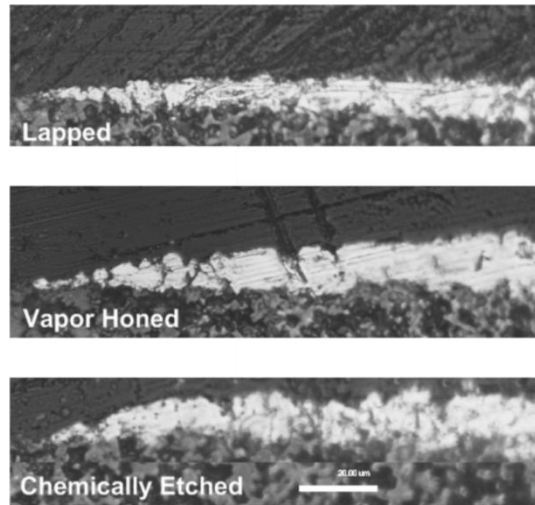


Figure 10 cross section of microstrip circuit, x50 magnification, across the width of the conductor at the edge. Shown is the AlN substrate with conductor ALN11 on Lapped (top), Vapor Honed (middle) and chemically etched (base) Surface finish.

Similarly, the edges of the ALN11 conductor change topography depending on the surface finish as shown by figure 10. The chemically etched surface has a conductor with an abrupt thick to thin thickness change when compared to the lapped surface which has a more tapered edge. The ALN11 and ALN33 conductors have the same results.

Table 2: Loss Rank for ALN11 and ALN33 Compared to Surface Roughness and Edge Topography

Surface Finish	Surface Roughness of AlN ceramic	Loss for ALN33	Loss for ALN11	Taper angle of Edge For ALN33	Taper angle of Edge For ALN11
Lapped	Lowest	Highest	Highest	Lowest	Lowest
Vapor Honed	Medium	Medium	Medium	Medium	Medium
Chemically Etched	Highest	Lowest	Lowest	Highest	Highest

For the ALN 33 conductor the width of the lapped conductor strip is wider than the width of the conductor strip, shown by figure 8, on the chemically etched substrate and the edge topography is also different, figure 9. When compared, the lapped surface conductor has a sharper edge implying that the lapped surface, which has a lower surface area, has had a larger lateral paste flow across the surface. The increased surface roughness/inclination and therefore surface area, figure 7, of the chemically etched surface, causes greater adhesion/inclination friction of the paste and less lateral motion of the conductor.

Conclusions

- Conductor loss, surface roughness and edge topography were measured for two conductor materials on three different substrate surface treatments.
- The ALN11 fired conductor trace is wider on the lapped surface than on the chemically etched surface.
- The sample with the chemically etched surface has a conductor edge with a more distinct thick to thin change than the lapped surface conductor sample.
- The conductor edge topography has been shaped by the ceramic surface characteristic between the printed conductor paste and the substrate.
- The differences in loss between the samples made with lapped, vapor honed, and chemically etched AlN substrates is as a result of the conductor edge topography and not as a result of the conductor/substrate interface roughness.
- The greater the angle of the conductor edge, the lower the transmission loss.

Acknowledgments

The authors would like to thank the Surface Metrology Laboratory at WPI.

References

- [1] Stephen Hall, Steven G. Pytel, Paul G. Huray, Daniel Hua, Anusha Moonshiram, Gary A. Brist, and Edin Sijercic, Multigigahertz Causal Transmission Line Modeling Methodology Using a 3-D Hemispherical Surface Roughness Approach, *IEEE Transactions on Microwave Theory and Techniques*, vol. 55, no. 12, December 2007.
- [2] S. Safavi-Naeini, R. Faraji-Dana, Y.L. Chow, Studies of Edge Current Densities in Regular and Superconducting Microstrip Lines of Finite Thickness, *IEE Proceedings-H*, Vol.140, No. 5, October 1993.
- [3] T. Vincent, I. Bar-On, C. A. Brown, Examination of Surface Roughness Effect on Insertion loss at Microwave Frequencies within LTCC Structures, *Conference Proceedings and Presentation iMAPS/ACerS 3rd International Conference and Exhibition on Ceramic Interconnect and Ceramic Microsystems Technologies (CICMT)*, April 23-26, 2007, Denver, Colorado USA, pp 138-144.
- [4] J. D. Kraus and D. A. Fleisch, *Electromagnetics with applications*, 5th Edition McGraw-Hill International Editions, 1999, p 35-115.
- [5] E. L. Barsotti, *Effect of Strip Edge Shape on Microstrip Conductor Loss*, MS Thesis University of Colorado 1990.

- [6] J. Meixner, The Behavior of Electromagnetic Fields at Edges, *Inst. Math. Sci. Res. Rept.* EM-72, New York University, New York, NY, 1954.
- [7] T. K. Gupta, *Handbook of Thick- and Thin-Film Hybrid Microelectronics*, Wiley Interscience, 2003, p 161-175.
- [8] Rangchi, A Model for Deposition of Thick Films by the Screen Printing Method, MS Thesis Louisiana State University, 1986.
- [9] G. Moeller-Johnson, The Importance of Rheology in the screen printing ink: Newtonian vs. Shear Thinning, *Proceeding of the International Symposium on Microelectronics*, 1987, p. 320-337.
- [10] P. M. Gerhart, *Fundamentals of Fluid Mechanics*, Addison-Wesley Publishing Company, 1985.
- [11] C.A. Brown and S. Siegmann, Fundamental Scales of Adhesion and Area-scale Fractal Analysis, *International Journal of Machine Tools and Manufacture*, vol. 41. 2001.
- [12] ASME B46.1, Surface Texture (Surface Roughness Waviness and Lay), an American National Standard, ch 10, American Society of Mechanical Engineers, New York, 2002.

[13] ALN11 Silver Conductor, DuPont Microcircuit Materials datasheet [www.dupont.com/mcm MCMALN11\(07/2002\)](http://www.dupont.com/mcm/MCMALN11(07/2002))

[14] ALN33 Silver/Palladium Conductor (10:1), DuPont Microcircuit Materials
[www.dupont.com/mcm MCMALN33\(06/2002\)](http://www.dupont.com/mcm/MCMALN33(06/2002))

[15] B. C. Wadell, *Transmission Line Design Handbook*, Artech House, 1991, pp25-27.

[16] Buehler SUMMET, *The Science Behind Materials Preparation*, a guide to Materials Preparation and Analysis, 2004, p 51.

[17] G. F. Vandervoort, *Metallography Principles and Practice*, ASM international, 1999, p 90.

[18] C. Lipson, *Statistical Design and Analysis of Engineering Experiments*, McGraw-Hill, Inc, New York, 1973, p196-201.

9.0 APPENDIX C

MATLAB PROGRAM FOR PAPER I, CHAPER III: MATLAB PROGRAM TO MEASURE THE LENGTH OF THE CONDUCTOR EDGE PROFILE

Matlab program for edge profile

```
%Tracey's edge length program
% read image file
I=imread('HMAP_11_7.bmp');
% Initialize, a, b variable denote the pixel position on the
% bitmap image, c, d are white & black pixel counters and the
% initial edge length is 1.

a=1;
b=1;
c=0;
d=0;
e=1;
f=1;
l=0;

% outer loop going to each pixel in image file (512x512)

while b<513
    if a<512
        a=a+1;
%Is it a white pixel?
        if I(a,b)>0
            d=d+1;
            switch I(a,b)>0
```

```

%Is it next to a black pixel?
    case I(a+1,b)==0
        l=l+1;
    case I(a,b+1)==0
        l=l+1;
    case I(e,b)==0
        l=l+1;
    case I(a,f)==0
        l=l+1;
    end
    else
        c=c+1;
    end
else
a=0;
b=b+1;
    if b>=2
        f=b-1;
        if a>=2
            e=a-1;
        end
    end
end
end
end

% output

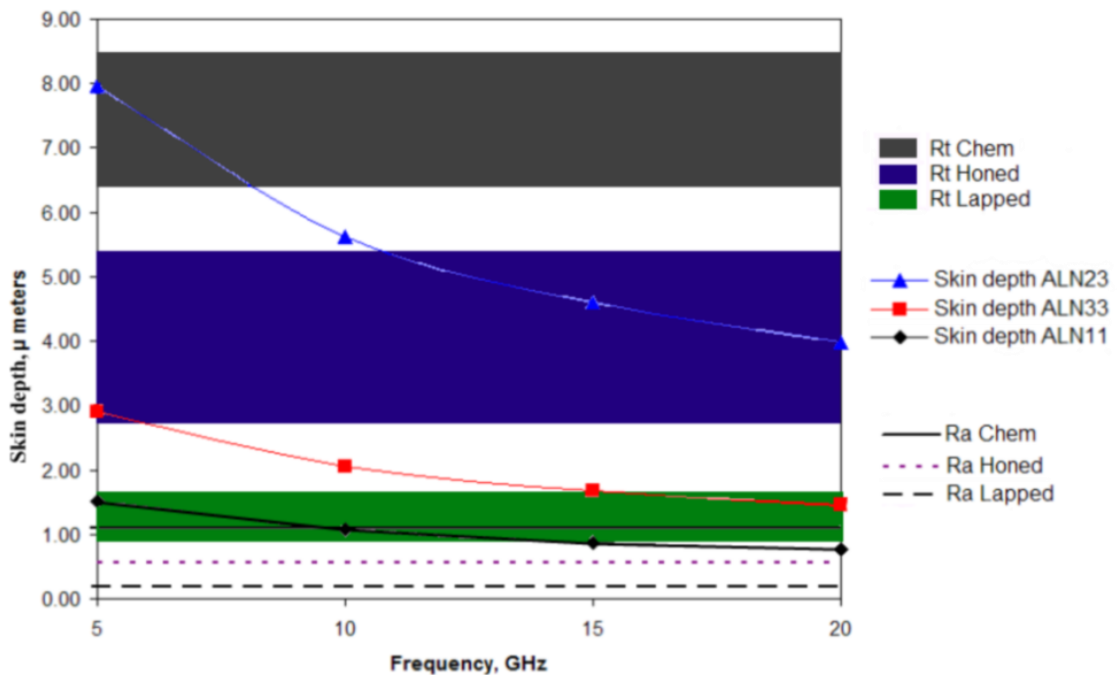
d
c
e
f
l
rel_length=1/512

```

10.0 APPENDIX D

ANALYZE SUBSTRATE SURFACES

The influence of roughness values on loss, for the different conductor lines, can be understood in terms of skin depth. The figure below depicts skin depth as a function of frequency for the three different conductor lines. The figure includes the values of roughness parameters, Ra and Rt that were measured for the surfaces.



Skin depth as a function of frequency for three different conductor lines including the values for roughness parameters, Ra (lines), and Rt (ranges).

These values show how the roughness values are of the same magnitude as the skin depth for the higher frequencies. For ALN11 and ALN33 this occurs at lower frequencies than for ALN23. It also shows that the effect of the frequency on loss should appear first, for the material with the greater roughness value, the chemically etched surface. This was only observed for the ALN23 line, and there only for the 10 and 15 GHz condition where the skin effect is not prominent. For all other cases, the surface with greater roughness shows lower loss.